Irena Dapic,[1]* Lucia Baljeu-Neuman,[2] Naomi Uwugiaren,[1] Jesper Kers,[3,4,5] David R. Goodlett,[1,6] and Garry L. Corthals,[4]**

[1]*International Centre for Cancer Vaccine Science, University of Gdansk, Gdansk, Poland*
[2]*University of Applied Sciences Inholland, Amsterdam, The Netherlands*
[3]*Department of Pathology, Amsterdam Infection & Immunity Institute (AI&II), Amsterdam Cardiovascular Sciences (ACS), Amsterdam UMC, University of Amsterdam, Amsterdam, The Netherlands*
[4]*van 't Hoff Institute for Molecular Sciences, University of Amsterdam, Amsterdam, The Netherlands*
[5]*Ragon Institute of Massachusetts General Hospital, Massachusetts Institute of Technology and Harvard University, Cambridge, MA*
[6]*University of Maryland, 20N. Pine Street, Baltimore, MD 21201*

Received 20 March 2019; accepted 17 June 2019

Published online 7 August 2019 in Wiley Online Library (wileyonlinelibrary.com). DOI 10.1002/mas.21598

Tissues and biofluids are important sources of information used for the detection of diseases and decisions on patient therapies. There are several accepted methods for preservation of tissues, among which the most popular are fresh-frozen and formalin-fixed paraffin embedded methods. Depending on the preservation method and the amount of sample available, various specific protocols are available for tissue processing for subsequent proteomic analysis. Protocols are tailored to answer various biological questions, and as such vary in lysis and digestion conditions, as well as duration. The existence of diverse tissue-sample protocols has led to confusion in how to choose the best protocol for a given tissue and made it difficult to compare results across sample types. Here, we summarize procedures used for tissue processing for subsequent bottom-up proteomic analysis. Furthermore, we compare protocols for their variations in the composition of lysis buffers, digestion procedures, and purification steps. For example, reports have shown that lysis buffer composition plays an important role in the profile of extracted proteins: the most common are tris(hydroxymethyl)aminomethane, radioimmunoprecipitation assay, and ammonium bicarbonate buffers. Although, trypsin is the most commonly used enzyme for proteolysis, in some protocols it is supplemented with Lys-C and/or chymotrypsin, which will often lead to an increase in proteome coverage. Data show that the selection of the lysis procedure might need to be tissue-specific to produce distinct protocols for individual tissue types. Finally, selection of the procedures is also influenced by the amount of sample available, which range from biopsies or the size of a few dozen of mm^2 obtained with laser capture microdissection to much larger amounts that weight several milligrams.

Keywords: *tissue; LC-MS; FF; FFPE; proteome; protocols; sample preparation*

**Correspondence to*: Irena Dapic, International Centre for Cancer Vaccine Science, University of Gdansk, Wita Stwosza 63, 80-308 Gdansk, Poland. E-mail: irena.dapic@ug.edu.pl
***Correspondence to*: Garry L. Corthals, University of Amsterdam, van 't Hoff Institute for Molecular Sciences (HIMS), Science Park 904, 1098 XH Amsterdam, The Netherlands. E-mail: G.L.Corthals@uva.nl

I. INTRODUCTION

A. Pathology and Mass Spectrometry: From a Visual Science to Molecular Science

To define the proteome is crucial to determine the pathophysiology of a disease. Therefore, today we witness a large increase in the methodologies that attempt to capture and monitor proteins in tissue samples. Specifically, clinical proteomics seeks novel approaches to lead to better clinical diagnosis and effective treatment. Expansion in proteomics has led to the development of technologies for more effective and sensitive detection of proteins and bioinformatic tools to convert data in knowledge (Silberring & Ciborowski, 2010; Binnig, Huss, & Schmidt, 2018).

Historically, tissue samples collected in the clinic formed the cornerstone to investigate biological functions and dynamics in order to ascertain the disease state. Goal to advance treatment of the patients drove discovery of new medical tools and methodologies. In this process, examination of tissue biopsy or clinical specimen by pathologists is somewhat dependent on the pathologist's experience and is unfortunately subjective. Considering that manual tissue examination using conventional immunohistochemical staining limits throughput of tissue analysis, there has been recently an increase in attempts to use proteomic methods as a surrogate or aid to the pathologist's historical approaches. Main struggle today in tissue proteomics represents urge to find cure for cancer and massive effort in this has the Clinical Proteomic Tumor Analysis Consortium (CPTAC; https://proteomics.cancer.gov/programs/cptac) launched in 2011. CPTAC organization developed proteogenomics work on variety of cancers to find mutations responsible for cancer progression (Ellis et al., 2013; Mertins et al., 2016; Zhang et al., 2014, 2016). Data from the proteomic studies and pipelines are publicly available on the CPTAC Data Portal together with experimental design and protocols (Edwards et al., 2015). Later, in 2016 two new programs: The Applied Proteogenomics OrganizationaL Learning and Outcomes and the International Cancer Proteogenome Consortium were released with the goal to share data and advance patient's care.

Mass spectrometry is an indispensable tool in proteome exploration, including definition of posttranslational modifications (PTMs). Today, there are two main proteomic approaches: discovery-based methods that are nontargeted in nature, and targeted methods where the proteome of interest has been previously defined. Both methods use high-performance liquid chromatography (HPLC)-electrospray ionization tandem mass spectrometry (LC-MS/MS) methods to elucidate proteomes. Discovery proteomics aims to define proteomes with automated methods that might use either data-dependent acquisition where the computer controlling data-analysis makes decisions based on what is observed, or data-independent acquisition (DIA) where the computer is preprogramed to collect data based on a previously defined proteome (Fig. 1). In both cases, it is typical to analyze samples in a so-called bottom-up proteomic approach, where peptides are obtained after digestion of all proteins in a biological sample. When on contrasts targeted proteomics to discovery proteomics, preselected sets of peptides are defined for detection with a method known as single reaction monitoring of which there are various permutations that depend on the type of instrument used; for example, parallel-reaction monitoring approaches would be used on quadrupole-orbitrap mass spectrometers. This targeted approach leads to highly reproducible, sensitive, and accurate data sets; however, only a limited number of the peptides present in the sample can be analysed per LC-MS/MS experiment. Both strategies have been widely used in proteomics and are described in detail elsewhere in the literature.

Regardless of which method would be used to analyze a proteome, sample preparation of tissue specimens prior to MS analysis requires effective and reproducible protein extraction. As alluded to above, the first step in bottom-up proteomics is protein extraction and subsequent digestion with endoproteases that produces a complex mixture of peptides. Although the sample preparation process is one of the key steps in proteomics, regrettably there is no standard method in use for preparation of protein samples from tissues or any source for that matter. Rather, the toolbox of available sample-preparation methods is often tied directly to the type of sample to be prepared and is highly variable. In this review, we outline factors that influence protein sample preparation from tissue, including types of tissue and the various chemical routes that lead from protein extraction to instrumental analysis. Notably, one of the most important factors that determine which sample-preparation method to choose is sample size or amount. Many of the existing methods have been used on single proteins and cell lines, that do not translate easily to small amounts of tissue. Detection of proteomes from small amounts of tissue represents a methodological challenge that is currently under constant refinement. Recently, Zhu et al. (Y Zhu, Dou et al., 2018; Y Zhu, Piehowski et al., 2018) have developed a nano-scale sample preparation platform which was further adapted to a nanowell-mediated 2D LC approach and demonstrate its use on only a dozen cells (Dou et al., 2018). Reduction of adsorptive losses of proteins is key to analyze small numbers of cells, and this point was elegantly made by the development of the nanoPOTS platform, which in combination with existing 2D-LC-MS/MS chromatography methods, allowed deep proteome profiling from only nanograms of protein and also was successfully combined with laser capture microdissection (LCM) of the tissues (Y Zhu, Dou et al., 2018).

In addition, technological development of the instrumentation required for depicting the proteome had led to large expansion of the methods used in proteomics. Ancillary techniques as mass spectrometry imaging (MSI) enables detection of spatial distribution of the molecules and can provide information about thousands of molecules in a single run (Balluff, Hanselmann, & Heeren, 2017; Dilillo et al., 2017; McDonnell et al., 2017; Buchberger et al., 2018). Alternatively, to benefit from matrix-less technologies some combined

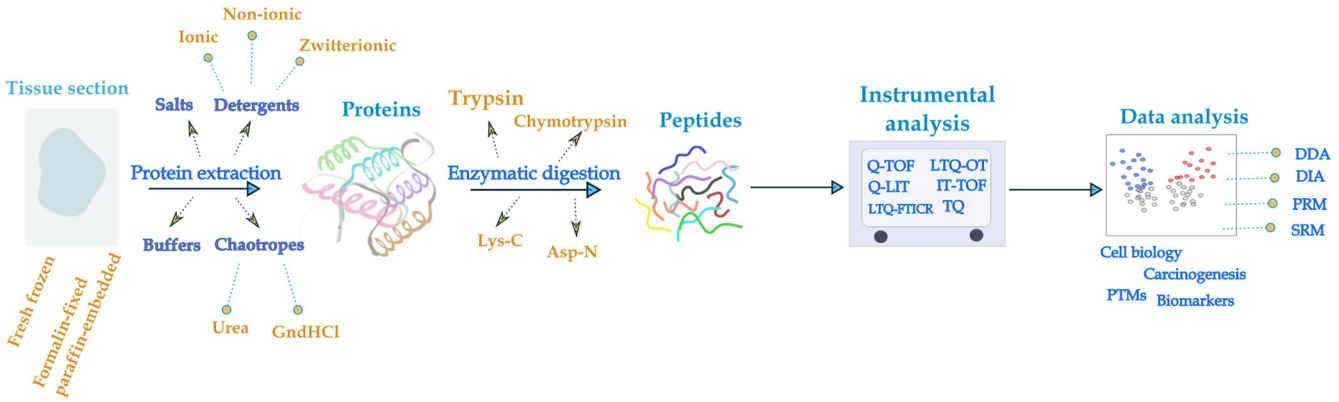

FIGURE 1. Typical tissue analysis workflow. Microdissected tissue sections can be obtained as FF or FFPE tissues. Tissue processing includes protein extraction followed by digestion to peptides enzymatically most often with trypsin. Next various cleanup methods are available for preparation for LC-MS/MS analysis. Bioinformatic analysis of the tandem MS data leads to the identification of peptides and their corresponding proteins. Further, this information is used to answer biological question of the experiment and to help in better understanding of biochemical processes behind the scene. DDA, data dependent acquisition; DIA, data independent acquisition; FF, fresh frozen; FFPE, formalin fixed paraffin embedded; IT-TOF, ion trap-time of flight mass spectrometry; LC-MS/MS, liquid chromatography tandem mass spectrometry; LTQ-FTICR, linear quadrupole ion trap Fourier transform ion cyclotron resonance mass spectrometry; LTQ-OT, linear trap quadrupole orbitrap mass spectrometry; PRM, parallel reaction monitoring; PTM, posttranslational modification; Q-LIT, linear quadrupole ion trap; Q-TOF, quadrupole-time of flight mass spectrometry; SRM, single reaction monitoring; TQ, triple quadrupole mass spectrometry. [Color figure can be viewed at wileyonlinelibrary.com]

techniques as matrix-free silicon nanowire arrays (Wang et al., 2012) or laser desorption/ionization on porous silicon (DIOS) (Beavis et al., 1990; Wei, Buriak, & Siuzdak, 1999) were developed. In this approach, after analytes deposition on the porous silicon surface laser is used to desorb analytes from the surface without matrix assistance. DIOS-MS showed to tolerate moderate amounts of contaminats and was applied in structural characterization and detection of proteins, *in situ* digests, small molecules (Thomas et al., 2001) and peptides from neurons (Kruse et al., 2001).

Moreover, mass cytometry (CyTOF) has gained attention in immunophenotyping and studying the range of the cells and their function. Cells are stained with antibodies conjugated to the metal isotopes reporters and are further resolved with ICP-qTOF. CyTOF had shown large range of applications to reveal heterogeneity of human cells including phenotyping of natural killer cells (Kay, Strauss-Albee, & Blish, 2016) and detecting cancer cell subsets (Leelatian et al., 2017). CyTOF has expanded to step further in imaging mass cytometry (IMC) whereas highly multiplexed assay couples imunohistochemical staining with immunocytochemical methods (Di Palma & Bodenmiller, 2015; Chang et al., 2017). Bodenmiller et al pioneered IMC and applied it to FFPE human breast cancer and mammary epithelial cells for simultaneous imaging of more than 30 proteins and their modifications at subcellular resolution (Giesen et al., 2014). Application of IMC on FFPE tissues with demonstrated power to reveal tumor microenvironment heterogeneity helped IMC to further rapidly evolve into the commercial instrument for screening of immunohistological tissue sections.

Technological advances that include cell sorting and/or further discover spatial distribution of the cells in tissues are an appealing paltform to provide phenotypic and functional markers in cancer. Progress in standardizing procedures and application on histological tissue sections lays down attention on these techniques and raises their chance to be accepted for clinical use. However, detailed discussion about these techniques is beyond the scope of this review, and we would like to point readers to some of the informative resources mentioned here as well as to the other existing literature.

II. TISSUE CLASSIFICATION AND COLLECTION

The advantage of molecular analysis compared to conventional pathology evaluation of tissues is that more unambiguous molecular information is acquired that can be used for decision-tree processes, and ultimately personalized disease management based on the molecular profile of the patient. High-throughput analyses can aid in further stratification of patients based on the molecular patterns in the tissue. Besides disease classification, molecular analysis of tissue can reveal pathways related to the underlying disease process that can be leveraged as targets for therapy (ie, theranostics; Yousem, 2012; Peer, 2014). The recently published randomized-controlled MINDACT trial in which 6,693 patients with early-stage breast cancer were randomized to adjuvant chemotherapy based on a 70-gene signature (MammaPrint) acquired from their tumor tissue, which has previously been shown to predict poor prognosis, is an example of such a clinical application (Cardoso et al., 2016). Compared to the clinical risk score, the 70-gene tumor signature selected low-risk patients that comprised 46% of the population under study that did not require adjuvant chemotherapy. This study exemplifies how molecular analyses can have an impact on patient management.

In pathology, tissue specimens can be divided into two groups; namely, the so-called "reactive diseases," which encompass immunologic and metabolic traits, and oncological diseases (ie, cancer). Figure 2a provides an overview of the tissue types and storage in regard to disease classification and study goals. Depended on the specimen group and at what time in the diagnostic process tissue is collected, the aim of proteomics, and how such an experiment is set up, will vary.

A. Small, Smaller, and Smallest: Resection, Biopsy, and Aspiration Specimens

Resection specimens are almost exclusively collected in oncologic diseases. Because the objective is to remove the tissue from the patient, the amount of tissue that can be used for molecular analyses is almost always adequate. Tumors are often compared with pre-existing tissue from the same organ typically part of the same resection as an internal control. Additionally, tissue sampling for proteomics done upon macroscopic evaluation by the pathologist could reduce sampling error to a minimum. Proteome analysis of resected material can be used to further stratify patients in a molecular subgroup and to identify possible candidate molecules or pathways that can be a target for adjuvant therapy. However, most specimens sent for pathology evaluation are biopsies that have been obtained for primary diagnostics. Because a biopsy is obtained for diagnostic purposes (eg, prior to tumor resection), less material is available for experimental purposes. There are two types of needle biopsies; the first is termed fine-needle aspiration (FNA), and the second is known as a core-needle biopsy (or core biopsy). The dimensions of the FNA are very small (25- to 27-gauge needles) and these needles are only used to remove a small amount of fluid and tissue pieces for the analysis of cellular and nuclear features (eg, FNA of lymph nodes to detect tumor metastasis). Typically, this process is guided visually with ultrasound or computed tomography (CT) scan. Although, the procedure often allows rapid diagnosis (same day), occasionally not enough tissue is removed for an unambiguous diagnosis and an aspirate does not allow the pathologist to observe the integrity of the tissue (only groups of cells or fluids are removed for analysis). Core-needle biopsies are larger, because the needles used in a core biopsy are slightly bigger than those used in FNA (typically 14- to 18-gauge). They remove a small cylinder of tissue about 1.5 mm (1/16'') diameter by 1.25 cm (1/2''). The big advantage of a core needle biopsy is the ability, when successful, to analyze the morphology and integrity of the microanatomy. In oncological diseases, normal tissue microanatomy can be distinguished from precursors of cancer (dysplasia) and invasive tumor. With FNA, it is not possible to distinguish dysplasia from invasive tumor cells, because tissue morphology is lost. In immunological or metabolic diseases, on the contrary, analysis of tissue morphology is crucial and FNA is not a suitable procedure to diagnose such diseases upon light microscopy. To process core biopsy samples, especially with formalin-based fixation protocols, usually takes longer than FNA biopsies. Although biopsies can be snap-frozen to reduce lead-time, tissue morphology is lost and is, therefore, primarily used for peroperative decisions and immunofluorescence staining. As with FNA, the core biopsy often uses an ultrasound, CT scan

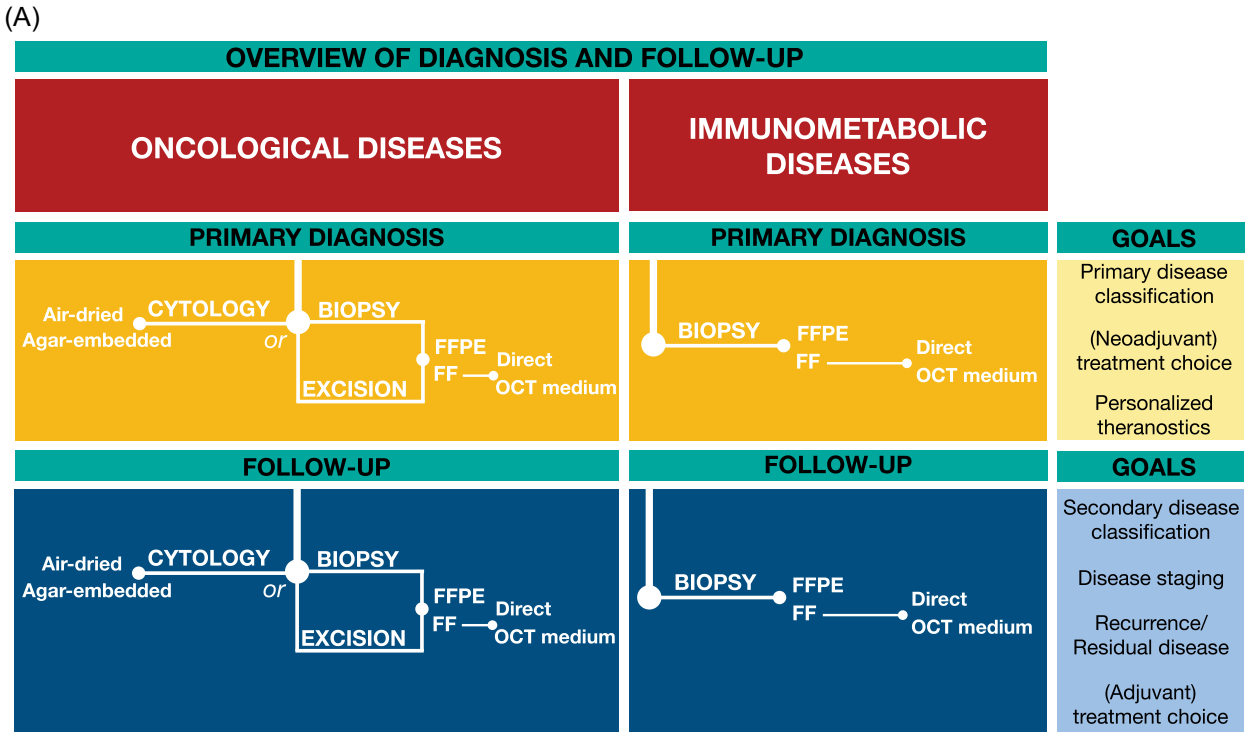

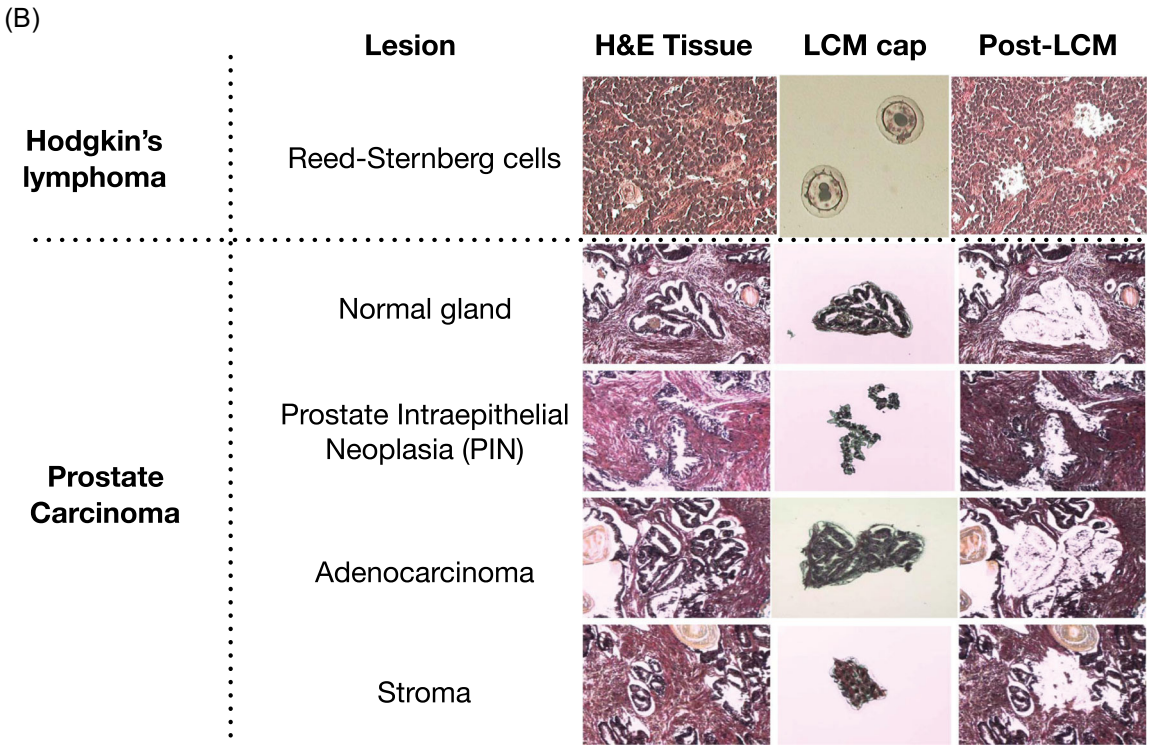

FIGURE 2. Overview of disease categories in use for LCM analysis. (a) Schematic overview of tissue types and their storage used in clinics for disease classification and diagnostics. In oncological diseases, microdissected tissue or biopsies are the main sources of the material. For metabolic and immunological diseases biopsies are main source of material for primary diagnosis and follow-up treatment. (b) H&E staining of tissues and LCM capture of Reed-Stenberg cells in research of Hodgkin's lymphoma and cell subpopulations including benign, PIN, malignant, and stromal cells in prostate cancer. In the middle column captured cells are shown in LCM cap. Reprinted with permission from Liu et al. (2010) copyright year 2010 (Journal of Biomolecular Techniques, Association of Biomolecular Resource Facilities) H&E, hematoxylin and eosin stain; LCM, laser capture microdissection; PIN, prostatic intraepithelial neoplasia; RS, Reed-Stenberg. [Color figure can be viewed at wileyonlinelibrary.com]

mammogram, or MRI to guide the needle toward the lesion of interest. Sometimes the tumor is palpable and can be directly biopsied. Compared to resection material, the yield of proteins when analyzing biopsy specimens will be drastically reduced, especially for FNA. In a recent study, Labots and colleagues revealed that phosphoproteome analysis of biopsy tissue from patients with colorectal cancer is feasible and reproducible, although there was no direct comparison of phosphoprotein yield loss compared to a corresponding resection sample from the same patient (Labots et al., 2017). Tumor heterogeneity, which can be defined as different tumor cell clones with variable mutation patterns, but also sampling errors in immunological and metabolic traits, are not necessarily detected with biopsy-based proteomics. However, sampling error is a problem of the biopsy procedure itself rather than any flaws in proteome analysis. In oncological cases, large number of biopsies are used to identify targets for neo-adjuvant therapy to reduce tumor mass prior to surgery. In pathology specimens from patients with immunologic and metabolic diseases, which represent disease processes that diffusely affect the entire organ, a biopsy is almost never followed by organ resection, especially when the disease affects visceral organs. Core-biopsy specimens, therefore, represent the main target and challenge in fast analysis of patient material. Studies that investigate clinical applications of proteomics should focus on relative and absolute quantitative analysis on small tissue samples.

B. Noise Reduction and Enrichment

There are various methods that can analyse the complex spatial multicellular organization of microscopic tissue sections. LCM of tissues on slides (a.k.a. tissue slides) is a method to cut out selected cellular patterns or regions that can be further processed for proteomics or other molecular techniques. Although there are many different LCM devices on the market, two main platforms exist; namely, infrared-LCM and ultraviolet-LCM (Datta et al., 2015). With an LCM system, samples can be purified with selection of only the regions of interest to reduce interference with proteomes from cells that are not of interest, and also was shown to be compatible with immunofluorescent staining (Moulédous et al., 2003). Invention of immuno-LCM to investigate tumour micro-environment (Buckanovich et al., 2006) was also used for recovery of high quality mRNA from isolated cell subpopulations from tissues (Fend et al., 1999) and was later combinated with FASP and LC-MS in proteomics study of CD24 cells in adenocarcinoma tissues to identify several pancreatic cancer biomarker candidates (Zhu et al., 2013). LCM is fast and is depended on the laser spot and the composition of the tissue. Single-cell LCM, however, is not straightforward and requires a skilled operator. Figure 2b shows microdissected single Reed-Sternberg cells from a patient with Hodgkin's lymphoma (typically scarce within lymph nodes) and separation of (*in situ*) prostate carcinoma that surrounded stroma and normal tissue. LCM is compatible with various tissue sources, including FFPE and fresh frozen (FF) samples. De Marchi et al compared the use of LCM to whole-tissue lysis of breast cancer specimens followed with MS, and found that LCM enrichment had a higher individual protein yield (3,404 vs 2,837 with 2,696 overlapping, respectively) and significantly reduced numbers of missing values at the peptide and protein level, possibly due to a reduction in interference from immune cells, metabolism-related proteins, and high-abundance proteins (De Marchi et al., 2016). Besides the selection of cell types, LCM can also be used to microdissect and enrich proteinaceous (eg, fibrillar) deposits like amyloids. Amyloid deposition is defined by the presence of congo-red reactivity under polarized light, and its presence is pathognomonic for amyloidosis. However, various protein substrates can form the typical amyloid beta-sheets that react with congo-red, including immunoglobulin light chains secondary to hematological malignancies (AL amyloidosis) or serum amyloid A secondary to chronic inflammation in, for instance, rheumatoid arthritis (AA amyloidosis). Mollee et al. performed LCM on congo-red stained amyloid deposits from different organ sites, and could identify the amyloid-forming protein in 94% of their cases, including rare disease-specific variants (Mollee et al., 2016). Cells subpopulation-characteristics could also be detected with flow cytometry (Bernas et al., 2006; Chang & Hedley, 2012) whereas purified cells can further be analyzed with MS (Turiák et al., 2011). Flow cytometry has already shown potential in tissue proteomics to study levels of the proteins among mouse spleen dendritic cells subsets which were sorted according to CD8α or CD4 surface molecules (Luber et al., 2010). Label-free quantitative approach identified more than 5000 identified proteins to reveal differences in subset specific signaling pathways whereas $CD4^+$ and cDC were activated and $CD8\alpha^+$ lacked activation to certain viruses. Further, proteomic analysis of glioblastoma stem-like cells (GSC) which are thought to have significant role in tumor recurrence, identified antigens that induce tumor-specific T cell responses and might be important targets in future therapies (Rapp et al., 2017). Moreover, cell sorting was further downstreamed to single cell proteomics by combination of fluorescence-activated cell sorting (FACS) and nanoPOTS platform whereas 485 proteins were identified across the single-cell samples (Y Zhu, Clair, et al., 2018).

An application that can leave the architecture of tissues intact in order to acquire spatially important architecture is mass spectral imaging (MSI). The comprehensive overview by Vaysse et al describes the history of MSI (matrix-assisted laser desorption/ionization-mass spectrometry imaging [MALDI-MSI], secondary ion mass spectrometry-MSI, and desorption electrospray ionization-MSI) and places it in a future clinical context (McDonnell et al., 2012; Vaysse et al., 2017). Single-cell preparations for MS have also provided interesting results, although these techniques can be technically more challenging than, for instance, single-cell RNA sequencing (Peterson et al., 2017). Recent advances in single-cell separation techniques and molecular barcoding (Prakadan, Shalek, & Weitz, 2017) have unraveled complex interactions and heterogeneous responses among cell types upon stimulation (Satija & Shalek, 2014; Shalek et al., 2014; Tirosh et al., 2016). A detailed description of these novel techniques is outside the scope of the current review, but can be found elsewhere (Svensson, Vento-Tormo, & Teichmann, 2018).

III. METHODS TO PRESERVE AND STORE TISSUES

After removal, tissues could either be analyzed with proteomics and other molecular methods, pathology laboratory, or stored for future research. For storage, preservation is required to minimize enzymatic and chemical degradation and to protect the integrity of the molecular content (Young, Bermes, & Haverstick, 2008; Mukherjee et al., 2013). Samples must be kept in a stable environment to avoid degradation and thermally, mechanically, or chemically induced alterations (Riondino

et al., 2015). However, a lack of standard operating procedures (SOP) compatible with proteomic methodologies for tissue storage has led to heterogeneity in the quality of the samples and inconsistent research results (Morente et al., 2006). Variations in sample and data quality is an obvious concern to the community and have led to the establishment of the EU COST program, a pan-European initiative aimed to define the most important concerns and discuss how to resolve them.

For further analysis, tissues are most commonly preserved with FF or FFPE methods, or they might be optimal cutting temperature (OCT) embedded as FF tissues (vide infra).

A. FFPE Tissues-Formalin-Fixed Paraffin-Embedded

Formalin fixation and paraffin-embedding represents standard method for preservation of tissue specimens that has been routinely performed since the late 1800s. The objective is to prepare tissue to be stable for storage for long periods of time. FFPE tissues are regularly used for histopathological studies (Giusti & Lucacchini, 2013) and are usually fixed in a 10% aqueous solution of formalin, which is typically 3.7–4% formaldehyde, that contains methanol to prevent the conversion of formaldehyde to formic acid, and is buffered with phosphate salts (Nirmalan et al., 2008). Fixation time depends on the sample size, clinical timing, and protocol, and can range from 12 to 72 hr. After fixation, the tissue is rinsed in water and washed with a series of ethanol (EtOH) solutions of different concentrations (70%, 95%, and 100%) at room temperature. Before the tissue is placed in a mold with melted paraffin (at 60–65°C), EtOH is removed. After heating, the paraffin mold with tissue is allowed to cool down to form a "tissue block" (Canene-Adams, 2013). Although this preservation procedure has been used since 1893, there is yet no standard preparation method of FFPE tissues.

FFPE tissues are highly stable and can be stored for a long period of time at room temperature with no visible destruction of the microscopic structure (Addis et al., 2009; Wolff et al., 2011). Although storage at room temperature has the advantage that it is cost- and space-effective, it is not standardized. Notably, recent studies have demonstrated that the presence of endogenous or exogenous water might result in protein degradation (Xie et al., 2011b; Giusti & Lucacchini, 2013). Obviously, variations in humidity and temperature between storage repositories might influence the quality of preserved tissues stored in laboratories in different climates. Although FFPE tissues can be stored at room temperature to avoid costs and complications related to storage associated with FF preserved tissues discussed below, formalin fixation is known to lead to chemical modifications on proteins and cross-linking between proteins. Therefore, to avoid these effects, alternative fixation with EtOH has been examined. EtOH preservation and paraffin embedding of murine tissues allow long preservation of tissues at room temperature to produce high-quality histological sections without cross-linking molecular content (Chaurand et al., 2008).

The impact of formaldehyde-induced protein modifications and the potential benefit of FFPE tissues as a surrogate for the FF tissues in the last decade has led to numerous studies that examined equivalence of FF- and FFPE-preserved tissues. Most of them used paired FFPE and FF tissues (Geoui et al., 2010; Bell et al., 2011; Gámez-Pozo et al., 2012; Kojima et al., 2012; Y Zhang, Muller, et al., 2015) to evaluate similarities in retrieved proteins; to a lesser extent, paired FFPE- and OCT-embedded FF tissues were also reported in proteomic studies (Scicchitano et al., 2009; Nirmalan et al., 2011; Holfeld et al., 2018). Measurement of the overlap of so-called diagnostically relevant proteins in paired FF and FFPE nonalcoholic steatohepatitis (NASH) 10 μm thick human liver tissues revealed that archived specimens could potentially be used for biomarker discovery of NASH (Bell et al., 2011). The number of proteins identified in the FFPE tissues was reduced by just over half compared to the number identified in the matched FF tissues (718 in FF and 367 in FFPE tissues); however, 860 total identified proteins and 493 unique proteins (57%) were found in FF tissues and 142 (17%) in FFPE tissues. Importantly, six proteins identified as proteins with functions involved in the pathogenesis of NASH have been expressed at similar levels in both tissues led to the conclusion that FFPE liver tissues can be used for proteomic analysis and biomarker identification studies (Bell et al., 2011). In another study, healthy and nephroblastoma kidney tissues that used paired FF an FFPE tissues were investigated. Nephroblastoma (Wilms tumor) is the most frequent renal cancer in children. In a study that analyzed paired healthy and tumor FFPE tissues 1,367 proteins were detected in both types of preserved tissues, whereas 262 proteins were differentially expressed in FFPE tumor tissue compared to healthy FFPE tissue (Hammer et al., 2014).

1. Chemical Modifications of Proteins Induced by Formalin-Fixation

Due to its physicochemical properties and small size, formaldehyde rapidly penetrates through tissues and reacts with amino acid residues to cause chemical modifications and cross-linking. Cross-linking leads to the preservation of cell complexes that allows study of intermolecular interactions in their native condition. The recognition of formaldehyde-induced modifications remains a cumbersome task. In one case, chemical modification of proteins induced by formalin preservation was addressed with model peptides (Metz et al., 2004; Toews et al., 2008; Toews, Rogalski, & Kast, 2010; Tanca, Pagnozzi, & Addis, 2012) and small proteins (ie, insulin) (Metz et al., 2006). In order to detect possible modifications that might be influenced by the complex biological environment in tissues, it is important to conduct these studies on FFPE tissues. Formaldehyde-induced modifications studied in human kidney tissues revealed lysine methylation (+14 Da) as a major modification, methylene (+12 Da) and methylol (+30 Da) adducts were also found (Jiang et al., 2007; Y Zhang, Muller, et al., 2015). In the analysis of prostate cancer, lysyl formylation that originated from formalin fixation was present on 6.5% of identified peptides (Hood et al., 2005). In addition, stable intra- and inter-chain methylene bridges might be formed with amine, amide, guanidyl, phenol, imidazole, and indole groups of amino acids residues (Nirmalan et al., 2008), whereas other as yet uncharacterized modifications also might occur (Magdeldin & Yamamoto, 2012).

After penetrating into the cells in tissues, formaldehyde initially reacts with nucleophilic groups (ie, basic side-chains on proteins) to form methylol adducts with a mass increase of 30 Da. Further dehydration and elimination of water produces a Schiff base with a final mass increase of 12 Da. The methylene group of the Schiff base undergoes nucleophilic attack from a nearby amino acid to produce interprotein and intraprotein cross-links via a methylene carbon bridge ($–CH_2–$) with a mass shift of +12 Da. The presence of formaldehyde methylene carbon cross-links might

affect the protein's physicochemical properties, like molecular weight and isoelectric point (Magdeldin & Yamamoto, 2012). Zhang et al in a study of four paired glomeruli and three paired renal cortical samples of FF and FFPE tissues reported lysine methylation (+14 Da) as the most frequent modification induced by FFPE preservation. A minor increase in methylene (+12 Da) and methylol (+30 Da) adducts was found as well, and these modifications affected about 2–6% of all peptide mass spectra. Collected LCM glomerular cross-sections (approximately 1 mm^2) showed a total number of 2,084 proteins with a 67% overlap in proteins between examined tissues, of which 15% were unique proteins to FF tissues, and 18% to FFPE tissues (Y Zhang, Muller, et al., 2015).

Multiple comparative proteomic reports showed that the retrieved molecular information varied by extraction method, tissue type, and instrument, and made comparison of results between studies difficult (Hood et al., 2005; Geoui et al., 2010; Kojima et al., 2012; Mason, 2016). Because the lysine side chains are mostly involved in the reaction with formaldehyde, some studies reported the lysine (K) to arginine (R) terminal peptide ratio (K/R), as a way to evaluate and classify chemical variations found in FFPE tissues. This type of classification of tissue by modification is by no means straightforward, because in another study on colon adenoma tissue, a reduction in the K/R ratio was shown for FFPE vs FF tissues. However, no peptide modifications related to formalin-induced chemistry were detected (Sprung et al., 2009). Underrepresentation of lysine C-terminal peptides was also found in other mammalian studies (Tanca, Pagnozzi, Burrai, et al., 2012), murine tissues (Broeckx et al., 2016), and glycopeptides (Tian et al., 2009).

Other research has focused on the identification of biochemical modifications prior to fixation like phosphorylation of proteins (Ostasiewicz et al., 2010; Gámez-Pozo et al., 2012; Gündisch et al., 2012; Wakabayashi et al., 2014). Phosphoproteome analysis of Wakabayashi et al study revealed 1413 and 1197 unique phosphopeptides for FF and FFPE tissue, respectively. Their results showed a lower content of phosphopeptides with terminal lysines for mouse liver tissue, at 42.8% for FFPE and 49.7% for FF tissues to indicate modifications of the ε-amino groups of the lysine (Wakabayashi et al., 2014).

Only a small number of studies exist that compared OCT-embedded FF and FFPE tissues for their protein content. Scicchitano et al. (2009) investigated five paired LCM and five non-LCM rat liver tissues and found a slightly lower protein yield from non-LCM FFPE tissues. Moreover, similar types of proteins and signaling pathways were identified in FFPE and OCT-embedded FF samples with similar subcellular distribution of the proteins. Nirmalan and colleagues compared FFPE to OCT-embedded FF normal human renal tissues from five patients (Nirmalan et al., 2011). Overall, they found 350 proteins between the different samples, where 283 were from FFPE, and 268 from OCT-embedded FF tissues. The overlap in proteins was 201 common proteins (57%), where 82 unique proteins were from FFPE (23%) and 67 from OCT-embedded FF tissues (19%). The protein distribution at the sub-cellular localization and the molecular function profiles were once again found broadly similar in both tissues.

Overall, there has been a large effort in the community to compare proteomes between different tissue-storage methods and how these might affect protein modifications. Modification of amino acid residues during fixation to preserve tissue morphology has been shown to be significant followed by numerous studies that depicted proteome differences induced by fixation. Reports in the literature have shown diversity in types of the tissues and, sample sizes used to study proteome. Numerous protocols used in laboratories and lack of uniformity represent challenge to compare results accross studies. Establishment of the standarized procedures would be important factor to ensure consistency and contribute to communication of the developments between the researchers.

2. *Retrieval of Proteins from FFPE Tissues*

Although the mechanism of protein fixation with formalin is not completely elucidated, development of knowledge of protein recovery from FFPE and proteome analysis of FFPE tissues has made great progress (Tanca, Pagnozzi, & Addis, 2012; Shi et al., 2013). A successful method for protein extraction from FFPE tissues should remove formaldehyde-induced cross-links (ie, intrachain and interchain methylene bridges), but avoid induction of new chemical changes in proteins. Already in 1991, Shi, Key, & Kalra (1991) successfully analyzed FFPE tissue with an antigen retrieval (AR) method. Tissue specimens were heated to 100°C in a buffer solution that contained water or saturated lead thiocyanate or 1% zinc sulfate that enhanced immunoreactivity of antibodies. Later, Ikeda et al. (1998) optimized high-temperature incubation and obtained 121.5 μg proteins (approximately efficiency of protein extraction was 164.2 μg/mg of dry cancer tissue) from a 5 $mm^2 \times 50$ μm FFPE colorectal tumor tissue sample dissolved in radioimmunoprecipitation assay (RIPA) buffer (100°C, 20 min), followed by incubation at 60°C for 2 hr. Since then, heat-induced AR in the presence of various buffers has been frequently used for protein recovery from FFPE tissues. The most common buffers used are RIPA buffer, tris(hydroxymethyl)aminomethane HCl (Tris-HCl) that contains 0.1–4% sodium dodecyl sulfate (SDS), and ammonium bicarbonate (Crockett et al., 2005; Addis et al., 2009; Azimzadeh et al., 2010; Craven et al., 2013; Wisniewski, Ostasiewicz, & Mann, 2011; Wisniewski, Duś, & Mann, 2013).

The efficiency of different extraction protocols versus protein recovery from different FFPE tissues has been investigated many times. Typically, protein yields from FFPE tissues were compared to matched FF tissues. The main variables to optimize are buffers and incubation time because the tissues are typically fixed onto glass slides. Numerous publications have investigated optimization of the extraction process using various combinations of custom-made or commercial buffers (Scicchitano et al., 2009; Gámez-Pozo et al., 2011; Wolff et al., 2011; Vincenti & Murray, 2013; Lai & Schneider 2014; Luebker & Koepsell, 2016; Föll et al., 2018; Holfeld et al., 2018), for example, with addition of solutions such as citraconic anhydride (0.05%, pH 7.4) (Namimatsu, Ghazizadeh, & Sugisaki, 2005). Numerous other methods have included sample incubation at higher temperatures (eg, approximately 100°C) with a Tris-HCl buffer supplemented with SDS (Table 1). Variations in protein yield might be due to the sample type. For example, range of the protein recovery was illustrated by a study of skeletal muscle and liver tissue where differences in protein yield were significant (Addis et al., 2009). Results showed that, with 35 mg of each tissue (incubated in Tris-HCl, SDS, dithiothreitol (DTT) buffer at 100°C for 20 min, then 2 hr at 80°C), yields for skeletal muscle tissue were: 1.3 μg/mg of tissue (FF) and 5.2 μg/mg of tissue (FFPE); liver tissue: 5.9 μg/mg of tissue (FF) and 31.3 μg/

TABLE 1. Description of some protocols used for proteome analysis of the tissues.

Tissue	Comment(s)	Tissue preservation	Sample size	Extraction buffer	Author
Aorta					
Human	Investigation of combination of heat and temperature on protein extraction	FF, FFPE	20–60 mg (wet weight)	100 mM Tris-HCl (pH 8), 100 mM DTT with later addition of SDS (4%)	Fu, 2013
Brain					
Human	LCM of neurons from Alzheimer's disease patients. All methods revealed similar number of proteins	FFPE	0.5–10 mm^2; 8 μm thick	Method adapted from Alkhas et al. (2011) 100 mM NH_4HCO_3/ 20% ACN 95°C 1 hr, 65°C 2 hrSeveral protocols tested:1. 20 mM DTT 57°C 1 hr/50 mM IAA RT 45 min2. 0.2% Rapigest/ 20 mM DTT 57°C 1 hr/50 mM IAA RT 45 min3. RIPA buffer. In-gel digestion. 20 mM DTT 57°C 1 hr/50 mM IAA RT 45 min	Drummond, 2015
	Glioblastoma multiforme tumor. iTRAQ 8-plex. Profiling of phosphotyrosine phosphorylation-mediated signaling	FF (OCT and LN_2)	8 mg (wet weight tumor) equivalent to 800 μg peptide	8 M urea/1 mM sodium orthovanadate/0.1% NP-40/ protease and phosphatase inhibitors/10 mM DTT 56°C 45 min/50 mM IAA RT 1 hr	Johnson, 2014
Mouse	Enriched plasma membrane samples from fore- and hind-brain. Identification of 1213 proteins (81% membrane proteins), brain receptors (glutamate, GABA), calcium channel units and ATPase	FF	30 mg	2 M NaCl/10 mM HEPES/ NaOH/1 mM EDTA. Centrifugation 900,000*g* 15 min. Pellets re-extraction 0.1 M Na_2CO_3/1 mM EDTA (pH 11). Ice incubation 30 min/ centrifugation 900,000*g* (15 min). Pellets re-extraction 4 M urea/100 mM NaCl/10 mM HEPES/1 mM EDTA (pH 7.4). 4 mg/mL digitonin/2 M sucrose/ 10 mM HEPES/NaOH (pH 7.4). Centrifugation 213,000*g* (20 min)	Le, 2006
	Membrane proteins profiling. Removal of detergents using equilibration of desalting column with 8 M urea. Identification of neurotransmitter glutamate and	FF	20 mg	2 M NaCl/10 mM HEPES-NaOH (pH 7.4)/1 mM EDTA; centrifugation 16,000*g* (15 min). Pellet re-extracted 2× 0.1 M Na_2CO/1 mM EDTA (pH 11).	Nagaraj, 2008

TABLE 1. Continued

Tissue	Comment(s)	Tissue preservation	Sample size	Extraction buffer	Author
	GABA receptors			Incubation 30 min pellet washed with 4 M urea/100 mM NaCl/ 10 mM HEPES/NaOH/1 mM EDTA (pH 7). Pellet solubilized in 100 mM phosphate buffer containing: (a) 2% SDS, (b) 0.5% Triton X-100, or (c) 3.5% CHAPS	
	Preparation of the cell lysates in presence of high content of SDS. FASP method for protein extraction and digestion using 3000 and 10,000 filters	FF	50 mg	0.1 M Tris-HCl (pH 7.6)/20% SDS/1 M DTT incubated 95°C (3 min). Aliquots of 1 mg protein mixed with 8 M urea/MWCO Microcon Centrifugation 14,000*g* (40 min). Addition 8 M urea/ 0.1 M Tris-HCl (pH 8.5). Centrifugation. Addition 8 M urea/0.1 M Tris-HCl (pH 8.5)/ 50 mM IAA. Centrifugation. 2× 8 M urea/0.1 M Tris-HCl (pH 7.9).	Wisniewski, 2009
	Multiple enzymes (trypsin, chymotrypsin, Lys-C, Glu-C, Arg-C, and Asp-N) used for sample digestion. MED-FASP. Brain and liver analyzed. Enrichment of phosphopeptides on TiO_2. Largest number of peptides and proteins after digestion with trypsin and Lys-c	FF		0.1 M Tris-HCl (pH 7.6)/2% SDS/0.1 M DTT. Sonication and then centrifugation 16,100*g* (10 min). 8 M urea/0.1 M Tris-HCl (pH 8.5). Centrifugation 14,000*g* (15 min). 8 M urea/ 50 mM IAA, incubation 10 min. Washing with urea, followed by 40 mM NH_4HCO_3	Wisniewski, 2012
Rat	Comparison of MS compatible detergents for protein solubilization. Identification of GABA and glutamate receptors	FF	100 µg of brain cells lysate used for analysis	Brain homogenized in 0.32 M sucrose/4 mM HEPES followed by protein precipitation with MeOH/CHF; pellet resuspended in: (a) invitrosol, (b) Rapigest, and (c) PPS. Incubation 60°C (5 min), addition of remaining solvent (80% ACN or Tris-HCl) and sonication for 2 hr in water bath	Chen, 2008
	Analysis of brain, heart, kidney,	FFPE	6 µm section, 2–6 sections	Several protocols tested:(1) 0.2%	Shen, 2015

TABLE 1. Continued

Tissue	Comment(s)	Tissue preservation	Sample size	Extraction buffer	Author
	heart, lungs, and liver. Different protocols and different volumes of Zwittergent-containing buffers tested for protein extraction		used for sample preparation; LMD (1,000,000 μm^2)	Zwittergent 3–16/10 mM Tris/ 1 mM EDTA(2) UPX buffer(3) 100 mM Tris/100 mM DTT/4% SDS (pH 8);(4) 0.5% PEG20000/ 100 mM Tris/100 mM DTT/4% SDS (pH 8)(5) 8 M urea/2 M thiourea/65 mM DTT/83 mM Tris/4% CHAPSIncubation 100°C (20 min) then 60°C (2 hr). 20 mM DTT 37°C (60 min)/ 25 mM IAA RT 45 min. Centrifugation 21,000*g* (10 min). Transfer to MWCO filter (10k) and washing with 25 mM NH_4HCO_3	
Breast					
Human	Analysis also of the cervix and cervix cancer cells in lymph node, kidney, lung, and liver	FFPE	4–5 um sections; 375,000 μm^2 (approximately 2,700 cells)	SDS (0.01%, 0.1%, 0.4%, and 4%); 10 mM citric acid; Rapigest (0.01%, 0.1%, and 1%)	Longuespée, 2016
Colon					
Human	Influence of tissue storage materials on data quality. Provided colon proteins data set for future use	FF, FFPE	1–2 mm^3 biopsies size	Modified FASP; 12 mM SDC/ 12 mM SDS/300 mM Tris-HCl (pH 9). Incubation 95°C (10 min, for FFPE 60 min), sonication 10 min. 100 µg proteins corresponding volume transferred to YM-30kDa, centrifugation 14,000*g* (15 min). 12 mM TCEP 37°C (30 min)/ 50 mM ClAA 37°C (50 min).	Bennike, 2016
	MED-FASP. Fractionation of the peptides on-pipette tip-SAX columns. Application to adenoma samples	FFPE		0.1 M Tris-HCl (pH 8)/0.1 M DTT/0.5% PEG 20000/4% SDS, incubation 99°C. 8 M urea/ 0.1 mM Tris-HCl (pH 8.5), centrifugation 14,000*g* (15 min). 50 mM IAA (20 min). 2× washing with 8 M urea/0.1 mM Tris-HCl (pH 8.5) followed by 2× 50 mM 0.1 Tris-HCl (pH 8.5).	Wisniewski, 2013
	Also analysis of murine liver (FF	FFPE	10 µm thick	Several protocols tested:	Broeckx, 2016

TABLE 1. Continued

Tissue	Comment(s)	Tissue preservation	Sample size	Extraction buffer	Author
	and FFPE) and human colon (FFPE). Buffer 1 showed best extraction efficiency. Inspection of modifications introduced by cross-linking			(1) Adapted from Addis et al. (2009)20 mM Tris HCl/2% SDS/ 200 mM DTT/20% glycerol/1% protease inhibitor (pH 8.8) (2) Adapted from Jiang et al. (2007)40 mM Tris-HCl/6 M guanidine-HCl/65 mM DTT (pH 8.2) (3) Adapted from Crockett et al. (2005) RIPA buffer (pH 7.6) (4) Adapted from Crockett et al. (2005) RIPA buffer/5 mM DTT/ 0.2% Rapigest (pH 8) (5) Adapted from Hwang et al (2007)RIPA buffer/2% SDS (pH 8) (6) Adapted from Hwang et al (2007) (7) Adapted from Sprung et al. (2009) 100 mM NH_4HCO_3/30% ACN (pH 8.4)50% 100 mM NH_4HCO_3/50% TFE(8) Adapted from Addis et al. (2009)20 mM Tris HCl/0.5% SDS/1.5% CHAPS/200 mM DTT/10% glycerol (pH 8.8)Incubation 98°C (20 min), then 80°C (2 hr). Centrifugation 14,000*g* (30 min). In gel digestion	
Mouse					
	Isoelectric focusing of the peptides. Comparable number of proteins detected in FF and FFPE. Underrepresentation of K/R in FFPE	FF, FFPE	60 μm slice	100 mM NH_4HCO_3 (pH 8) with or without 1 mM EDTA or 100 mM pyridoxamine. Incubation 80°C (2 hr). Addition of TFE and 2× sonication (20 sec) and on ice incubation (30 sec). Incubation 60°C (1 hr). 10 mM TCEP/25 mM DTT 60°C (30 min) then 50 mM IAA RT (20 min)	Sprung, 2009

TABLE 1. Continued

Tissue	Comment(s)	Tissue preservation	Sample size	Extraction buffer	Author
Endometrium					
Human	Application on endometrial cancer. Investigation of peptide/protein recovery for different tissue amounts and trypsin to protein ratios	FFPE	8 μm thick	100 mM NH_4HCO_3/20% ACN. Incubation 95°C (1 hr), then 65°C (2 hr)	Alkhas, 2011
Heart					
Mouse	Comparison of gel-based and gel-free approaches. Buffer 5 yielded most proteins Alternation of the protein migration from the regions of expected M_w indicated presence of cross-linked protein complexes or protein degradation due to storage	FF, FFPE	20 μm thick, 80 mm^2	Several protocols tested: (1) Laemmli buffer with 2% SDS (2) 9 M urea/2% CHAPS/1% immobilized pH gradient buffer pH 3–10 NL/50 mM DTT (3) Buffer containing 0.2% Tween 20 (4) RIPA buffer (5) 20 mM Tris-HCl/2% SDS/1% β-octylglucosyde/200 mM DTT/200 mM glycineIncubation 100°C (20 min). Centrifugation 14,000*g* (30 min). Protein extract precipitation with 2 D clean up kit	Azimzadeh, 2010
Swine		FF	200–300 mg (approximately 2 mm^3)	(1) HEPES/50 mM NaF/0.25 mM Na_3VO_4/0.25 mM PMSF/2.5 mM EDTA/protease inhibitor cocktail (2) 25 mM NH_4HCO_3 with addition of (a) MasDes, (b) ProteaseMax, (c) Rapigest, (d) PPS silent surfactant, (e) octyl-β-glucopyranoside, (f) dodecyl-β-maltoside, (g) digitonin, and (h) SDS	Chang, 2015
Intestine					
Human	Also analysis of liver samples. Impact of preanalytical factors as procedural delay on protein and phosphoprotein levels. Analysis of biopsies and resections	FF, FFPE	5 × 5 × 5 mm	FF: EXB Plus/Complete protease inhibitor cocktail/PhosSTOP phosphatase inhibitors/kinase inhibitors (staurosporine, genistein). Centrifugation 12,500 rpm (5 min)	Gündisch, 2012

TABLE 1. Continued

Tissue	Comment(s)	Tissue preservation	Sample size	Extraction buffer	Author
				FFPE:Qproteome FFPE tissue kit	
Kidney					
Human	Comparison of FF and FFPE tissues for Wilms' tumor (nephroblastoma)	FFPE	10 × 10 mm, 10 μm thick	Adapted from Geoui et al. (2010) PEB/2% SDS/2% Tris. Homogenization, ice sonication. Heating 100°C (20 min), then 80°C (2 hr). Centrifugation 14,000*g* (15 min). Contaminats removal by MeOH-chloroform precipitation. Protein precipitate dissolved in 25 mM NH_4HCO_3/ 1% Rapigest. 50 mM DTT/ 10 mM IAA	Hammer, 2014
		FF		Homogenization in 8 M urea/2 M thiourea, sonication on ice. Centrifugation 16,000*g* (20 min). 5 μg proteins diluted in 20 mM NH_4HCO_3, then 2.5 mM DTT/ 10 mM IAA	
	Also analysis of lung, liver, and urinary bladder. Development of an integrated method for deparafinization and protein extraction in one tube using nontoxic solvents	FFPE	5 × 2.5 × 1 mm (50 mg slices)	100 mM NH_4HCO_3 (pH 8). Incubation 99°C (30 min), ice incubation (8 min). Centrifugation in Ultrafree-MC filter 3,500*g* (1 min). 2× extraction with 100 mM NH_4HCO_3 (pH 8), incubation 99°C (60 min), centrifugation 15,000*g* (10 min)	Lai, 2014
	Effect of tissue block age on data quality. Profiling of normal and renal cell carcinoma tissues	FFPE	10 μm thick, approximately 5 cm^2	62.5 mM Tris-HCl/4% SDS/10% glycerol/100 mM DTT. Incubation 105°C (45 min). Incubation on ice (5 min), shear DNA (optional). Centrifugation 10 min. FASP digestion	Craven, 2013
	Also analysis of lung tissues. Phosphopeptide enrichment using Fe(III) and Ga(III) based IMAC	FF, FFPE	FF: 10 μm thickFFPE: 7 μm thick	FF: TRIzol reagent, 6 M guanidine hydrochloride. Heating 95°C (10 min)FFPE: 7 μm thickFFPE (several protocols tested):FFPE: 7 μm thick	Gámez-Pozo, 2011

TABLE 1. Continued

Tissue	Comment(s)	Tissue preservation	Sample size	Extraction buffer	Author
				(1) 40 mM Tris, 2% SDS, (pH 8.2)FFPE: 7 μm thick (2) 40 mM Tris, 6 M Gnd-HCl (pH 8.2)FFPE: 7 μm thick (3) 30% ACN/100 mM ABC; FFPE PES from Agilent; Qproteome FFPE tissue Kit (Qiagen)	
Mouse	Chemical immobilization of proteins to beads via amino groups and proteolyzed release of the peptides. Comparison of OCT and noncontaminated samples and their quantification using iTRAQs	FF	…	RIPA buffer (100 mM sodium citrate/50 mM Na_2CO_3/1% NP-40, ice sonication (4 min). Buffer exchange with 40 mM Na-citrate/ 20 mM Na_2CO_3. 1 mg of protein captured on AminoLink resin. Washing steps/incubation, then centrifugation 2,000*g*. PBS/ 50 mM Na-cyanoborohydrate, incubation (4 hr), centrifugation (2,000*g*). Tris-HCl (pH 7.6)/ 50 mM Na-cyanoborohydrate, incubation (1 hr). Washing with PBS/1.5 M NaCl. 10 mM DTT/ 50 mM NH_4HCO_3 then 15 mM IAA/50 mM NH_4HCO_3	Shah, 2015
Liver					
Human	Comparison of direct tissue trypsiniztion (DT), FASP, and IS protocols for tissue processing. DT showed to be more depleted in membrane proteins and enriched in cytoskeleton, nucleolus, ER lumen, and mitochondrial matrix. IS showed higher abundance of membrane proteins, while intermediate results were obtained when FASP was used	FFPE	5 μm thick	Several protocols tested: (1) Direct tissue trypsinization: 50 mM NH_4HCO_3 incubation 99°C (60 min). 100 mM DTT/ 50 mM NH_4HCO_3 incubation 56°C (30 min), then 100 mM IAA incubation RT (20 min) (2) Protein extraction: 20 mM Tris-HCl (pH 8.8)/2% SDS/ 200 mM DTT, incubation 99°C (60 min). Centrifugation 16,000*g* (10 min). After protein extraction 2 protocols test ed:(a) FASP(b) 0.2% SDS,	Tanca, 2014

TABLE 1. Continued

Tissue	Comment(s)	Tissue preservation	Sample size	Extraction buffer	Author
				extract dispensed on detergent removal spin column, incubation 2 min, centrifugation 1,500*g* (2 min). 10 mM DTT/50 mM NH_4HCO_3 incubation 56°C (30 min), then 25 mM IAA incubation RT (20 min)	
Mouse	Combination of heat and pressure for protein extraction	FF, FFPE	10 μm thick, 750 μm thick	FF: (1) Homogenization in 50 mM Tris-HCl/2% SDS (pH 7). One protocol incubation on ice 2.5 hr. Second protocol 100°C 30 min, then 80°C 2 hr atmospheric pressure (2) Homogenization in 100 mM Tris-HCl/4% SDS (pH 8)/ 100 mM DTT. Incubation 95°C (3 min) atmospheric pressureFFPE: (1) Adapted from Shi et al. (2006)50 mM Tris-HCl/2% SDS (pH 7), sonication 3× 5 sec, split in 2 fractions. 1st fraction incubated 100°C (30 min), then 80°C (2 hr) atmospheric pressure (14.7 psi). 2nd fraction incubated 100°C (30 min), then 80°C (2 hr) elevated pressure (40 000 psi) (2) Adapted from Ostasiewicz et al. (2010)100 mM Tris-HCl/ 4% SDS (pH 8)/100 mM DTT. Sonication 3× 5 sec. One fraction incubated 95°C (1 hr). Second fraction incubated 95°C (1 hr) at elevated pressure (40 000 psi)	Fowler, 2012
	SILAC labeling and SAX peptide fractionation. Phosphopeptide enrichment and *N*-glycopeptide enrichment	fresh tissue/LN_2, FFPE	5 μm thick, 40 mm^2	0.1 M Tris-HCl (pH 8)/0.1 M DTT/4% SDS. Incubation 95°C (3 min), centrifugation 16,000*g* (10 min). FASP digestion.	Ostasiewicz, 2010
	All the tissue samples were taken	FF, FFPE		Several protocols	Jiang, 2007

TABLE 1. Continued

Tissue	Comment(s)	Tissue preservation	Sample size	Extraction buffer	Author
	from same mouse liver, does not say how large sections were			tested:FF:Guanidine-HCl/40 mM Tris-HCl/65 mM DTT (pH 8.2). Sonication 180 sec, centrifugation 25,000*g* (1 hr). Reduction/alkylationFFPE:(1) Guanidine-HCl/40 mM Tris-HCl/ 65 mM DTT (pH 8.2) (with or without heating at 100°C for 30 min)(2) 2% SDS/40 mM Tris (pH 8.2) (incubation at 100°C and 60°C)(3) Guanidine-HCl/ 40 mM Tris-HCl/65 mM DTT (pH 8.2) (heating at 100°C) and further addition of HCOOH and CNBr	
Rat	LCM and non-LCM of rat liver samples. Identification of atorvastatin-regulated proteins	FF, FFPE	7 μm thick, 7 cm × 3 cm (non-LCM) or 0.8 × 0.8 cm (LCM)	FF: 1 M Tris-HCl (pH 7.5)/2 M sucrose/0.5 M EDTA/1 M DTT/ protease inhibitor cocktail. Homogenization. 3× freeze/thaw cycles in dry ice. Centrifugation. 5 mM DTT 60°C (1 hr)/15 mM IAA RT (1 hr)FFPE:Liquid tissue buffer/ 0.5% Rapigest SF. Homogenization. 3× freeze/thaw cycles in dry ice. Incubation 95°C 90 min. Centrifugation. 5 mM DTT 60°C (1 hr)/15 mM IAA RT (1 hr)	Scicchitano, 2009
Sheep	Analysis of sheep muscle and human thyroid gland	FF, FFPE	FF: approximately 35 mg FFPE: 10 μm thick, 80 mm2	20 mM Tris-HCl (pH 8.8), 2% SDS, 200 mM DTT. Incubation 100°C (20 min), then 80°C (2 hr) while shaking. Centrifugation 15 min 12,000 g 4°C	Addis, 2009
Lung					
Rat	Analysis of native and decellularized lung scaffold	5 mg of nondecellularized		50 mM Tris-HCl/0.25% CHAPS/ 25 mM EDTA/3 M NaCl (pH	Hill, 2015

TABLE 1. Continued

Tissue	Comment(s)	Tissue preservation	Sample size	Extraction buffer	Author
		(native) and native lungs		7.4)/protease inhibitor. Centrifugation 15,000 rpm (15 min). Pellet extraction 2× 50 mM Tris-HCl/0.25% CHAPS/ 25 mM EDTA/3 M NaCl (pH 7.4)/protease inhibitor. 8 M urea/ 100 mM NH_4HCO_3/25 mM TCEP (pH 8) (30 min). Mixed ion exchange resin. 100 mM CNBr in 86% TFA to pellet overnight dark. Washed with H_2O. 3× speedvac. 8 M urea/ 100 mM/NH_4HCO_3/25 mM TCEP (pH 8)	
Mammary					
Canine	Comparison of FF and FFPE tissue. Identification of proteins overexpressed in tumor tissue compared with normal tissue	FF, FFPE	8 μm thick	2% SDS/0.2 M DTT/20 mM Tris-HCl (pH 8.8)	Tanca, 2012
Mesenchymal tumors					
Human	Influence of storage time on protein extraction	FFPE	10 μm thick, 100 mm^2	20 mM Tris-HCl/2% SDS. Incubation 100°C (20 min) then 60°C (2 hr). Supernatant dialyzed overnight in a dialysis cup at 4°C against 100 mM Tris-HCl (pH 8.2). Addition urea to final concentration of 8 M. Addition of DTT to final concentration of 10 mg/mL. Addition of IAA to final concentration of 20 mg/mL. Incubation 37°C (1 hr) in the dark. Eightfold dilution with 100 mM ammonium acetate (pH 8) to 10 mL	Balgley, 2009
Muscle					
Mouse		N/A		6 M guanidine-HCl/10 mM TCEP/40 mM 2-ClAA. Heating 5 min, sonication 15 min. Addition of 20 mM Tris-HCl (pH	Murgia, 2015

TABLE 1. Continued

Tissue	Comment(s)	Tissue preservation	Sample size	Extraction buffer	Author
				8.5)/10% ACN	
Pancreas					
Mouse, human	Comparison of FF and FFPE tissue. Comparison of pancreatic cancer tissue and healthy tissue	FF, FFPE	FF: 10 μm FFPE: 3 mm × 3 mm × 10 μm	FF: (1) Mammalian protein extraction reagent (2) QProteome FFPE tissue kitFFPE: QProteome FFPE Tissue Kit	Kojima, 2012
Renal					
Human	Paired cancer and noncancer tissue. Identification of potential biomarkers for renal cell carcinoma	FF	15–25 mg	FASP	Atrih, 2014
Skin					
Human	Several washing protocols for removal of salts, lipids, and phospholipids tested	FF	12 μm thick, approximately 8 mm^2	Different tissue washing protocols tested:(1) 2× 70% EtOH (60 sec), 100% EtOH (120 sec)(2) 70% EtOH (30 sec)/ 100% EtOH (30 sec)/Carnoy's fluid (120 sec)/100% EtOH (30 sec)/0.2% TFA (30 sec)/ 100% EtOH (30 sec)(3) 70% EtOH (30 sec)/100% EtOH (30 sec)/Carnoy's fluid (120 sec)/ 100% EtOH (30 sec)/0.2% TFA (30 sec)/100% EtOH (30 sec)(4) No washing(5) 75% EtOH (cold) (30 sec)/95% EtOH (cold) (30 sec)/chloroform (30 sec)(6) 70% EtOH (30 sec)/100% EtOH (30 sec)/H_2O (30 sec)/70% EtOH (30 sec)/100% EtOH (30 sec)(7) 70% EtOH (30 sec)/100% EtOH (30 sec)/H_2O/70% EtOH (30 sec)/100% EtOH (30 sec)	Enthaler, 2013

Abbreviations: ACN, acetonitrile; CHAPS, 3-((3-cholamidopropyl) dimethylammonio)-1-propanesulfonate; DTT, dithiothreitol; EDTA, ethylenediaminetetraacetic acid; EtOH, ethanol; FASP, filter-aided sample preparation; FFPE, formalin fixed paraffine embedded; HEPES, 4-(2-hydroxyethyl)-1-piperazineethanesulfonic acid; GABA, γ-minobutyric acid; Gnd-HCl, guanidine hydrochloride: IAM, iodoacetamide; LCM, laser capture microdissection; MED, multienzyme digestion; MWCO, molecular weight cut-off; OCT, optimal cutting temperature; PEG, polyethylene glycol; ProteaseMAX, sodium 3-((1-(furan-2-yl)undecyloxy)-carbonylamino)propane-1-sulfonate; RIPA, radioimmunoprecipitation assay; SAX, strong anion exchange; SDC, sodium deoxycholate; SDS, sodium dodecyl sulfate; TFA, trifluoro acetic acid; TCEP ,tris(2-carboxyethyl)phosphine; TFE, 2,2,2-trifluoroethanol.

mg of tissue (FFPE). Interestingly, the highest yields (>80%) were found in a study with tissue surrogates to evaluate influence of pH, detergents, denaturants, reducing agents, and temperature with three different types of buffers: Tris-HCl (at pH 4.0, 6.0, and 9.0, with/without SDS, glycine, or β-mercaptoethanol [BME]), Gnd-HCl with BME, and citraconic anhydride (pH 2.0). The highest yields were observed (>80%) with Tris-HCl, SDS, and citraconic anhydride solution, at 100°C for 20 min, followed by incubation at 60°C for 2 hr. Furthermore, they concluded that the best protein recovery was achieved with various combinations of heat, detergent, and protein denaturant, but the use of reducing reagents did not improve recovery (Fowler et al., 2007).

Tris-HCl is one of the most widely used buffers for protein extraction. Additives, protein-retrieval procedures, and sample size and type have been the main differences among methods used for sample processing. Kawashima et al. (2014) examined the effect of buffer concentration on protein recovery, and whereas most experiments used a Tris-HCl concentration in the range 20–100 mM (Table 2), evaluation of the extraction efficiency on mouse liver tissue showed that an increase in Tris-HCl concentration beyond this range promoted protein extraction that plateaued at 300 mM Tris-HCl. FFPE tissue sections have also been studied with direct on-tissue digestion, where enzymes are directly sprayed onto the tissue surface to enable subsequent analysis of released peptides or glycans (Wisztorski et al., 2013; Heijs et al., 2016). Glycans have diverse biological functions and are important node to understand cancer mechanism and seek for therapeutic targets (Pinho & Reis, 2015). Imaging of glycans is a new emerging field and recently it was pioneered for resolving spatial distribution and depiction of *N*-glycans in brain (Powers et al., 2013; Eshghi et al., 2014), breast (Scott et al., 2019), renal, and hepatocellular carcinoma (Powers et al., 2015). Holst et al. (2016) in their work on leiomyosarcoma reported on-tissue linkage-specific sialic acid derivatization applied on FFPE tissue sections which showed improved detection of sialylated *N*-glycans. Study on brain with *in situ* release with PNGase F enzyme on brain sections identified 42 *N*-linked glycans (30 were fucosylated, seven were nonfucosylated, and five were oligomannose glycans). Further results on the glioblastoma xenograft indicated 13 *N*-linked glycans with different expression levels in tumor and normal brain tissue with low-abundance glycans in tumor being more fucosylated (Eshghi et al., 2014).

Although we focus here on protein extraction and digestion from the sample, other pre-analytical factors such as size and origin of sample, fixation time, temperature and storage conditions might also affect the outcome as judged by number of identified peptides and proteins and some of these elements have been discussed in details elsewhere (Thompson et al., 2013; Broeckx et al., 2016). Experiments need to be carefully planned with special attention to the choice of sample (sub)groups and numbers. Moreover, analytical methods used for these experiments must be validated with respect to the type of the samples analyzed, including sample amount, origin and instrument used for detection.

B. FF Tissues

The lack of complications produced by chemical fixation discussed above makes FF tissues the preferred material to study molecular diagnostics, such as cancer. When material is limited, however, tissue morphology primarily drives the choice to only fixate material with FFPE.

FF tissues are obtained with snap freezing in liquid nitrogen or in a mixture of dry ice and alcohol. Preservation with freezing has the advantage that it is fast and circumvents the molecular changes induced by FFPE processes (Mukherjee et al., 2013). After freezing, tissue samples are usually cut into sections of about 6 to 12 μm thick with a cryostat microtome. Tissue preservation by freezing has been regulated since 2006 by the European Human Frozen Tumor Tissue Bank (TuBa-Frost) with regard to collection, storage, retrieval, and tracking of tissues (Morente et al., 2006). As a result of standard protocols, translational research can be facilitated to avoid intrinsic bias of frozen tissues. Briefly, the collected tissues are placed in labeled sterile containers and transported on ice to the histopathology department. After the pathologist has taken representative parts for routine diagnosis (ie, 0.5 cm^3), the remaining tissue is directly frozen, or embedded in OCT medium and frozen. For best results, tissues should be frozen within 30 min of excision; however, when a delay up to 2 hr occurs, tissues should be still preserved and the interval of time recorded in the database (Morente et al., 2006).

Although free of the chemical modifications that occur with the FFPE process, freezing tissue has its own challenges because there is a chance that freezing artifacts might form. Artifacts might include accidental addition of a foreign substance or alteration in tissue structure. Comparison of freezing procedures on skeletal muscle tissue (Fig. 3) showed that the morphology was best preserved when isopentane was used. Besides the freezing medium, it was shown that formation of ice crystals can be due to various factors such as speed of the freezing process, excessive moisture within the tissue, or a freezing temperature (Chatterjee, 2014; Meng et al., 2014).

Frozen tissues are usually stored at low temperatures (−80°C) or in liquid nitrogen-cooled Dewar flasks (−196°C). Accordingly, the storage facilities should be provided with a back-up power system and appropriate alarms (eg, triple-layer alarm) to monitor and warn when the temperature warms. If an increase of more than 10% above the set temperature is detected, then a progressive series of alarms will be activated and changes automatically recorded in a database. The database should also be updated when samples are moved, issued, or depleted (Morente et al., 2006).

Numerous methods and approaches have been developed for tissue sampling, profiling and/or increasing protein recovery from frozen tissue all in order to elucidate biological processes and diseases mechanisms. Each tissue sample is of great value and inherently unique by time, location and patient. However, for minute tissue amounts (up to 20 μm thickness) the challenges are significant because they are more likely than larger tissue samples to produce a poor protein recovery due to physical losses during cutting and immobilization. Additionally, protein extraction and solubilization depend on physicochemical properties of the protein collection such as thermal stability, solubility, and proclivity to aggregate and/or degrade. In 2000, Corthals and colleagues first reported that the dynamic range of protein expression is a significant challenge in proteome analysis (Corthals et al., 2000). Although this report dealt with bacterial, yeast, and human cell lines, Corthals' and the broader community's efforts since then have focused on similar problems in tissues from patients.

In order to facilitate optimal analysis, additional steps like protein/peptide cleanup, purification, enrichment or a combination

TABLE 2. Comparison of protein yields identified in FFPE tissues using Tris-HCl buffer.

Extraction buffer	Sample type	Protein retrieval procedure	Sample size	Proteins	References
100 mM Tris-HCl, 4% SDS, 100 mM DTT, 0.5% PEG, pH 8.0	Colon	99°C, 1 hr (shaking)	250 nL of cells	9,700–10,500	Wisniewski et al. (2015)
20 mM Tris-HCl, 2% SDS, pH 9.0	Liver	100°C, 20 min; 60°C, 2 hrdialyzed overnight at 4°C	10 μm thick	4,098	Xu et al. (2008)
20 mM Tris-HCl, 2% SDS, pH 7.0 20 mM Tris-HCl, 2% SDS, pH 9.0	Kidney	100°C, 20 min; 60°C, 2 hr	10 μm thick	326 3,254	Shi et al. (2006)
20 mM Tris-HCl, 2% SDS, pH 9.0	Brain	100°C, 20 min; 60°C, 2 hr; dialyzed overnight at 4°C	100,000 cells	2,845	Guo et al. (2007)
62.5 mM Tris-HCl, 4% SDS, 100 mM DTT, 10% glycerol, pH 6.8	Kidney	105°C, 45 min; cooled on ice5 min	5 $cm^2$10 μm thick	2,266	Craven et al. (2013)
20 mM Tris-HCl, 2% SDS, pH 7.0	Nasopharynges	100°C, 20 min; 60°C, 2 hr	7 μm thick	730	Xiao et al. (2010)
20 mM Tris-HCl, 2% SDS, 200 mM DTT,200 mM glycine, 1% β-octylglucoside, pH 8.8	Heart	100°C, 20 min; 80°C, 2 hr (shaking)	80 mm^2 20 μm thick	192	Azimzadeh et al. (2010)
20 mM Tris-HCl, 2% SDS, 200 mM DTT, pH 8.8	Skeletal muscle liver	100°C, 20 min; 80°C, 2 hr (shaking)	35 mg	16.3 μg 86.8 μg	Addis et al. (2009)

Abbreviations: DTT, dithiothreitol; FFPE, formalin fixed paraffin embedded; PEG, polyethylene glycol; SDS, sodium dodecyl sulfate; Tris, tris(hydroxymethyl)aminomethane.

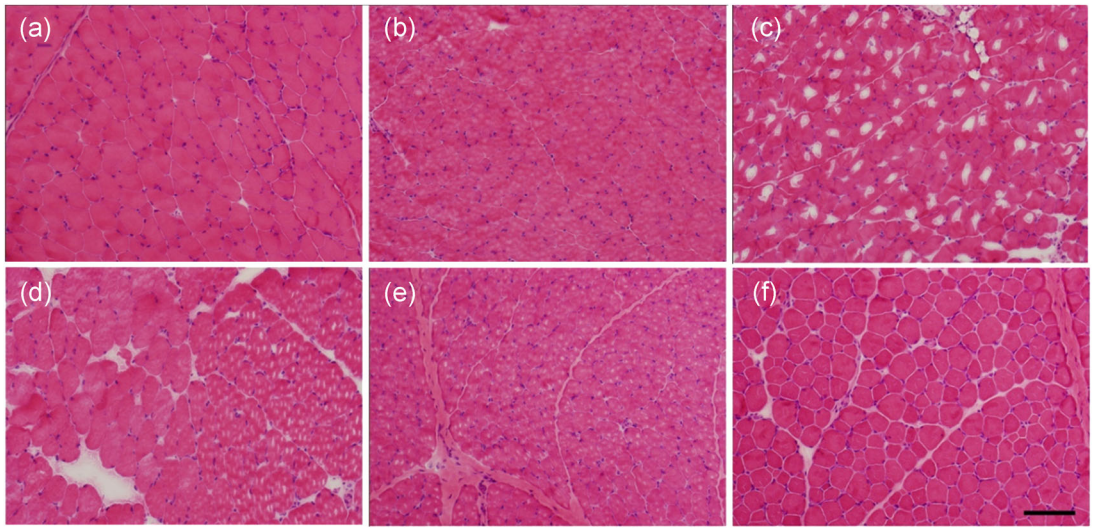

FIGURE 3. Formation of freezing artifacts after muscle preservation using different procedures: (a) isopentane-frozen muscle; (b) muscle frozen in isopentane and also in contact with OCT medium. Formation of the freezing artifacts also can be caused by liquid content of OCT; (c) muscle frozen at −80°C freezer and (d) muscle frozen in liquid nitrogen. Slow freezing procedure can cause formation of artifacts (c,d). Thawed and refrozen sample from OCT medium (e) showed improved intracellular morphology after represervation using method described (f). Reprinted with permission from Meng et al. (2014), copyright year 2014 (Journal of Visualized experiments). OCT, optimal cutting temperature. [Color figure can be viewed at wileyonlinelibrary.com]

of homogenization methods have been used (Butt & Coorssen, 2006; Bodzon-Kulakowska et al., 2007). Like proteins, lipids are pervasive in tissue samples but often require removal in order to facilitate optimal proteome analysis. Removal of lipids by washing specimens in butanol and heating at 95°C for 5 min produced improved protein recovery in a study of renal carcinoma FF tissues (Atrih et al., 2014) to allow discovery of 596 proteins that were differentially expressed between cancer and noncancer tissues. In addition, the detection of different molecular classes from the same tissue material or even region adds to the value in comparison to only one compound class analysis. Simultaneous analysis of glycosaminoglycans, *N*-glycans, and peptides were demonstrated for small tissue regions of bovine cerebral cortex in paired, FF, and FFPE tissues (Turiák et al., 2014). Samples were processed with microwave-assisted on-tissue digestion and, multiple enzymes were used to digest different compound classes. Multiple tissue spots analysis has an advantage to enable spatial comparison between tissue regions rather than simple analyses of bulk material.

Consequently, more studies have focused on microspotted arrays and *in situ* trypsin digestion of tissue, with some of the challenges described in a recent review (Cillero-Pastor & Heeren, 2014). MALDI-MSI has recently become very popular to characterize proteins digested *in situ* because of the preservation of protein spatial information (Groseclose et al., 2007). Here, though lower yields of the proteins compared to traditional extraction from the bulk solution have motivated further breakthrough of technologies to analyze proteins. For example, recent reports described incorporation of surfactants to improve yield (Djidja et al., 2009; Patel et al., 2015). Yet another approach that allows identification of proteins from discrete regions of the tissues is liquid extraction surface analysis (LESA). In LESA, a droplet of solvent is dispensed on a region of interest on tissue to thereby create a liquid microjunction between pipette tip and tissue from where soluble molecules are extracted. This extracted droplet, which contains proteins of interest, is subsequently reaspirated and further analyzed with traditional LC-MS/MS methods. LESA has also been combined with on-tissue digestion (Quanico et al., 2013) and top-down proteomics coupled to high-field asymmetric waveform ion mobility spectrometry (FAIMS) to analyze thin liver sections (Sarsby et al., 2015). Further, LESA-FAIMS-MSI was used in a study of mouse brain and liver tissue (Griffiths et al., 2016) whereas spatial tissue microextraction with subsequent MALDI-MSI detection was used to study bovine ocular lens, mouse brain and kidney tissue sections (Schey, Anderson, & Rose, 2013). Moreover, LESA sampling has been used on whole-body thin-tissue sections of drug-dosed mice to locate the distribution of drugs and drug-metabolite analysis (Kertesz & Van Berkel, 2010). Even though LESA shows low spatial resolution (0.5–1 mm^2), which is restricted by the size of the liquid droplet, its potential to couple to high-resolution mass analyzers gives it an advantage for use as a complementary approach to techniques like MALDI-MSI.

1. OCT Compound in FF Tissue Analysis

Use of cryopreservation media such as OCT-compound represents an alternative to snap freezing to preserve FF tissues. With OCT, tissue samples are cut in cubes, put in cryomolds, covered with an OCT compound, frozen in liquid nitrogen or isopentane/dry ice (−120°C) and stored at low temperature (−80°C or lower) (Micke et al., 2006; Scicchitano et al., 2009; Lim et al., 2010; Nirmalan et al., 2011; W Zhang, Sakashita, et al., 2015). The OCT compound, a viscous aqueous product that contains polyvinyl alcohol (PVA), benzalonium chloride (antifungal agent), and polyethylene glycol (PEG) surrounds the tissue without penetrating it (Young et al., 2008). In this way, molecular information and structural details are preserved,

sample dryness is prevented by freezing, and the samples can be easily cut in thin slices due to the regular-shaped tissue blocks (Weston & Hummon, 2013). Samples are usually cut into tissue sections (6 to 12 μm thick) with the same type cryostat microtome as used for FF tissues. However, the OCT compound must be removed before MS analysis because it will cause ion suppression and consecutively will limit the dynamic range of the analytes of interest (Enthaler et al., 2013; Weston & Hummon, 2013). In addition to ease of use, the OCT compound is soluble in polar solvents and can be removed by washing with water or water in combination with another polar solvent. For example, OCT from skin tissue samples (12 μm thick, approximately 8 mm^2) was removed by a tissue wash with different polar solvents that consisted of a gradient of EtOH concentrations, Carnoy's fluid (EtOH:chloroform:acetic acid, 6:3:1, vol/vol/vol) or H_2O with 0.2% trifluoroacetic acid to improve spectral quality and protein yield. Protein quantification with bicinchoninic acid assay showed that protein recovery in the washed tissues varied from 62 to 83% compared to the nonwashed samples (Enthaler et al., 2013) and the best protein recoveries were produced when tissues were washed with EtOH only or with cold EtOH and chloroform. These studies noted that wash protocols that included aqueous components produced higher protein losses, and that traces of OCT compound were still observed in the MALDI spectra. However, when aqueous-only wash steps were included (short dips of tissue in two different aqueous solution), there was complete removal of PEG from the samples (Fig. 4).

In another approach, efficiency of the OCT removal was investigated with protocols used commonly to remove detergents (Weston & Hummon, 2013). In these studies, colorectal cancer cell lines were embedded into OCT, and protocols to remove OCT included ether-methanol precipitation, filter-aided sample preparation (FASP), and SDS-PAGE purification. MALDI-MS spectra before removal of OCT contained predominant characteristic PEG ion series indicated by evenly spaced peaks with a difference of 44 *m/z*, whereas for all three methods after removal of OCT the mass spectra were free of PEG peaks. Further, after LC-MS/MS analysis, 3,307, 3,165, and 2,781 unique proteins were found when precipitation, FASP, and SDS-PAGE were used, respectively. The overall number of proteins was, 3,917 and the number of common proteins among the three methods was 2,305. The high degree of protein overlap (59%) and the low percentage of unique proteins per method (lower than 12%) demonstrated similarities among the methods. In other research, OCT removal after enzymatic digestion and quantification of glycoproteins was shown on prostate cancer samples (Tian, Bova, & Zhang, 2011). After protein digestion, OCT was removed with an SPE column after which *N*-linked glycopeptides were isolated with SPE of glycopeptides (SPEG) (Tian et al., 2007). Briefly, the glycosylated peptides were oxidized and coupled to a solid support, and nonglycopeptides were removed with successive washes. The amino-terminus of each glycopeptide was labeled, and *N*-linked glycopeptides were released with PNGase F digestion and analyzed with mass spectrometry. Results showed that glycosylation is retained in OCT-embedded tissues, and that 102 unique formerly *N*-linked glycopeptides that represented 79 unique glycoproteins were identified (Tian et al., 2011).

With regard to whole-proteome studies after removal of OCT, information is relatively scarce. One such publication reported the influence of OCT medium on proteome analysis in brain tumor samples of protein expression and phosphorylation-mediated signaling networks in paired FF and OCT-embedded FF tissues (Johnson & White, 2014). In this study, OCT-embedded frozen tissues were first rinsed with ice-cold PBS buffer to remove the OCT compound from the tissue. Subsequently, samples were mechanically homogenized on ice (Polytron homogenizer) in the presence of ice-cold urea (8 M) or ice-cold modified RIPA buffer that contained 1 mM sodium orthovanadate (Na_3VO_4, enzymes inhibitor), 0.1% NP-40 (lysis buffer containing NaCl and Tris HCl), and protease and phosphatase inhibitors. Quantification of the protein-expression profiles across the FF- and OCT-embedded FF samples identified 402 phosphotyrosine peptides and 1037 protein groups. These authors used hierarchical clustering and correlation analysis to show a high degree of similarity by between FF and OCT samples, which indicated that OCT-embedding did not significantly alter the protein expression and phosphorylation-mediated signaling networks.

IV. BIOCHEMICAL PROTOCOLS AND THEIR IMPACT ON THE PROTEOME DATA MATRIX

Protein extraction is a critical step in tissue-sample preparation with disparate goals to release proteins from cells and cells from tissues. Disruption of intra- and inter-protein interactions to solubilize proteins has a direct impact on the end-results that represents a formidable challenge. Therefore, extraction buffers contain various additives such as chaotropes, surfactants, or salts (Bodzon-Kulakowska et al., 2007), all with the goal to harvest proteins from their native environment in order to facilitate their solubilization.

Although various protocols have been reported for tissue analysis, it is unavoidable that some amount of each protein will be lost and, to reduce losses is critical with small amounts of tissue. To minimize loss of protein during sample transfer or detergent removal steps, methods that minimize transfer of the sample, sometimes called "single pot" methods have been pursued (Wang et al., 2005; Hughes et al., 2014; Kanshin & Thibault, 2014; Wang et al., 2005). Hughes et al. developed a method in which the entire preparation is carried out in a single tube, called single-pot solid-phase-enhanced sample preparation (SP3) (Hughes et al., 2014). The SP3 method is based on carboxylate-coated paramagnetic beads that use a hydrophilic layer on the magnetic beads developed via addition of organic solvent to the aqueous buffer. Proteins and peptides are attracted toward the hydrophilic layer of the magnetic beads, and contaminants are removed by a change in the composition of the buffer. A simple decrease in the organic component of the buffer and pH elutes proteins and peptides. SP3-clinical tissue proteomics was successfully applied to detect differential protein expression in ovarian tumor tissues (Hughes et al., 2016). Moreover, an in-stage tip technology was recently reported for very small sample analysis. This method also uses a single closed volume to minimize loss during sample processing, and although originally tested on Hela cells (Kulak et al., 2014), it was also applied to muscle-fiber tissue (Murgia et al., 2015).

A. Buffers, Chaotropes, and Salts

Most buffers for protein extraction maintain an alkaline pH that favors protein stability and is important during subsequent proteolytic digestion steps (Rabilloud, 1996). Control of the pH

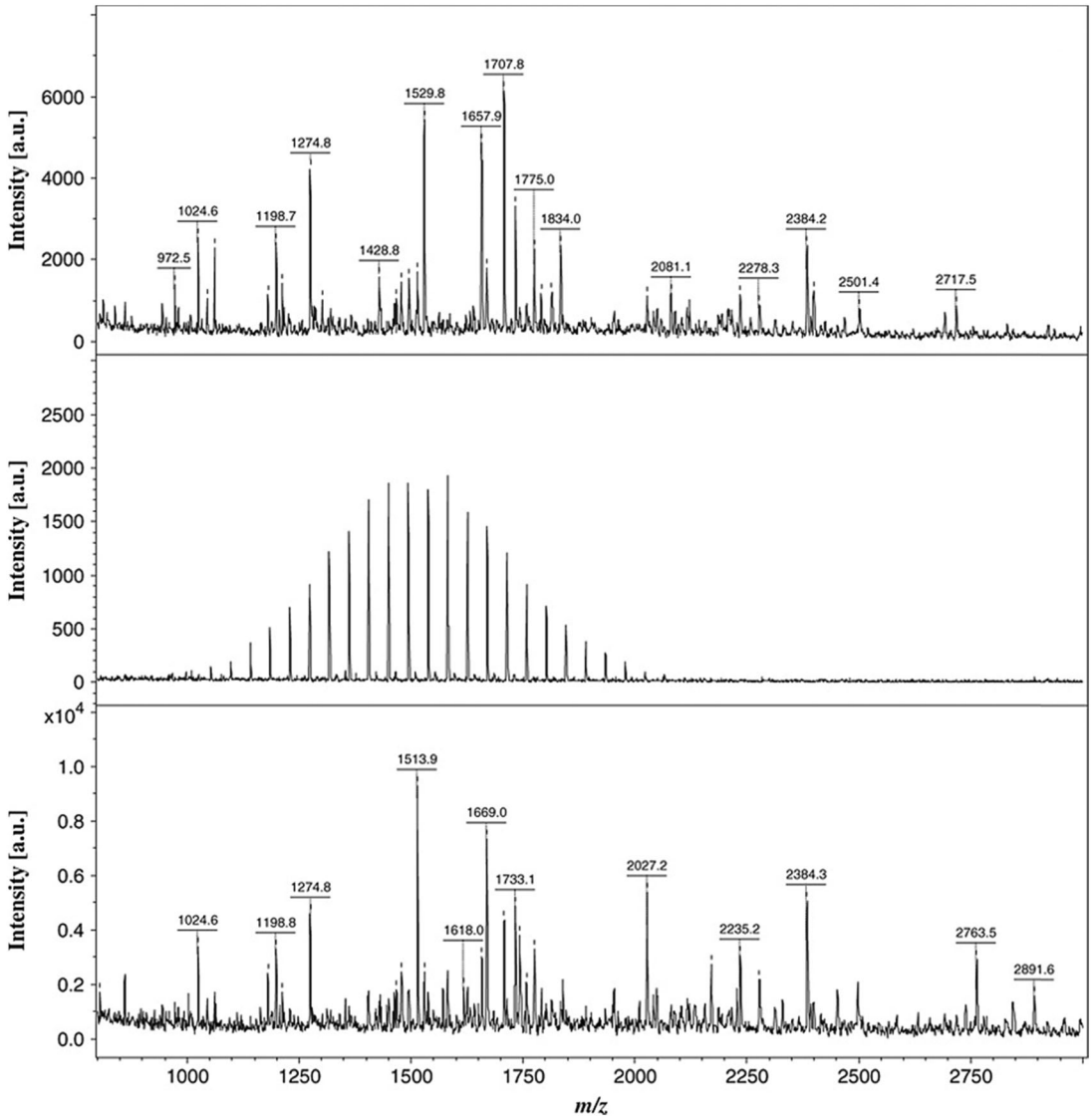

FIGURE 4. Influence of various on-tissue washing procedures on the recovered protein quantity and the quality of matrix-assisted laser desorption/ionization spectra. Tissue washing procedures as follows: (a) 70% EtOH (30 s), 100 EtOH (30 s), Carnoy's fluid (120 s), 100% EtOH (30 s), 0.2% TFA (dip-washing), 100% EtOH (30 s); (b) no washing; (c) 70% EtOH (30 s), 100 EtOH (30 s), deionized water (dip-washing), 70% EtOH (30 s), 100% EtOH (30 s). Middle-panel shows control with displayed PEG signal present compared to on-tissue digests after PEG removal with described aqueous washing protocols. Reprinted with permission from Enthaler et al. (2013), copyright year 2013 (John Wiley & Sons, Ltd.). EtOH, ethanol; PEG, polyethylene glycol; TFA, trifluoroacetic acid

in solution is defined by the buffering capacity (pH of approximately 0.5 units around pKa values). Commonly used buffers for protein extraction from tissues are NH_4HCO_3 (ammonium bicarbonate), 4-(2-hydroxyethyl)-1-piperazineethanesulfonic acid, RIPA buffer, and Tris/TrisHCl. Also, several commercial buffer solutions like Liquid Tissue MS Protein Prep Kit (Expression Pathology Inc) (Scicchitano et al., 2009; Vincenti & Murray 2013), EXB, and EXB Plus (Qproteome FFPE Tissue Kit from Qiagen) (Wolff et al., 2011; Yoshida et al., 2013), or FFPE PES (Agilent) (Gámez-Pozo et al., 2011) are used for protein extraction.

The addition of organic molecules into the buffers can significantly influence protein structure and stability. Due to the wide range of biophysical characteristics of the proteins and our limited knowledge on the solvent interaction during denaturation, the mechanism(s) that control or influence protein denaturation are not yet fully understood. However, denaturation might occur in one or more steps: for example, impact of a denaturant on the biomolecules themselves or alterations on the protein environment (by a solvent) can also affect protein stability and unfolding.

Urea is one of the most widely used denaturants to promote protein solubilization. Urea stabilizes the protein denatured state by hydrogen bonding to exposed polar moieties (ie, amide groups) of proteins and helps to uncover hydrophobic regions (Lim, Rosgen, & Englander, 2009). Urea has been successfully

used in extraction buffers for protein extraction from FF and FFPE tissues (Ronci et al., 2008; Bell et al., 2011; Rodríguez-Rigueiro et al., 2011; Dapic et al., 2017; Guo et al., 2007, 2015; Lai & Chen, 2015; Luebker & Koepsell, 2016; Dapic et al., 2017). However, heating samples with urea can lead to carbamylation of amino and sulfhydryl groups, and to chemical modification of lysine and arginine residues (Sun et al., 2014; Luebker, Wojtkiewicz, & Koepsell, 2015; Betancourt et al., 2018). These modifications might cause incomplete protein digestion and subsequently change of retention time, intensity, and masses of the modified peptides. Some of these chemical artifacts, like carbamylation caused by urea, can interfere with *in vivo* carbamylation, an important PTM associated with renal and cardiovascular diseases (Ok et al., 2005; Wang et al., 2007). In order to prevent modifications induced by urea, cyanate scavengers such as ammonium bicarbonate, methylamine, and Tris-HCl are often added to the extraction buffer (Lin et al., 2004; Sun et al., 2014).

Guanidine hydrochloride (GndHCl) can also be used for protein denaturation (Jiang et al., 2007; Önnerfjord et al., 2012; Yamamoto et al., 2016). Unlike urea, GndHCl denaturation is driven more by its ionic properties than urea, which is neutral. Gnd^+ can denature proteins in order to break salt bridges and competitive binding to carboxylate groups (Meuzelaar, Panman, & Woutersen, 2015). Given that urea and GndHCl use different mechanisms for protein denaturation, their choice should be based on the nature of the protein instead of treating them as analog (Monera, Kay, & Hodges, 1994). Chaotropes can also interfere with digestion, and it is known that the activity of trypsin is decreased in the presence of urea at a concentration higher than 4 M or GndHCl at a concentration higher than 0.1 M. Therefore, for proteases to work effectively, the concentration of chaotropes must be reduced before enzyme addition (Brownridge & Beynon, 2011). Protein extraction from FF tissues with GndHCl with no heating showed nearly an eightfold higher number of identified proteins than to FFPE tissues, 480 and 57, respectively. However, heating FFPE tissues for 30 min at 100°C in the presence of 40 mM Tris-HCl, 6 M guanidine HCl and 65 mM DTT gave results comparable to FF tissues (480 and 470 identified proteins with two unique peptides minimum, respectively) (Jiang et al., 2007).

Moreover, the presence of thiourea can increase solubility of hydrophobic and transmembrane proteins, and has been widely used in lysis buffers to extract of proteins from tissues in concentrations of up to 2 M (Ngoka, 2008; Fowler, O'Leary, & Mason, 2014; Luebker et al., 2015; Shen et al., 2015). Its importance has also been demonstrated in two-dimensional gel electrophoresis (2DGE), where it has been shown that inclusion of thiourea improved electrophoretic resolution.

Beside urea-based buffers, RIPA buffer is found to be efficient in cell and tissue lysis. It has several variants, but typically contains Tris-HCl, NaCl, NP-40, sodium deoxycholate (SDC), and SDS (Ngoka, 2008; Drummond et al., 2015). RIPA lysis buffer has been widely reported in tissue proteomic preparations with multiple variations in the basic ingredients; addition of protease and phosphatase inhibitors has also been used.

During cell lysis, many proteolytic enzymes can be excreted to give rise to artefactual modifications (eg, protein degradation). To minimize these biochemical reactions, inhibitors to inactivate proteases and phosphatases are often; selection of the most suitable methods should be tested for optimal results. Phosphatases and proteases bind reversibly or irreversibly to a protease and defend proteins from modifications during extraction. Inhibitors have specific targeting classes of compounds. To cover inadvertent proteolysis against a higher number of proteases, it is common to use "protease inhibitor cocktails" available for use in the form of solutions or tablets (Drummond et al., 2015). Although some cocktails inhibit serine and cysteine endopeptidases, others such as ethylenediaminetetraacetic acid (EDTA) operate through metal chelation and inhibit metaloproteases. However, to maintain the function and stability of metal-ion dependent proteins, EDTA-free inhibitor cocktails might also be used.

The choice of buffer can influence extracted classes of proteins. For example, the extraction of proteins from breast tissue with RIPA buffer followed by an additional extraction with an urea-based buffer revealed that these two buffers discriminated proteins according to their molecular weight (Ngoka, 2008). In this study, proteins extracted with urea had an approximately 12% higher molecular weight compared to proteins extracted with RIPA. Most of the extracellular matrix proteins were soluble in urea-based buffers, but insoluble in RIPA buffer. Protein solubility in any given buffer is influenced by several factors that contribute to the overall structure, including the mass and amino acid composition of the protein and the presence of hydrophobic regions and folds intrinsic in its tertiary structure. Gamez-Pozo et al. compared five protein-extraction protocols on non-small cell lung cancer 7 μm thick FFPE tissues (Gámez-Pozo et al., 2011). Protocols were based on extraction with three commonly used buffers: (1) 30% acetonitrile (ACN) in 100 mM NH_4HCO_3; (2) 40 mM Tris with 6 M GdnHCl; and (3) 40 mM Tris and 2% SDS. Two other protocols used commercial kits: (4) Qproteome and (5) FFPE PES. The SDS-based protocol (Protocol 3) yielded the highest amount of protein from FFPE tissues, followed by the commercial kit (Protocol 5) FFPE PES, which yielded 20% less. The ACN-NH_4HCO_3 buffer (Protocol 1) had the lowest yield in this study about 25% lower than Protocol 3, 40 mM Tris and 2% SDS.

Together with salts and chaotropes, the amount of organic solvent used is an important factor for protein denaturation. In an aqueous environment, hydrophilic protein domains become exposed to solvents, whereas with the addition of an organic solvent they tend to avoid exposure because proteins alter conformation. Conformation change results in interruption of ionic and hydrogen bonds that contribute to an "unraveling" of the functional protein "architecture." Another advantage of addition of organic solvent is that their removal is easy to accomplish through evaporation or lyophilization. Furthermore, the addition of an organic solvent can help to extract membrane proteins, because of their preference for organic-aqueous buffers compared to aqueous buffers (Blonder et al., 2002). Several studies have reported the addition of different organic solvents, such as ACN and methanol (MeOH), to extraction buffers, whereas addition of 2,2,2-trifluoroethanol (TFE) in range of 40–50% showed improved solubilization and separation of membrane proteins detected with isoelectric focusing (Deshusses et al., 2003). Different concentrations of organic solvents in a range of 20–80% ACN (Russell, Park, & Russell, 2001; Alkhas et al., 2011; Longuespée et al., 2016) have been found optimal in different reports. Large extent of organic solvents concentration suggests that the results of various buffers might be sample-specific. For example, Hervey et al. reported that 6 M GdnHCl and 80% ACN yielded a higher

number of peptides than 0.1% RapiGest (Hervey, Strader, & Hurst, 2008), and in another study on a yeast lysate the opposite trend was was attributed to a decrease of trypsin activity (Wall et al., 2011).

Addition of certain salts promotes protein solubility. Therefore, salts are often added to extraction buffers (Guo et al., 2007; GE Healthcare, 2010). Salts interrupt electrostatic forces formed by charged groups in proteins, and salts most often used in tissue analysis are KCl, NaCl, and Tris-HCl. The influence of salts on protein solubility can be estimated from the Hoffmeister (lyotropic) series. Ions at the end of the series have the most influence on protein stability. So-called salting-in ions weaken hydrophobic interactions and increase entropy of water and are used to solubilize proteins; by comparison, salting-out ions strengthen hydrophobic interactions and can be used for protein precipitation.

B. Surfactants

Surfactants (surface-active agents) or detergents are commonly used in sample preparation for protein extraction from tissues and cells. Surfactants can be classified as ionic, nonionic, or zwitterionic, and the invention of MS-compatible surfactants (acid-labile, thermo-labile) provided an effective way to overcome unwanted side effects during their removal from a sample.

Ionic surfactants are the most widely used because they have cationic- or anionic-charged head groups and a hydrophobic (SDS) or steroidal (SDC) backbone. They are very effective in protein solubilization and denaturation because they disrupt hydrophobic interactions; these structural characteristics allow them to make self-associated structures (ie, micelles). Hydrophobic domains of proteins are surrounded by a hydrophobic backbone of surfactant to form protein-detergent micelles (Rabilloud, 1996; Speers & Wu 2007). The concentration of detergent needed to form micelles is called critical micelle concentration. The size and stability of a micelle can be controlled with surfactant hydrophobic chain length. SDS is a commonly used ionic detergent that very efficiently solubilizes hydrophobic and amphipathic membrane proteins. SDS, as an anionic detergent, binds to positively charged side chains of proteins to hamper aggregation. Although this beneficial steric effect will also limit availability of cleavage sites during proteolysis, it is mitigated by dilution to roughly 0.1% prior to digestion, however a wide range of concentrations (0.1–4%) of SDS have been used for lysis in tissue proteomics (Palmer-Toy et al., 2005; Gräntzdörffer et al., 2010; Craven et al., 2013; Dapic et al., 2017).

Even though SDS is so powerful for protein solubilization, it is an MS-incompatible chemical that reduces peptide detection and interferes with electrospray ionization, which is most commonly used to couple HPLC peptide separations with MS detection. Numerous methods such as protein precipitation with organic solvents or acids, surfactant precipitation, membrane filtration, strong-cation exchange, or electrophoretic techniques have been used to remove SDS prior to LC-MS analysis (Bereman, Egertson, & Maccoss, 2011). The most commonly used method is protein precipitation with acetone, which causes proteins to aggregate and form a pellet with surfactant retention in the supernatant. However, a drawback of this technique is that many proteins are difficult to solubilize afterward. Recently, it has been shown that protein recovery after acetone precipitation can be improved with ion-pairing by addition of salt (ie, NaCl) (Crowell, Wall, & Doucette, 2013). Besides acetone, other solvents used for detergent removal include ethyl acetate, methanol/chloroform, and trifluoroacetic acid (Yeung et al., 2008; Zhou et al., 2012; Leon et al., 2013; Kachuk, Stephen, & Doucette, 2015). Moreover, SDS can be removed with KCl precipitation through formation of a K-SDS precipitate. Another recently reported method used greather than or equal to 0.5% SDS for protein extraction, and in a later step, SDS was removed in the form of K-SDS precipitate (Zhou et al., 2012). This method was tested on mouse brain tissue, and showed a similar number of protein identifications compared to filter-aided sample preparation (FASP), TFE, and urea-based protocols; those indicated that SDS can be alternatively removed after peptides have been produced.

Molecular weight cut-off (MWCO) filters have also been described in tissue proteomics, and can be an effective way of contaminant elimination. Wisniewski et al. reported use of the FASP method (Wisniewski et al., 2009; Wiśniewski, 2016), which was pioneered by Manza et al. (Manza et al., 2005), on several tissue studies (Ostasiewicz et al., 2010; Wisniewski et al., 2011, 2015; Shen et al., 2015; Bennike et al., 2016; Dowling et al., 2016; Föll et al., 2018). Proteins were first solubilized in a 4% SDS solution and with exchange with urea buffer SDS was washed off the sample and proteins were captured on MWCO filter. This procedure was followed by enzymatic digestion, after which peptides were eluted in a final step while high-molecular-weight substances were retained on the filter to minimize interference. FASP was further extended to a so-called enhanced FASP (eFASP) (Liu et al., 2014) that was applied to analysis of *Escherichia coli* with 0.2% deoxycholic acid; reported an increase in trypsin activity was found for cytosolic and membrane proteins compared to the original FASP method. However, in another report, Nel et al. (2015) showed no significant difference with FASP or eFASP. Colorectal tissue samples processed with FASP and strong anion exchange (SAX) peptide fractionation revealed approximately 10,000 proteins to yield more than 2,000 proteins with significant modifications between normal (N), adenoma (A), and colon cancer (C) tissues (23% between N and A, 17.8% between A and C, and 21.6% between N and C) (Wisniewski et al., 2015). Also, in a FASP study of renal cell carcinoma, a total of 1761 identified proteins were identified, 596 were differentially expressed in cancer and noncancer samples (Atrih et al., 2014). Yet another variation, called *N*-glyco FASP, was developed to enrich glycopeptides after they were bonded to lectin-immobilization supports (Zielinska et al., 2010; Wiśniewski, Zielinska, & Mann, 2011). Use of multiple enzymes for protein digestion, multienzyme digestion-FASP (MED-FASP) applied on tissue lysates yielded an increase in protein identifications (Wiśniewski & Mann, 2012), while its improved version thiol-activated polyethylene glycol FASP enriched cysteine-containing peptides (Wisniewski & Pruś, 2015).

Drawbacks of SDS include ion suppression and incompatibility with enzymatic digestion, and resulted in development of alternative detergents to assist in protein extraction and denaturation. Proc et al. (2010) have reported that the ionic detergent SDC is a good alternative for SDS with a similar efficiency in denaturation, but easier to remove from plasma samples. SDC is a bile acid salt and a mild detergent that

contains a steroidal group that has a polar and apolar face rather than polar "head" and hydrophobic "tail" like SDS (Seddon, Curnow, & Booth, 2004). Comparison of protein extraction from mitochondrial samples with buffers that contained 5% SDC and 8 M urea showed that SDC yielded more identified proteins compared to urea alone (Leon et al., 2013).

Mild detergents like polyoxyethylene that are based on nonionic surfactants (Triton X-100, Brij, Tween) and alkyl-glycosides (*n*-dodecyl-β-D-maltoside, octyl-glucoside) have hydrophilic polar head groups that are not charged and a hydrophobic tail (Dong, Li, & Mo, 2013; Liu et al., 2015). For example, their head group might contain an alkylpolyethylene ether domain (Brij) or phenyl group (Triton X-100, NP-40). They are considered mild detergents because they disrupt lipid-lipid and protein-lipid associations rather than protein-protein interactions. Because they are considered to be nondenaturants, they are often used to isolate proteins in their biochemically active forms.

Moreover, zwitterionic compounds such as 3-((3-cholamidopropyl) dimethylammonio)-1-propanesulfonate (Wang et al., 2005; Hill et al., 2015) combine properties of ionic and nonionic detergents. As nonionic detergents, they interrupt protein-protein interactions, but do not possess a net charge and, therefore, lack electrophoretic mobility. Although they might be less effective in protein extraction than SDS, they can, however, be added to the buffer in order to complement protein extraction (Shen et al., 2015; Broeckx et al., 2016). Preference for buffer composition can also be tissue-dependent due to the diversity of proteins in various tissues. Shen et al. (2015) showed that zwittergent-containing buffers extracted more unique proteins and peptides for kidney and lung, whereas for brain a PEG20000-containing buffer was better compared to a urea-based buffer that extracted fewest proteins among those tested. Due to their chemistry, zwitterionic detergents solubilize proteins better than nonionic detergents, but are not as good as linear alkyl chain-containing compounds.

Alternatively, to minimize interference with ionization and to simplify sample processing, MS-compatible detergents were developed and tested on different tissue types (Norris, Porter, & Caprioli, 2003; Chen et al., 2007, 2008). Specifically, acid-labile surfactants contain functional moieties with a hydrophobic tail and hydrophilic head that can be separated by cleavage of an acid labile-bond at low pH (Table 3). Although in their intact form they are MS-incompatible, after hydrolysis at low pH they break down into noninterfering by-products. One example is sodium 3-((1-(furan-2-yl)undecyloxy)-carbonylamino)propane-1-sulfonate (ProteaseMAX), an anionic surfactant that contains a sulfonate group and is structurally similar to SDS, which allowed rapid digestion of membrane proteins like bacteriorhodopsin (Saveliev et al., 2013). ProteaseMAX under acidic conditions decomposes into two components: (1) a neutral
1-(furan-2-yl)undecan-1-ol and (2) a zwitterionic 3-aminopropane-1-sulfonic acid. This detergent also shows a concentration- and temperature-dependent degradation at neutral pH probably due to destabilization of the labile bond by furanyl group. Protocols can be optimized so that this type of surfactant can be degraded during digestion to eliminate the need for an additional degradation step. Several other acid-labile detergents such as RapiGest SF, Invitrosol, or MaSDeS have also been reported (Nomura et al., 2004; Chen et al., 2007; Y-H Chang, Gregorich, et al., 2015). The MasDes surfactant is structurally similar to SDS, and showed comparable efficiency to SDS to extract membrane proteins (Y-H Chang, Gregorich, et al., 2015). In addition, although several studies have reported a similar or higher protein-extraction efficiency of the MS-compatible detergents compared to SDS, their main disadvantage is their high cost (Chen et al., 2007; Waas et al., 2014).

Waas et al. compared several buffers that contained MS-compatible surfactants, namely Invitrosol, which is a PPS Silent Surfactant; Progenta, an anionic acid-labile surfactant; Progenta, a cationic acid-labile surfactant; ProteaseMax; and RapiGest SF (Waas et al., 2014). They showed that Progenta surfactants produced the largest number of identified transmembrane proteins. Among the chaotropes tested, GndHCl was preferable to urea for greater production of hydrophobic peptides while its combination with ACN was favored to increase sequence coverage of transmembrane proteins. GndHCl was also shown to have a solvent preference toward MS-compatible detergents. The combination of Rapigest and PPS detergents with Tris buffer showed an increase of 22.7% and 40.6% in protein identifications compared to their combination with 80% ACN (Chen et al., 2007). However, when IVS detergent was combined with Tris buffer, results showed a decrease of 30.4% in identified proteins compared to combination with 80% ACN.

C. Protein Digestion

In all bottom-up proteomic applications, proteins are proteolytically digested into highly complex mixtures of peptides that are further subjected to LC-MS/MS analysis. However, before digestion, additional steps include reduction of protein disulfide bonds to improve protease access and facilitate unfolding and subsequent alkylation to prevent reoxidation. Reagents for disulfide bond reduction between cysteine residues are commonly DTT, tris(2-carboxyethyl)phosphine, BME, or dithioerythritol.

Breakage of disulfide bonds leads to protein unfolding, which in turn improves solubility. DTT is the most commonly used reducing agent, and after formation of thiol groups is converted into cyclic disulfide (Hustoft et al., 2010). Subsequently, the thiol groups of the cysteine residues are alkylated to prevent the reformation of disulfide bonds. Alkylation is generally achieved by addition of iodoacetamide or iodoacetic acid (Rabilloud, 1996; Hustoft et al., 2010).

Currently, trypsin is considered the "gold standard" in protein proteolysis in all aspects of proteomics, including tissue proteomics (Palmer-Toy et al., 2005; Tanca et al., 2014; Luebker et al., 2015; Shah et al., 2015). However, to supplement digestion or increase protein coverage, sometimes other proteinases such as Lys-C (Le Bihan et al., 2006; Nagaraj et al., 2008; Wakabayashi et al., 2014) or chymotrypsin are used alone or in combination with trypsin. For example, trypsin has shown a lower cleavage efficiency toward lysine compared to arginine (Tsiatsiani & Heck, 2015) and to increase cleavage efficiency, trypsin can be combined with Lys-C, which cleaves at the carboxyl site of lysine residues. Another advantage of Lys-C is that it has activity in the same pH range as trypsin and can be used with urea concentrations already present for denaturation (6–8 M); however for trypsin digestion urea needs to be diluted to <2 M (Klammer & MacCoss, 2006).

TABLE 3. Overview of selection acid-labile detergents and their decomposition products after acidification.

Detergent names	Detergent	Concentration (%)	Sample	References
ProteaseMAX	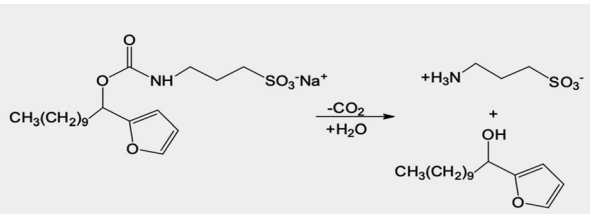	0.01	Model proteins	Saveliev et al. (2013)
		0.05, 0.1	Membrane pellet	Waas et al. (2014)
		0.05	Kidney, lung scaffolds	Nakayama et al. (2013)
Rapigest	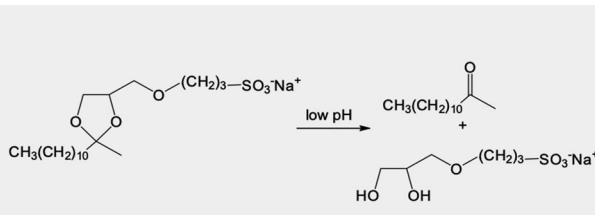	0.5	FFPE rat liver tissue	Scicchitano et al. (2009)
		0.2	Neuronal tissue	Drummond et al. (2015)
		0.1	Different cancer FFPE tissues	Longuespée et al. (2016)
MasDes	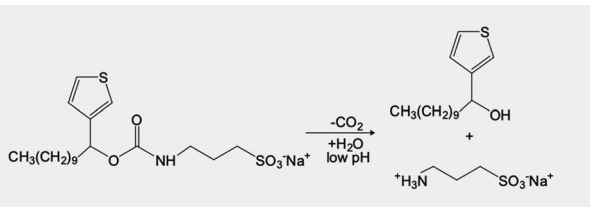	0.2	Snap frozen swine tissues	Y-H Chang, Gregorich, et al. (2015)
		0.1–0.5	Heart, liver, lung	Y-H Chang, Ye et al. (2015)
PPS Silent	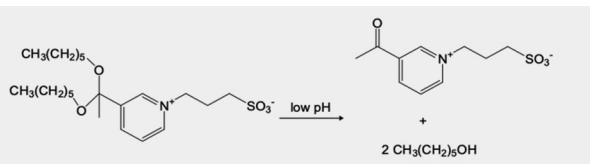	1	Rat brain	Chen et al. (2008)

Abbreviations: FFPE, formalin-fixed paraffin embedded; ProteaseMAX, sodium 3-((1-(furan-2-yl)undecyloxy)-carbonylamino)propane-1-sulfonate

More specifically, trypsin belongs to the serine protease S1, family and catalyzes hydrolysis of a peptide bond in two steps. The binding pocket of trypsin has an aspartate residue in the binding cleft to allow basic amino acids that are protonated at low pH to bind. However, in practice, only amino acids with long basic side chains, such as lysine and arginine, will make a stable salt bridge with aspartate that lasts long enough for cleavage to occur (Polgár, 2005).

Lysine and arginine are two of the most abundant amino acids in the human body; that fact led to the popularity of trypsin as a proteomic reagent. Furthermore, trypsin has an optimal activity at pH 7.5–8.5, and peptides produced by trypsin are typically a favorable length for tandem MS (Tsiatsiani & Heck, 2015). The quality of trypsin is an important factor in its use for digestion. Its susceptibility to autolysis and generation of fragments that interfere with sample analysis has been reduced with laboratory-modified trypsin that is highly resistant to autocatalytic reactions. Moreover, trypsin autolysis can be decreased by the addition of calcium ions when Ca^{2+} in natural concentration in samples is low (Hustoft et al., 2010). Several attempts have been carried out to improve the digestion efficiency. In 2015, Fang and co-workers tried to reduce the number of nonspecific trypsin cleavages and to investigate the effect of protein-to-trypsin ratio (Fang et al., 2015). They found that a higher ratio resulted in a higher number of nonspecific trypsin cleavages. Importance of protein-to-trypsin ratio might be explained by the fact that trypsin autolysis depends on concentration, because the higher chance that a trypsin encounters another trypsin molecule might result in a higher autolytic rate. However, eventhough trypsin has been dominantly used in proteomics so far, it also comes with limitations (ie generated peptides might be too short and not detected by MS), and therefore alternative proteases should be considered (Swaney, Wenger, & Coon, 2010; Tsiatsiani & Heck, 2015).

As alluded to above, the combination of trypsin and Lys-C can result in higher digestion efficiency and thus more identified proteins compared to use of trypsin alone. However, although multiple examples exist on use and comparison of multi-protease digestion on HeLa cell lines, *E. coli*, yeast and model proteins (Choudhary et al., 2003; Glatter et al., 2012; Chiva, Ortega, & Sabid, 2014; Guo et al., 2014; Cui et al., 2019; Morsa et al., 2019), information on methodological comparisons on complex samples such as tissues is limited. Biringer et al. demonstrated that a combination of the data of the digestion of cerebrospinal fluid with Glu-C, chymotrypsin, and trypsin resulted in an increase of sequence coverage for detected proteins (Biringer et al., 2006). In another report, digestion of 300 Duke's type C colorectal adenocarcinoma (DLD-1) cells showed a higher number of identified proteins with trypsin alone in comparison to chymotrypsin alone or a combination of trypsin and chymotrypsin (278, 104, and 173 respectively) (Chen, Yan, & Zhang, 2015). However, even though trypsin alone showed an advantage to identify most proteins, combination with chymotrypsin typically produced increased protein sequence coverage. Interestingly, decades ago trypsin was typically contaminated with chymotrypsin due to secretion together for digestion (Kostka & Carpenter, 1964). In later research, chymotrypsin activity was removed to create the pure version of trypsin we use today. Another possibility to use multi-enzyme digestion on tissue lysates is the aforementioned MED-FASP. The use of MED-FASP on brain and liver lysates with a two-step digestion process that combined Lys-C and trypsin showed a twofold increase in detected phosphorylation sites compared to trypsin digestion alone (Wiśniewski & Mann, 2012). MED with Lys-C, trypsin, and chymotrypsin confirmed their advantage over single enzyme digestion evidenced by increased number of peptides, proteins and increase in sequence coverage (Wiśniewski, Wegler, & Artursson, 2018). Another protease, Arg-C cleaves peptide bond at C-terminus of the arginine to generate longer peptides that contain basic residue and has been somewhat less used in proteomics compared to Lys-C. Alternatively, reversible- or irreversible-amine derivatization to block lysine residues might be used to utilize Arg-C like digestion with trypsin (Garcia et al., 2007; Wu et al., 2018). Further, proteases used for middle-down proteomics as Arg-C, Asp-N, and Glu-C can be used to reveal information about posttranslational modifications (PTMs) or protein isoforms, as that is in histones that have many isoforms, are lysine- and arginine-rich and generated tryptic peptides might be too short and difficult to detect (Arnaudo et al., 2011; Kalli, Sweredoski, & Hess, 2013). Convenience of MED to overcome limitations of trypsin to generate too short or too long peptides was also showed with pepsin, thermolysin and trypsin in study of *N*-glycosites in liver tissue. Generated *N*-glycopeptides were enriched with hydrazide chemistry and further processed with PNGase F. Only 20 *N*-glycosites were shared among proteases whereas 622 *N*-glycosites were identified with trypsin alone and additional 317 (33.7%) with pepsin and thermolysin which led to increased coverage of N-glycosilation sites (Chen et al., 2009). However, although multi-enzyme digestion has shown potential to increase sequence coverage and the number of identified proteins, it is not fully recognized as a standard protocol for proteomic analysis of tissue (Tsiatsiani & Heck, 2015).

Moreover, chemical digestion with various chemical agents as acid (ie, formic or acetic acid), cyanogen bromide (CNBr) or 2-nitro-5-thiobenzoic acid (NTCB) can also be used to cleave proteins, even though their use has been so far more applied on protein mixtures rather than tissues (Aiqun et al., 2001; Swatkoski et al., 2008; Srzentić et al., 2018). One of the most used reagents for chemical cleavage is CNBr that cleaves at methionine residues (Hill et al., 2015; Goddard et al., 2016; Sato et al., 2016), and also can be used in combination with trypsin to obtain smaller length peptides (Quach et al., 2003). Chemical digestion with CNBr prior to trypsin digestion showed advantageous to solubilize insoluble extracellular matrix (iECM) components as that is collagen in lung and liver (Hill et al., 2015; Goddard et al., 2016). However, drawbacks as toxicity of CNBr led to development of alternative methods as hydroxylamine (NH_2OH) for digestion of iECM components (Barrett et al., 2017). Further option for chemical digestion might be acid hydrolysis whereas peptides generated from the ribosomal proteins presented middle-mass range peptides (Cannon et al., 2010) that were longer and carried more basic residues compared to tryptic peptides (Swatkoski et al., 2008). In addition, most of the studies reported were focused on investigation of particular protein modifications or were restricted to some proteins (ie, individual proteins or complex proteins mixtures). Several reports have shown that chemical-mediated digestion could improve sequence coverage of the proteins, improve their solubilization, aid to cleavage efficiency and might be valuable step in a sample preparation protocol. However, systematic evaluation of

the digestion with small molecules compared to enzymatic proteolysis still needs to be investigated on larger number of tissue samples.

V. MECHANICAL AND PHYSICAL PROCEDURES TO FACILITATE PROTEIN RETRIEVAL FROM TISSUES

Use of buffers for chemical extraction of proteins from their natural environment is the most common sample treatment approach. However, proteins can also be extracted with physical procedures where mechanical or thermal external energy is used. Advantages of these methods is the possibility to shorten long-chemical extraction procedures, which might introduce unwanted side reactions, and to minimize adsorptive sample loss as well as to simplify sample preparation. Numerous physical methods such as mechanical, freeze-thaw, ultrasonication, or pressure can be used for cell disruption. Here, we discuss some of these methods on tissues and their recent applications. Ideally, optimization of one of these methods would lead to integration in tissue analysis for standard workflows in clinics.

A. Ultrasonication

Ultrasonication can be used as a fast and efficient method to extract proteins as well as to speed up protein digestion. Ultrasonication has proven successful in proteomic experiments for cell lysis and to facilitate protein digestion. The mechanism of ultrasound-assisted digestion of proteins is not completely understood; however, an important role is attributed to the increase in diffusion rates and temperature related to the cavitation phenomena. Cavitation occurs in liquids when pressure rapidly changes. This change in pressure causes air pockets or cavities to form as the bonds between water molecules are disrupted. The consequence of production of these microbubbles is a force strong enough to disrupt cellular architecture. When a cavitation bubble collapses near a solid-particle surface, the microjets of solvent can cause disruption and mechanical erosion of a structure. In this way, enzymes might also be brought closer to regions of interest (López-Ferrer, Capelo, & Vázquez, 2005) (Fig. 5a). High-intensity focused ultrasound (HIFU) can be used to accelerate protein digestion to a few minutes (López-Ferrer et al., 2005). In addition, HIFU has also proved to be a promising tool for regional treatment of tumors (Al-Bataineh, Jenne, & Huber, 2012), and has been applied for treatment of different organs and cancer types (Zhou, 2011; Xie et al., 2011a).

A variety of ultrasonic devices such as ultrasonic baths, ultrasonic probes, cup-horns, and sonoreactors can be used to provide ultrasonic energy (Santos & Capelo, 2007; Araujo et al., 2014). The possibility to produce ultrasonic energy also depends on the device used, and it has been shown that a slightly longer time is needed to digest α-lactabumin when a sonoreactor is used compared to an ultrasonic probe (Rial-Otero et al., 2007). However, the possibility to simultaneously process several samples with a sonoreactor can decrease the total time needed for analysis. Moreover, variables such as amplitude, sonication volume, and type of sample container can influence effectiveness of enzymatic digestion (Carreira et al., 2007).

Along with model proteins and cell lines, application of ultrasound energy has also been demonstrated on complex samples such as tissues. For example, Santos et al. sped up enzymatic digestion of liver tissue to 30 sec with an on-target ultrasonic approach (Santos et al., 2013). This group used glass slides coated with indium oxide used in MSI in conjunction with a sonoreactor for digestion. Short digestion times processed 20 samples in 5 min to improve the potential of the method for high-throughput applications. In another approach, Hansen et al. used a combination of ultrasound and surfactant-assisted digestion of extracellular matrix proteins, which are difficult to digest with standard methods (Hansen et al., 2009). Ultrasonication-facilitated digestion of Matrigel resulted in nearly 50% more identified proteins compared to a traditional digestion procedure. With ultrasound, they identified 248 proteins and increased sequence coverage for several proteins in rat mammary matrix, where perlecan, collagen α3, decorin, fibrillin 1, and fibronectin were among the top five identified proteins.

B. Pressure-Based Systems

Recently, it has been shown that elevated hydrostatic pressure can improve protein extraction and reduce the digestion time of proteins from complex biological samples (Tao et al., 2007; Yang et al., 2010; Freeman & Ivanov, 2011; Olszowy, Burns, & Ciborowski, 2013). This type of technology was shown to be suitable for protein extraction from biopsy-sized tissues and is known as a pressure-cycling technology (PCT). The technology uses cycles of hydrostatic pressure between ambient and ultra-high pressure, and promotes water penetration into the protein core to destabilizae the sample complexes and disassemble protein aggregates (Fig. 5b). Another advantage of PCT is extraction of proteins without the use of detergents in extraction buffers to thus simplify sample preparation and to make it potentially more compatible with LC-MS/MS analysis.

Moreover, it has been shown that heat-high pressure combinations improved protein extraction from FFPE tissues (Namimatsu et al., 2005; Fowler et al., 2012, 2014; Fu et al., 2013). Although pressure causes denaturation and stimulates water penetration, heat contributes to protein unfolding. Consequently, the combined effect of heat and high pressure facilitates the rehydration of cross-linked protein in FFPE tissue, and in reverses cross-links and protein solubilization. Fu et al. showed on aortic tissue samples that a combination of heat and elevated pressure increased protein yield 1.5-fold compared to heat only, and 8.3-fold compared to extraction at room temperature (Fu et al., 2013).

In the last several years, PCT systems have gained interest and are available as Barocycler technology (Rosenberger et al., 2014) or PCT-MicroPestle (Shao et al., 2016). The PCT approach has been successfully used with the sequential window acquisition of all theoretical spectra-MS, which is a mass spectrometric method that combines DIA with targeted data analysis. In the application of PCT for sample processing, results showed that applied pressure and pressure-cycle number played an important role. In one report, PCT-MicroPestle, mechanical tissue homogenizer significantly increased the amount of extracted proteins from liver, heart, and brain tissue compared to conventional PCT. The method was shown to be suitable for use on small amounts of tissue, whereas for extraction of proteins from large tissue samples (>10 mg), a defined volume of extraction buffer might be a limiting factor (Shao et al., 2016).

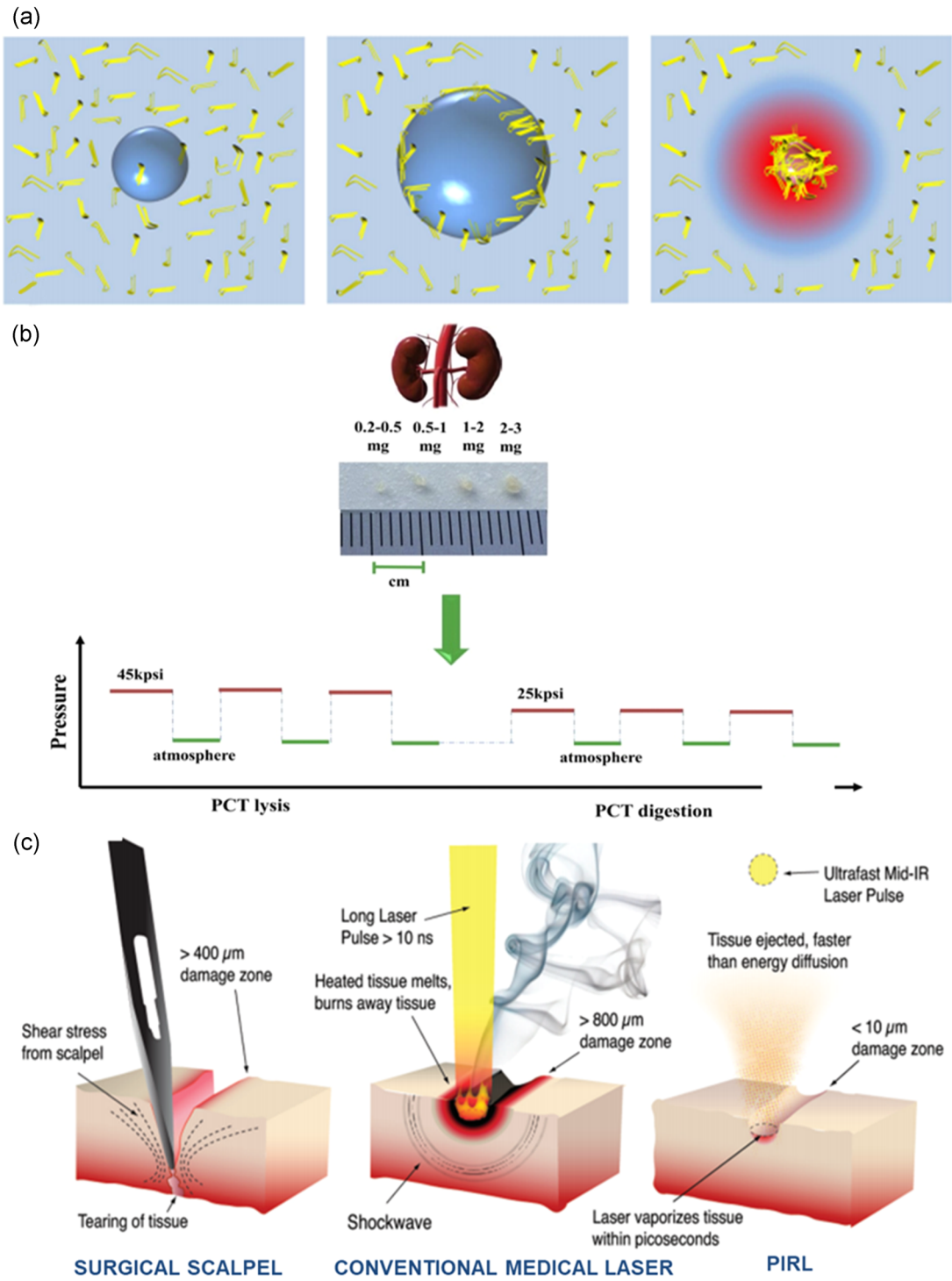

FIGURE 5. Overview of some physical methods for releasing proteins from human tissues. (a) Ultrasonication. Reproduced with permission from Nakajima et al. (2016) copyright year 2016 (Nature publishing group) (b) Pressure based systems. Reproduced with permission from Shao, Guo, & Aebersold (2015) copyright year 2015 (Elsevier). (c) Picosecond infrared laser. Reproduced with permission from (Amini-Nik et al. (2010) copyright year 2010 (PLoS ONE). [Color figure can be viewed at wileyonlinelibrary.com]

C. Picosecond infrared laser

Laser techniques are recognized as an important tool in surgery, and recently it was demonstrated that (picosecond infrared laser [PIRL]) could be used for ablation of tissues to minimize thermal damage of surrounding tissue areas. PIRL uses IR pulses that are tuned to resonate OH vibration stretch bands in water in the 3 μm wavelength range. Ultrafast relaxation of the vibrationally excited

OH bond can lead to energy transfer to translational motions, which are related to the ablation process of the local tissue (Fig. 5c).

Due to its high abundance in tissues, water is the most targeted compound. Under pulsed irradiation, water goes into a phase transition in an ultrafast explosive manner that leads to ablation of tissue. Pulse durations are one of the most important factors during laser treatment, and whereas microsecond or nanosecond lasers might cause surrounding tissue damage by leakage of deposited energy, picosecond lasers are the least invasive. As such, PIRL was recognized as a tool in laser surgery and for ablation of different tissue types such as corneal tissue (Linke et al., 2015), kidney (Zou et al., 2015), vocal folds (Böttcher et al., 2013; Hess et al., 2013), tooth enamel (Franjic et al., 2009) or skin (Jowett et al., 2013). Also, PIRL can extract intact proteins from biomaterials, and PIRL-LESI was used for molecular imaging of proteins, phospholipids and small molecules (Zou et al., 2015).

Recently, it was shown that PIRL with desorption by impulsive excitation (DIVE) can be used to extract proteins from tissues (Kwiatkowski et al., 2015). PIRL-DIVE generated aerosol from muscle tissue yielded nearly sixfold more proteins compared to a traditional mortar- and pestle-method of protein extraction. The ablation process was shown to be soft enough to extract proteins from tissue without any change in their chemical composition, and samples of human blood plasma were shown to have detectable enzymatic activities after sample treatment. PIRL-DIVE showed a high quality of tissue homogenate with a higher number of intact proteins and recovery compared to mechanical homogenization (Kwiatkowski et al., 2016).

VI. CONCLUSIONS AND FUTURE PERSPECTIVES

Sample preparation plays a major role in proteome discovery and is considered one of the most important steps in tissue analysis. Typical methods include several steps that consist of tissue lysis, digestion, instrumentation, and data analysis. One of the most important aspects of available analytical methods is to carry out analysis in a reproducible manner. However, this goal might be challenging when the amount of tissue available is limited. Thus, together with traditional approaches for tissue analysis, there has been a constant development in technologies to attempt to address analysis of small amounts of sample (eg, 1 to several dozen cells). Extensive manipulation of the sample often leads to adsorptive losses of proteins. Various methods have been suggested to avoid this problem: one is simply to try to directly detect proteins from tissues and avoid as many intermediate steps as possible. On-tissue digestion or FASP methods are good alternatives when one reduces the number of steps in sample preparation. Nanodroplet-processing platforms have extended proteome-profiling capabilities down to a dozen cells. Also, some novel technologies, such as microfluidic devices, have been developed to process small numbers of cells that might be integrated into standard nano-LC-MS workflows to provide opportunities to automate the entire process. These types of developments could eventually lead to high-throughput methods that would benefit clinicians and patients.

Today, considerable effort is dedicated to develope technologies that will address specific needs of proteome analysis for tissues. Pressure has been made to bridge the gap between the deep proteome profiling of small numbers of cells from clinical samples whereas to maintain demonstrated reproducibility and robustness of the methods. Further integration of the present-day technologies into clinical laboratories will bring opportunities for routine proteome detection from clinical samples. In this fashion, translation of results in a biological context together with pathologists' interpretations of proteomic data from tissue might lead to more precise protein biomarker discoveries. Moreover, a systematic integration of the acquired proteome and the interpretation together with pathological insights of patient-specific information might lead to improved patient treatment decisions.

ACKNOWLEDGMENT

This work was supported by the International Centre for Cancer Vaccine Science, carried out within the International Research Agendas program of the Foundation for Polish Science cofinanced by the European Union under the European Regional Development Fund. The authors also thank Dutch National Sectorplan Natuur-en Scheikunde (SNS-10.0119/D). J. Kers was financially supported by a grant from the Dutch Kidney Foundation (grant number 17OKG23).

ABBREVIATIONS

2DGE	two-dimensional gel electrophoresis
ACN	acetonitrile
AR	antigen retrieval
BME	β-mercaptoethanol
CHAPS	3-((3-cholamidopropyl) dimethylammonio)-1-propanesulfonate
CMC	critical micelle concentration
COST	European Cooperation in Science and Technology
CT	computer tomography
DDA	data dependent acquisition
DESI	desorption electrospray ionization
DIA	data independent acquisition
DIVE	desorption by impulsive excitation
DTE	dithioerythritol
DTT	dithiothreitol
EDTA	ethylenediaminetetraacetic acid
eFASP	enhanced FASP
EPPE	ethanol preservation and paraffine embedding
EtOH	ethanol
FAIMS	field asymmetric waveform ion mobility - spectrometry
FASP	filter aided sample preparation
FF	fresh frozen
FFPE	formaline fixed paraffine embedded
FNA	fine needle aspiration
H&E	hematoxylin and eosin stain
HEPES	4-(2-hydroxyethyl)-1-piperazineethanesulfonic acid
HIFU	high-intensity focused ultrasound
HPLC	high performance liquid chromatography
IAA	iodoacetamide
IEF	isoelectric focusing
IR	infrared
LC-MS /MS	liquid chromatography tandem mass spectrometry
LCM	laser capture microdissection

LESA	liquid extraction surface analysis
MALDI-MSI	matrix-assisted laser desorption/ionization-mass spectrometry imaging
MED-FASP	multienzyme digestion-FASP
MeOH	methanol
MWCO	molecular weight cut-off
NASH	nonalcoholic steatohepatitis
OCT	optimal cutting temperature
PCT	pressure cycling technology
PEG	polyethylene glycol
PIN	prostatic intraepithelial neoplasia
PIRL	picosecond infrared laser
PRM	parallel reaction monitoring
Protease MAX	sodium 3-((1-(furan-2-yl)undecyloxy)-carbonylamino)propane-1-sulfonate
PTM	posttranslational modification
PVA	polyvinyl alcohol
RIPA	radioimmunoprecipitation assay
RS	Reed-Stenberg
SAX	strong anion exchange
SDC	sodium deoxycholate
SDS	sodium dodecyl sulfate
SDS-PAGE	sodium dodecyl sulfate polyacrylamide gel electrophoresis
SIMS	secondary ion mass spectrometry
SOP	standard operating pocedure
SP3	single-pot solid-phase-enhanced sample preparation
SP3-CTP	SP3-clinical tissue proteomics
SPEG	solid-phase extraction of glycopeptides
SRM	single reaction monitoring
SWATH	sequential window acquisition of all theoretical spectra
TAPEG	thiol-activated polyethylene glycol
TCEP	tris(2-carboxyethyl)phosphine
TFA	trifluoro acetic acid
TFE	2,2,2-trifluoroethanol
Tris	tris(hydroxymethyl)aminomethane
TuBaFrost	European Human Frozen Tumour Tissue Bank

REFERENCES

Addis MF, Tanca A, Pagnozzi D, Crobu S, Fanciulli G, Cossu-Rocca P, Uzzau S. 2009. Generation of high-quality protein extracts from formalin-fixed, paraffin-embedded tissues. Proteomics 9(15):3815–3823.

Aiqun L, Sowder RC, I, Henderson LE, Moore SP, Garfinkel DJ, Fisher RJ. 2001. Chemical cleavage at aspartyl residues for protein identification. Anal Chem 73:5395–5402.

Al-Bataineh O, Jenne J, Huber P. 2012. Clinical and future applications of high intensity focused ultrasound in cancer. Cancer Treat Rev 38(5):346–353.

Alkhas A, Hood BL, Oliver K, Teng PN, Oliver J, Mitchell D, Hamilton CA, Maxwell GL. 2011. Standardization of a Sample Preparation and Analytical Workflow for Proteomics of Archival Endometrial Cancer Tissue. J Proteome Res 10(11): 5264–5271. https://doi.org/10.1021/pr2007736

Amini-Nik S, Kraemer D, Cowan ML, Gunaratne K, Nadesan P, Alman BA, Dwayne Miller RJ. 2010. Ultrafast Mid-IR Laser Scalpel: Protein Signals of the Fundamental Limits to Minimally Invasive Surgery. PLOS One 5(9): e13053. https://doi.org/10.1371/journal.pone.0013053

Araujo JE, Oliveira E, Kouvonen P, Corthals GL, Lodeiro C, Santos HM, Capelo JL. 2014. A journey through PROTEOSONICS. Talanta 121: 71–80.

Arnaudo AM, Molden RC, Garcia BA. 2011. Revealing histone variant induced changes via quantitative proteomics. Crit Rev Biochem Mol Biol 46(4):284–294.

Atrih A, Mudaliar MAV, Zakikhani P, Lamont DJ, Huang JT-J, Bray SE, Barton G, Fleming S, Nabi G. 2014. Quantitative proteomics in resected renal cancer tissue for biomarker discovery and profiling. Br J Cancer 110(6): 1622–1633.

Azimzadeh O, Barjaktarovic Z, Aubele M, Calzada-Wack J, Sarioglu H, Atkinson MJ, Tapio S. 2010. Formalin-fixed paraffin-embedded (FFPE) proteome analysis using gel-free and gel-based proteomics. J Proteome Res 9(9): 4710–4720.

Balluff B, Hanselmann M, Heeren RMA. 2017. Mass spectrometry imaging for the investigation of intratumor heterogeneity. Adv Cancer Res 134: 201–230.

Barrett AS, Wither MJ, Hill RC, Dzieciatkowska M, D'Alessandro A, Reisz JA, Hansen KC. 2017. Hydroxylamine chemical digestion for insoluble extracellular matrix characterization. J Proteome Res 16(11): 4177–4184.

Beavis RC, Chait BT, Podtelejnikov AV, Sagliocco F, Wilm M, Vorm O, Mortensen P, Boucherie H, Mann M. 1990. Rapid, sensitive analysis of protein mixtures by mass spectrometry. Proc Natl Acad Sci USA 87(17): 6873–6877.

Bell LN, Saxena R, Mattar SG, You J, Wang M, Chalasani N. 2011. Utility of formalin-fixed, paraffin-embedded liver biopsy specimens for global proteomic analysis in nonalcoholic steatohepatitis. Proteomics Clin Appl 5(7–8):397–404.

Bennike TB, Kastaniegaard K, Padurariu S, Gaihede M, Birkelund S, Andersen V, Stensballe A. 2016. Proteome stability analysis of snap frozen, RNAlater preserved, and formalin-fixed paraffin-embedded human colon mucosal biopsies. Data Br 6: 942–947.

Bereman MS, Egertson JD, Maccoss MJ. 2011. Comparison between procedures using SDS for shotgun proteomic analyses of complex samples. Proteomics 11(14):2931–2935.

Bernas T, Grégori G, Asem EK, Robinson JP. 2006. Integrating cytomics and proteomics. Mol Cell Proteomics 5(1):2–13.

Betancourt LH, Sanchez A, Pla I, Kuras M, Zhou Q, Andersson R, Marko-Varga G. 2018. Quantitative assessment of urea in-solution Lys-C/trypsin digestions reveals superior performance at room temperature over traditional proteolysis at 37°C. J Proteome Res 17(7): 2556–2561.

Binnig G, Huss R, Schmidt G. 2018. Tissue phenomics: Profiling cancer patients for treatment decisions. New York: Pan Stanford.

Biringer RG, Amato H, Harrington MG, Fonteh AN, Riggins JN, Hühmer AFR. 2006. Enhanced sequence coverage of proteins in human cerebrospinal fluid using multiple enzymatic digestion and linear ion trap LC-MS/MS. Brief Funct Genomic Proteomic 5(2):144–153.

Blonder J, Goshe MB, Moore RJ, Pasa-Tolic L, Masselon CD, Lipton MS, Smith R. 2002. Enrichment of integral membrane proteins for proteomic analysis using liquid chromatography-tandem mass spectrometry. J Proteome Res 1(4): 351–360.

Bodzon-Kulakowska A, Bierczynska-Krzysik A, Dylag T, Drabik A, Suder P, Noga M, Jarzebinska J, Silberring J. 2007. Methods for samples preparation in proteomic research. J Chromatogr B Analyt Technol Biomed Life Sci 849(1–2): 1–31.

Böttcher A, Clauditz TS, Knecht R, Kucher S, Wöllmer W, Wilczak W, Krötz P, Jowett N, Dalchow CV, Münscher A, Dwayne Miller RJ. 2013. A novel tool in laryngeal surgery: Preliminary results of the picosecond infrared laser. Laryngoscope 123(11): 2770–2775.

Broeckx V, Boonen K, Pringels L, Sagaert X, Prenen H, Landuyt B, Schoofs L, Maes E. 2016. Comparison of multiple protein extraction buffers for GeLC-MS/MS proteomic analysis of liver and colon formalin-fixed, paraffin-embedded tissues. Mol BioSyst 12(2): 553–565.

Brownridge P, Beynon RJ. 2011. The importance of the digest: proteolysis and absolute quantification in proteomics. Methods 54(4):351–360.

Buchberger AR, DeLaney K, Johnson J, Li L. 2018. Mass spectrometry imaging: A review of emerging advancements and future insights. Anal Chem 90(1):240–265.

Buckanovich RJ, Sasaroli D, O'Brien-Jenkins A, Botbyl J, Conejo-Garcia JR, Benencia F, Liotta LA, Gimotty PA, Coukos G. 2006. Use of immuno-LCM to identify the in situ expression profile of cellular constituents of the tumor microenvironment. Cancer Biol Ther 5(6): 635–642.

Butt RH, Coorssen JR. 2006. Pre-extraction sample handling by automated frozen disruption significantly improves subsequent proteomic analyses. J Proteome Res 5(2):437–448.

Canene-Adams K. 2013. Preparation of formalin-fixed paraffin-embedded tissue for immunohistochemistry. Methods Enzymol 533: 225–233.

Cannon J, Lohnes K, Wynne C, Wang Y, Edwards N, Fenselau C. 2010. High-throughput middle-down analysis using an orbitrap. J Proteome Res 9(8):3886–3890.

Cardoso F, van't Veer LJ, Bogaerts J, Slaets L, Viale G, Delaloge S, Pierga J-Y, Brain E, Causeret S, DeLorenzi M, Glas AM, Golfinopoulos V, Goulioti T, Knox S, Matos E, Meulemans B, Neijenhuis PA, Nitz U, Passalacqua R, Ravdin P, Rubio IT, Saghatchian M, Smilde TJ, Sotiriou C, Stork L, Straehle C, Thomas G, Thompson AM, van der Hoeven JM, Vuylsteke P, Bernards R, Tryfonidis K, Rutgers E, Piccart M. 2016. 70-gene signature as an aid to treatment decisions in early-stage breast cancer. N Engl J Med 375(8): 717–729.

Carreira RJ, Cordeiro FM, Moro AJ, Rivas MG, Rial-Otero R, Gaspar EM, Moura I, Capelo JL. 2007. New findings for in-gel digestion accelerated by high-intensity focused ultrasound for protein identification by matrix-assisted laser desorption ionization time-of-flight mass spectrometry. J Chromatogr A 1153(1–2): 291–299.

Chang Q, Hedley D. 2012. Emerging applications of flow cytometry in solid tumor biology. Methods 57(3):359–367.

Chang Q, Ornatsky OI, Siddiqui I, Loboda A, Baranov VI, Hedley DW. 2017. Imaging mass. Cytometry Cytom Part A 91(2):160–169.

Chang Y-H, Gregorich ZR, Chen AJ, Hwang L, Guner H, Yu D, Zhang J, Ge Y. 2015. New mass-spectrometry-compatible degradable surfactant for tissue proteomics. J Proteome Res 14(3): 1587–1599.

Chang Y-H, Ye L, Cai W, Lee Y, Guner H, Lee Y, Kamp TJ, Zhang J, Ge Y. 2015. Quantitative proteomics reveals differential regulation of protein expression in recipient myocardium after trilineage cardiovascular cell transplantation. Proteomics 15(15): 2560–2567.

Chatterjee S. 2014. Artefacts in histopathology. J Oral Maxillofac Pathol 18(suppl 1):S111–S116.

Chaurand P, Latham JC, Lane KB, Mobley JA, Polosukhin VV, Wirth PS, Nanney LB, Caprioli RM. 2008. Imaging mass spectrometry of intact proteins from alcohol-preserved tissue specimens: Bypassing formalin fixation. J Proteome Res 7(8): 3543–3555.

Chen EI, Cociorva D, Norris JL, Yates JR. 2007. Optimization of mass spectrometry-compatible surfactants for shotgun proteomics. J Proteome Res 6(7):2529–2538.

Chen EI, McClatchy D, Sung KP, Yates JR. 2008. Comparisons of mass spectrometry compatible surfactants for global analysis of the mammalian brain proteome. Anal Chem 80(22):8694–8701.

Chen Q, Yan G, Zhang X. 2015. Applying multiple proteases to direct digestion of hundred-scale cell samples for proteome analysis. Rapid Commun Mass Spectrom 29(15):1389–1394.

Chen R, Jiang X, Sun D, Han G, Wang F, Ye M, Wang L, Zou H. 2009. Glycoproteomics analysis of human liver tissue by combination of multiple enzyme digestion and hydrazide chemistry. J Proteome Res 8(2): 651–661.

Chiva C, Ortega M, Sabid E. 2014. Influence of the digestion technique, protease, and missed cleavage peptides in protein quantitation. J Proteome Res 13(9):3979–3986.

Choudhary G, Wu S-L, Shieh P, Hancock WS. 2003. Multiple enzymatic digestion for enhanced sequence coverage of proteins in complex proteomic mixtures using capillary LC with ion trap MS/MS. J Proteome Res 2(1):59–67.

Cillero-Pastor B, Heeren RMA. 2014. Matrix-assisted laser desorption ionization mass spectrometry imaging for peptide and protein analyses: A critical review of on-tissue digestion. J Proteome Res 13(2):325–335.

Corthals GL, Wasinger VC, Hochstrasser DF, Sanchez J-C. 2000. The dynamic range of protein expression: A challenge for proteomic research. Electrophoresis 21(6):1104–1115.

Craven RA, Cairns DA, Zougman A, Harnden P, Selby PJ, Banks RE. 2013. Proteomic analysis of formalin-fixed paraffin-embedded renal tissue samples by label-free MS: Assessment of overall technical variability and the impact of block age. Proteomics - Clin Appl 7(3-4):273–282.

Crockett DK, Lin Z, Vaughn CP, Lim MS, Elenitoba-Johnson KSJ. 2005. Identification of proteins from formalin-fixed paraffin-embedded cells by LC-MS/MS. Lab Invest 85(11):1405–1415.

Crowell AMJ, Wall MJ, Doucette AA. 2013. Maximizing recovery of water-soluble proteins through acetone precipitation. Anal Chim Acta 796: 48–54.

Cui C, Liu T, Chen T, Lu J, Casaren I, Lima DB, Carvalho PC, Beuve A, Li H. 2019. Comprehensive identification of protein disulfide bonds with pepsin/trypsin digestion, orbitrap HCD and spectrum identification machine. J Proteomics 198: 78–86.

Dapic I, Uwugiaren N, Jansen PJ, Corthals GL. 2017. Fast and simple protocols for mass spectrometry-based proteomics of small fresh frozen uterine tissue sections. Anal Chem 89(20):10769–10775.

Datta S, Malhotra L, Dickerson R, Chaffee S, Sen CK, Roy S. 2015. Laser capture microdissection: Big data from small samples. Histol Histopathol 30(11):1255–1269.

De Marchi T, Braakman RBH, Stingl C, van Duijn MM, Smid M, Foekens JA, Luider TM, Martens JWM, Umar A. 2016. The advantage of laser-capture microdissection over whole tissue analysis in proteomic profiling studies. Proteomics 16(10): 1474–1485.

Di Palma, S, & Bodenmiller, B. 2015. Unraveling cell populations in tumors by single-cell mass cytometry. Curr Opin Biotechnol, 31, 122–129.

Dilillo M, Ait-Belkacem R, Esteve C, Pellegrini D, Nicolardi S, Costa M, Vannini E, de Graaf EL, Caleo M, McDonnell LA. 2017. Ultra-high mass resolution MALDI imaging mass spectrometry of proteins and metabolites in a mouse model of glioblastoma. Sci Rep 7(1): 603.

Djidja MC, Francese S, Loadman PM, Sutton CW, Scriven P, Claude E, Snel MF, Franck J, Salzet M, Clench MR. 2009. Detergent addition to tryptic digests and ion mobility separation prior to MS/MS improves peptide yield and protein identification for in situ proteomic investigation of frozen and formalin-fixed paraffin-embedded adenocarcinoma tissue sections. Proteomics 9(10): 2750–2763.

Dong J, Li Y, Mo X. 2013. The study of a new detergent (octyl-glucopyranoside) for decellularizing porcine pericardium as tissue engineering scaffold. J Surg Res 183(1):56–67.

Dou M, Zhu Y, Liyu A, Liang Y, Chen J, Piehowski PD, Xu K, Zhao R, Moore RJ, Atkinson MA, Mathews CA, Qian W-J, Kelly RT. 2018. Nanowell-mediated two-dimensional liquid chromatography enables deep proteome profiling of. Chem Sci 9(34): 6944–6951.

Dowling P, Moran B, McAuley E, Meleady P, Henry M, Clynes M, McMenamin M, Leonard N, Monks M, Wynne B, Ormond P, Larkin A. 2016. Quantitative label-free mass spectrometry analysis of formalin-fixed, paraffin-embedded tissue representing the invasive cutaneous malignant melanoma proteome. Oncol Lett 12(5): 3296–3304.

Drummond ES, Nayak S, Ueberheide B, Wisniewski T. 2015. Proteomic analysis of neurons microdissected from formalin-fixed, paraffin-embedded Alzheimer's disease brain tissue. Sci Rep 5: 15456.

Edwards NJ, Oberti M, Thangudu RR, Cai S, McGarvey PB, Jacob S, Madhavan S, Ketchum KA. 2015. The CPTAC data portal: A resource for cancer proteomics research. J Proteome Res 14(6): 2707–2713.

Ellis MJ, Gillette M, Carr SA, Paulovich AG, Smith RD, Rodlans KK, Townsend RR, Kinsinger C, Mesri M, Rodriguez H, Liebler DC. 2013. Connecting genomic alterations to cancer biology with proteomics: The NCI Clinical Proteomic Tumor Analysis Consortium. Cancer Discov. 3(10): 1108–1112.

Enthaler B, Bussmann T, Pruns JK, Rapp C, Fischer M, Vietzke J-P. 2013. Influence of various on-tissue washing procedures on the entire protein quantity and the quality of matrix-assisted laser desorption/ionization spectra. Rapid Commun Mass Spectrom 27(8):878–884.

Eshghi ST, Yang S, Wang X, Shah P, Li X, Zhang H. 2014. Imaging of N-linked glycans from formalin-fixed paraffin-embedded tissue sections Using MALDI mass spectrometry. ACS Chem Biol 9(9):2149–2156.

Fang P, Liu M, Xue Y, Yao J, Zhang Y, Shen H, Yang P. 2015. Controlling nonspecific trypsin cleavages in LC-MS/MS-based shotgun proteomics using optimized experimental conditions. Analyst 140(22): 7613–7621.

Fend F, Emmert-Buck MR, Chuaqui R, Cole K, Lee J, Liotta LA, Raffeld M. 1999. Immuno-LCM: Laser capture microdissection of immunostained frozen sections for mRNA Analysis. Am J Pathol 154(1): 61–66.

Föll MC, Fahrner M, Oria VO, Kühs M, Biniossek ML, Werner M, Bronsert P, Schilling O. 2018. Reproducible proteomics sample preparation for single FFPE tissue slices using acid-labile surfactant and direct trypsinization. Clin Proteomics 15(1): 11.

Fowler CB, Cunningham RE, O'Leary TJ, Mason JT. 2007. "Tissue surrogates" as a model for archival formalin-fixed paraffin-embedded tissues. Lab Invest 87(8):836–846.

Fowler CB, O'Leary TJ, Mason JT. 2014. Improving the proteomic analysis of archival tissue by using pressure-assisted protein extraction: A mechanistic approach. J. Proteomics Bioinform. 7(6):151–157.

Fowler CB, Waybright TJ, Veenstra TD, OLeary TJ, Mason JT. 2012. Pressure-assisted protein extraction: A novel method for recovering proteins from archival tissue for proteomic analysis. J Proteome Res 11(4):2602–2608.

Franjic K, Cowan ML, Kraemer D, Miller RJD. 2009. Laser selective cutting of biological tissues by impulsive heat deposition through ultrafast vibrational excitations. Opt Express 17(25):22937.

Freeman E, Ivanov AR. 2011. Proteomics under pressure: Development of essential sample preparation techniques in proteomics using ultrahigh hydrostatic pressure. J Proteome Res 10(12):5536–5546.

Fu Z, Yan K, Rosenberg A, Jin Z, Crain B, Athas G, Heide RSV, Howard T, Everett AD, Herrington D, van Eyk JE. 2013. Improved protein extraction and protein identification from archival formalin-fixed paraffin-embedded human aortas. Proteomics-Clin Appl 7(3–4): 217–224.

Gámez-Pozo A, Sánchez-Navarro I, Calvo E, Agulló-Ortuño MT, López-Vacas R, Díaz E, Camafeita E, Nistal M, Madero R, Espinosa E, López JA, Vara JÁF. 2012. PTRF/Cavin-1 and MIF proteins are identified as non-small cell lung cancer biomarkers by label-free proteomics. PLOS One 7(3): 1–10.

Gámez-Pozo A, Sánchez-Navarro I, Calvo E, Díaz E, Miguel-Martín M, López R, Agulló T, Camafeita E, Espinosa E, López JA, Nistal M, Vara JÁF. 2011. Protein phosphorylation analysis in archival clinical cancer samples by shotgun and targeted proteomics approaches. Mol BioSyst 7(8): 2368–2374.

Garcia BA, Mollah S, Ueberheide BM, Busby SA, Muratore TL, Shabanowitz J, Hunt DF. 2007. Chemical derivatization of histones for facilitated analysis by mass spectrometry. Nat Protoc 2(4): 933–938.

GE Healthcare. 2010. Protein sample preparation. Handbooks from GE Healthcare. p. 121

Geoui T, Urlaub H, Plessmann U, Porschewski P. 2010. Extraction of proteins from formalin-fixed, paraffin-embedded tissue using the Qproteome extraction technique and preparation of tryptic peptides for liquid chromatography/mass spectrometry analysis. Curr Protoc Mol Biol 90(1):10.27.1–10.27.12.

Giesen C, Wang HAO, Schapiro D, Zivanovic N, Jacobs A, Hattendorf B, Schüffler PJ, Grolimund D, Buhmann JM, Brandt S, Varga Z, Wild PJ, Günther D, Bodenmiller B. 2014. Highly multiplexed imaging of tumor tissues with subcellular resolution by mass cytometry. Nat Methods 11(4): 417–422.

Giusti L, Lucacchini A. 2013. Proteomic studies of formalin-fixed paraffin-embedded tissues. Expert Rev Proteomics 10(2):165–177.

Glatter T, Ludwig C, Ahrné E, Aebersold R, Heck AJR, Schmidt A. 2012. Large-scale quantitative assessment of different in-solution protein digestion protocols reveals superior cleavage efficiency of tandem Lys-C/trypsin proteolysis over trypsin digestion. J Proteome Res 11(11):5145–5156.

Goddard ET, Hill RC, Barrett A, Betts C, Guo Q, Maller O, Borges VF, Hansen KC, Schedin P. 2016. Quantitative extracellular matrix proteomics to study mammary and liver tissue microenvironments. Int J Biochem Cell Biol 81: 223–232.

Gräntzdörffer I, Yumlu S, Gioeva Z, von Wasielewski R, Ebert MPA, Röcken C. 2010. Comparison of different tissue sampling methods for protein extraction from formalin-fixed and paraffin-embedded tissue specimens. Exp Mol Pathol 88(1):190–196.

Griffiths RL, Creese AJ, Race AM, Bunch J, Cooper HJ. 2016. LESA FAIMS mass spectrometry for the spatial profiling of proteins from tissue. Anal Chem 88(13):6758–6766.

Groseclose MR, Andersson M, Hardesty WM, Caprioli RM. 2007. Identification of proteins directly from tissue: In situ tryptic digestions coupled with imaging mass spectrometry. J Mass Spectrom 42(2):254–262.

Gündisch S, Hauck S, Sarioglu H, Schott C, Viertler C, Kap M, Schuster T, Reischauer B, Rosenberg R, Verhoef C, Mischinger HJ, Riegman P, Zatloukal K, Becker KF. 2012. Variability of protein and phosphoprotein levels in clinical tissue specimens during the preanalytical phase. J Proteome Res 11(12): 5748–5762.

Guo T, Kouvonen P, Koh CC, Gillet LC, Wolski WE, Röst HL, Rosenberger G, Collins BC, Blum LC, Gillessen S, Joerger M, Jochum W, Aebersold R. 2015. Rapid mass spectrometric conversion of tissue biopsy samples into permanent quantitative digital proteome maps. Nat Med 21(4): 407–413.

Guo T, Wang W, Rudnick PA, Song T, Li J, Zhuang Z, Weil RJ, DeVoe DL, Lee CS, Balgley BM. 2007. Proteome analysis of microdissected formalin-fixed and paraffin-embedded tissue specimens. J Histochem Cytochem 55(7): 763–772.

Guo X, Trudgian DC, Lemoff A, Yadavalli S, Mirzaei H. 2014. Confetti: A multiprotease map of the HeLa proteome for comprehensive proteomics. Mol Cell Proteomics 13(6):1573–1584.

Hammer E, Ernst FD, Thiele A, Karanam NK, Kujath C, Evert M, Völker U, Barthlen W. 2014. Kidney protein profiling of Wilms' tumor patients by analysis of formalin-fixed paraffin-embedded tissue samples. Clin Chim Acta 433: 235–241.

Hansen KC, Kiemele L, Maller O, O'Brien J, Shankar A, Fornetti J, Schedin P. 2009. An in-solution ultrasonication-assisted digestion method for improved extracellular matrix proteome coverage. Mol Cell Proteomics 8(7): 1648–1657.

Heijs B, Holst S, Briaire-De Bruijn IH, Van Pelt GW, De Ru AH, Van Veelen PA, Drake RR, Mehta AS, Mesker WE, Tollenaar RA, Bovée JVMG, Wuhrer M, McDonnell LA. 2016. Multimodal mass spectrometry imaging of N-glycans and proteins from the same tissue section. Anal Chem 88(15): 7745–7753.

Hervey WJ, Strader MB, Hurst GB. 2008. Comparison of digestion protocols for microgram quantities of enriched protein samples. J Proteome Res 6: 3054–3061.

Hess M, Hildebrandt MD, Müller F, Kruber S, Kroetz P, Schumacher U, Reimer R, Kammal M, Püschel K, Wöllmer W, Miller D. 2013. Picosecond infrared laser (PIRL): An ideal phonomicrosurgical laser? Eur Arch Oto-Rhino-Laryngology 270(11): 2927–2937.

Hill RC, Calle EA, Dzieciatkowska M, Niklason LE, Hansen KC. 2015. Quantification of extracellular matrix proteins from a rat lung scaffold to provide a molecular readout for tissue engineering. Mol Cell Proteomics 14(4):961–973.

Holfeld A, Valdés A, Malmström P-U, Segersten U, Lind SB. 2018. Parallel proteomic workflow for mass spectrometric analysis of tissue samples preserved by different methods. Anal Chem 90(9):5841–5849.

Holst S, Heijs B, de Haan N, van Zeijl RJM, Briaire-de Bruijn IH, van Pelt GW, Mehta AS, Angel PM, Mesker WE, Tollenaar RA, Drake RR, Bovée JVMG, McDonnell LA, Wuhrer M. 2016. Linkage-specific in situ sialic acid derivatization for N-glycan mass spectrometry imaging of formalin-fixed paraffin-embedded tissues. Anal Chem 88(11): 5904–5913.

Hood BL, Darfler MM, Guiel TG, Furusato B, Lucas DA, Ringeisen BR, Sesterhenn IA, Conrads TP, Veenstra TD, Krizman DB. 2005. Proteomic analysis of formalin fixed prostate cancer tissue. Mol Cell Proteomics 4: 1741–1753.

Hughes CS, Foehr S, Garfield DA, Furlong EE, Steinmetz LM, Krijgsveld J. 2014. Ultrasensitive proteome analysis using paramagnetic bead technology. Mol Syst Biol 10(10):757–757.

Hughes CS, McConechy MK, Cochrane DR, Nazeran T, Karnezis AN, Huntsman DG, Moring GB. 2016. Quantitative profiling of single formalin fixed tumour sections: Proteomics for translational research. Sci Rep 6(1): 34949.

Hustoft HK, Malerod H, Wilson SR, Reubsaet L, Lundanes E, Greibrokk T. 2010. A critical review of trypsin digestion for LC-MS based. Proteomics Integr Proteomics 73–92.

Ikeda K, Monden T, Kanoh T, Tsujie M, Izawa H, Haba A, Ohnishi T, Sekimoto M, Tomita N, Shiozaki H, Monden M. 1998. Extraction and analysis of diagnostically useful proteins from formalin-fixed, paraffin-embedded tissue sections. J Histochem Cytochem 46(3): 397–403.

Jiang X, Jiang X, Feng S, Tian R, Ye M, Zou H. 2007. Development of efficient protein extraction methods for shotgun proteome analysis of formalin-fixed tissues. J Proteome Res 6(3):1038–1047.

Johnson H, White FM. 2014. Quantitative analysis of signaling networks across differentially embedded tumors highlights interpatient heterogeneity in human glioblastoma. J Proteome Res 13(11): 4581–4593.

Jowett N, Wöllmer W, Mlynarek AM, Wiseman P, Segal B, Franjic K, Krötz P, Böttcher A, Knecht R, Miller RJD. 2013. Heat generation during ablation of porcine skin with erbium: YAG laser vs a novel picosecond infrared laser. JAMA Otolaryngol Neck Surg 139(8): 828.

Kachuk C, Stephen K, Doucette A. 2015. Comparison of sodium dodecyl sulfate depletion techniques for proteome analysis by mass spectrometry. J Chromatogr A 1418: 158–166.

Kalli A, Sweredoski MJ, Hess S. 2013. Data-dependent middle-down nanoliquid chromatography–electron capture dissociation-tandem mass spectrometry: An application for the analysis of unfractionated histones. Anal Chem 85(7):3501–3507.

Kanshin E, Thibault P. 2014. Efficient sample processing for proteomics applications — Are we there yet? Mol Syst Biol 758(10):1–3.

Kawashima Y, Kodera Y, Singh A, Matsumoto M, Matsumoto H. 2014. Efficient extraction of proteins from formalin-fixed paraffin-embedded tissues requires higher concentration of tris(hydroxymethyl)aminomethane. Clin Proteomics 11(1):4.

Kay AW, Strauss-Albee DM, Blish CA. 2016. Application of mass cytometry (CyTOF) for functional and phenotypic analysis of natural killer cells. Methods Mol Biol 1441: 13–26.

Kertesz V, Van Berkel GJ. 2010. Fully automated liquid extraction-based surface sampling and ionization using a chip-based robotic nanoelectrospray platform. J Mass Spectrom 45(3):252–260.

Klammer AA, MacCoss MJ. 2006. Effects of modified digestion schemes on the identification of proteins from complex mixtures. J Proteome Res 5(3):695–700.

Kojima K, Bowersock GJ, Kojima C, Klug CA, Grizzle WE, Mobley JA. 2012. Validation of a robust proteomic analysis carried out on formalin-fixed paraffin-embedded tissues of the pancreas obtained from mouse and human. Proteomics 12(22):3393–3402.

Kostka V, Carpenter F. 1964. Inhibition of chymotrypsin activity in crystalline trypsin preparations. undefined. J Biol Chem 239: 1799–1803.

Kruse RA, Rubakhin SS, Romanova EV, Bohn PW, Sweedler JV. 2001. Direct assay of Aplysia tissues and cells with laser desorption/ionization mass spectrometry on porous silicon. J Mass Spectrom 36(12):1317–1322.

Kulak NA, Pichler G, Paron I, Nagaraj N, Mann M. 2014. Minimal, encapsulated proteomic-sample processing applied to copy-number estimation in eukaryotic cells. Nat Methods 11(3):319–324.

Kwiatkowski M, Wurlitzer M, Krutilin A, Kiani P, Nimer R, Omidi M, Mannaa A, Bussmann T, Bartkowiak K, Kruber S, Uschold S, Steffen P, Lübberstedt J, Küpker N, Petersen H, Knecht R, Hansen NO, Zarrine-Afsar A, Robertson WD, Miller RJD, Schlüter H. 2016. Homogenization of tissues via picosecond-infrared laser (PIRL) ablation: Giving a closer view on the in-vivo composition of protein species as compared to mechanical homogenization. J Proteomics 134: 193–202.

Kwiatkowski M, Wurlitzer M, Omidi M, Ren L, Kruber S, Nimer R, Robertson WD, Horst A, Miller RJD, Schlüter H. 2015. Ultrafast extraction of proteins from tissues using desorption by impulsive vibrational excitation. Angew. Chemie 54: 285–288.

Labots M, van der Mijn JC, Beekhof R, Piersma SR, de Goeij-de Haas RR, Pham TV, Knol JC, Dekker H, van Grieken NCT, Verheul HMW, Jiménez CR. 2017. Phosphotyrosine-based-phosphoproteomics scaled-down to biopsy level for analysis of individual tumor biology and treatment selection. J Proteomics 162: 99–107.

Lai X, Chen S. 2015. Identification of novel biomarker and therapeutic target candidates for diagnosis and treatment of follicular adenoma. Cancer Genomics Proteomics 12(6):271–281.

Lai X, Schneider BP. 2014. Integrated and convenient procedure for protein extraction from formalin-fixed, paraffin-embedded tissues for LC-MS/MS analysis. Proteomics 14(21–22):2623–2627.

Le Bihan T, Goh T, Stewart II, Salter AM, Bukhman YV, Dharsee M, Ewing R, Wiśniewski JR. 2006. Differential analysis of membrane proteins in mouse fore- and hindbrain using a label-free approach. J Proteome Res 5(10): 2701–2710.

Leelatian N, Doxie DB, Greenplate AR, Mobley BC, Lehman JM, Sinnaeve J, Kauffmann RM, Werkhaven JA, Mistry AM, Weaver KD, Thompson RC, Massion PP, Hooks MA, Kelley MC, Chambless LB, Ihrie RA, Irish JM. 2017. Single cell analysis of human tissues and solid tumors with mass cytometry. Cytom. Part B Clin Cytom 92(1): 68–78.

Leon IR, Schwammle V, Jensen ON, Sprenger RR. 2013. Quantitative assessment of in-solution digestion efficiency identifies optimal protocols for unbiased protein analysis. Mol Cell Proteomics 12(10):2992–3005.

Lim J, Kim Y, Lee W, Kim M, Lee EJ, Kang CS, Han K. 2010. Fresh-frozen, optimal cutting temperature (OCT) compound-embedded bone marrow aspirates: a reliable resource for morphological, immunohistochemical and molecular examinations. Int J Lab Hematol 32(1 PART.1): e34–e39.

Lim WK, Rosgen J, Englander SW. 2009. Urea, but not guanidinium, destabilizes proteins by forming hydrogen bonds to the peptide group. Proc Natl Acad Sci USA 106(8):2595–2600.

Lin M-F, Williams C, Murray MV, Conn G, Ropp PA. 2004. Ion chromatographic quantification of cyanate in urea solutions: Estimation of the efficiency of cyanate scavengers for use in recombinant protein manufacturing. J Chromatogr B 803: 353–362.

Linke SJ, Frings A, Ren L, Gomolka A, Schumacher U, Reimer R, Hansen NO, Jowett N, Richard G, Miller RJDA. 2015. A new technology for applanation free corneal trephination: The picosecond infrared laser (PIRL). PLOS One 10(3): e0120944.

Liu A. 2010. Laser capture microdissection in the tissue biorepository. J Biomol Tech 21(3):120–125.

Liu J, Wang F, Mao J, Zhang Z, Liu Z, Huang G, Cheng K, Zou H. 2015. High-sensitivity N-glycoproteomic analysis of mouse brain tissue by protein extraction with a mild detergent of N-dodecyl β-D-maltoside. Anal Chem 87(4): 2054–2057.

Liu Y, Fire AZ, Boyd S, Olshen RA. 2014. Estimating clonality. J Proteome Res 13(4):1885–1895.

Longuespée R, Alberts D, Pottier C, Smargiasso N, Mazzucchelli G, Baiwir D, Kriegsmann M, Herfs M, Kriegsmann J, Delvenne P, de Pauw E. 2016. A laser microdissection-based workflow for FFPE tissue microproteomics: Important considerations for small sample processing. Methods 104: 154–162.

López-Ferrer D, Capelo JL, Vázquez J. 2005. Ultra fast trypsin digestion of proteins by high intensity focused ultrasound. J Proteome Res 4(5):1569–1574.

Luber CA, Cox J, Lauterbach H, Fancke B, Selbach M, Tschopp J, Akira S, Wiegand M, Hochrein H, O'Keeffe M, Mann M. 2010. Quantitative proteomics reveals subset-specific viral recognition in dendritic cells. Immunity 32(2): 279–289.

Luebker SA, Koepsell SA. 2016. Optimization of urea based protein extraction from formalin-fixed paraffin-embedded tissue for shotgun proteomics. Int J Proteomics 2016: 1–6.

Luebker SA, Wojtkiewicz M, Koepsell SA. 2015. Two methods for proteomic analysis of formalin-fixed, paraffin embedded tissue result in differential protein identification, data quality, and cost. Proteomics 15(21):3744–3753.

Magdeldin S, Yamamoto T. 2012. Toward deciphering proteomes of formalin-fixed paraffin-embedded (FFPE) tissues. Proteomics 12(7):1045–1058.

Manza LL, Stamer SL, Ham A-JL, Codreanu SG, Liebler DC. 2005. Sample preparation and digestion for proteomic analyses using spin filters. Proteomics 5(7):1742–1745.

Mason JT. 2016. Proteomic analysis of FFPE tissue: Barriers to clinical impact. Expert Rev Proteomics 13(9):801–803.

McDonnell LA, Angel PM, Lou S, Drake RR. 2017. Mass spectrometry imaging in cancer research: Future perspectives. Adv Cancer Res 134: 283–290.

McDonnell LA, Heeren RMA, Andrén PE, Stoeckli M, Corthals GL. 2012. Going forward: Increasing the accessibility of imaging mass spectrometry. J Proteomics 75(16):5113–5121.

Meng H, Janssen PML, Grange RW, Yang L, Beggs AH, Swanson LC, Cossette SA, Frase A, Childers MK, Granzier H, Gussoni E, Lawlor MW. 2014. Tissue triage and freezing for models of skeletal muscle disease. J Vis Exp 89: e51586.

Mertins P, Mani DR, Ruggles KV, Gillette MA, Clauser KR, Wang P, Wang X, Qiao JW, Cao S, Petralia F, Kawaler E, Mundt F, Krug K, Tu Z, Lei JT, Gatza ML, Wilkerson M, Perou CM, Yellapantula V, Huang K-L, Lin C, McLellan MD, Yan P, Davies SR, Townsend RR, Skates SJ, Wang J, Zhang B, Kinsinger CR, Mesri M, Rodriguez H, Ding L, Paulovich AG, Fenyö D, Ellis MJ, Carr SA, NCI CPTAC. 2016. Proteogenomics connects somatic mutations to signalling in breast cancer. Nature 534(7605): 55–62.

Metz B, Kersten GFA, Baart GJE, de Jong A, Meiring H, ten Hove J, van Steenbergen MJ, Hennink WE, Crommelin DJA, Jiskoot W. 2006. Identification of formaldehyde-induced modifications in proteins: Reactions with insulin. Bioconjug Chem 17(3): 815–822.

Metz B, Kersten GFA, Hoogerhout P, Brugghe HF, Timmermans HAM, de Jong A, Meiring H, ten Hove J, Hennink WE, Crommelin DJA, Jiskoot W. 2004. Identification of formaldehyde-induced modifications in proteins: reactions with model peptides. J Biol Chem 279(8): 6235–6243.

Meuzelaar H, Panman MR, Woutersen S. 2015. Guanidinium-induced denaturation by breaking of salt bridges. Angew. Chemie 54(50): 15255–15259.

Micke P, Ohshima M, Tahmasebpoor S, Ren Z-P, Ostman A, Pontén F, Botling J. 2006. Biobanking of fresh frozen tissue: RNA is stable in nonfixed surgical specimens. Lab Invest 86(2): 202–211.

Mollee P, Boros S, Loo D, Ruelcke JE, Lakis VA, Lê Cao K-A, Renaut P, Hill MM. 2016. Implementation and evaluation of amyloidosis subtyping by laser-capture microdissection and tandem mass spectrometry. Clin Proteomics 13(1): 30.

Monera OD, Kay CM, Hodges RS. 1994. Protein denaturation with guanidine hydrochloride or urea provides a different estimate of stability depending on the contributions of electrostatic interactions. Protein Sci 3: 1984–1991.

Morente MM, Mager R, Alonso S, Pezzella F, Spatz A, Knox K, Kerr D, Dinjens WNM, Oosterhuis JW, Lam KH, Oomen MHA, van Damme B, van de Vijver M, van Boven H, Kerjaschki D, Pammer J, Lopez-Guerrero JA, Llombart Bosch A, Carbone A, Gloghini A, Teodorovic I, Isabelle M, Passioukov A, Lejeune S, Therasse P, van Veen EB, Ratcliffe C, Riegman PHJ. 2006. TuBaFrost 2: Standardising tissue collection and quality control procedures for a European virtual frozen tissue bank network. Eur J Cancer 42(16): 2684–2691.

Morsa D, Baiwir D, La Rocca R, Zimmerman TA, Hanozin E, Grifnée E, Longuespée R, Meuwis M-A, Smargiasso N, de Pauw E, Mazzucchelli G. 2019. Multi-enzymatic limited digestion: The next-generation sequencing for proteomics? J Proteome Res. acs.jproteome.9b00044.

Moulédous L, Hunt S, Harcourt R, Harry JL, Williams KL, Gutstein HB. 2003. Proteomic analysis of immunostained, laser-capture microdissected brain samples. Electrophoresis 24(12):296–302.

Mukherjee S, Rodriguez-Canales J, Hanson J, Emmert-Buck MR, Tangrea MA, Prieto DA, Blonder J, Johann DJ. 2013. Proteomic Analysis of frozen tissue samples using laser capture microdissection. Methods Mol Biol 1002: 71–83.

Murgia M, Nagaraj N, Deshmukh AS, Zeiler M, Cancellara P, Moretti I, Reggiani C, Schiaffino S, Mann M. 2015. Single muscle fiber proteomics reveals unexpected mitochondrial specialization. EMBO Rep 16(3): 387–395.

Nagaraj N, Lu A, Mann M, Wiśniewski JR. 2008. Detergent-based but gel-free method allows identification of several hundred membrane proteins in single LC-MS runs. J Proteome Res 7(11):5028–5032.

Nakajima K, Ogi H, Adachi K, Noi K, Hirao M, Yagi H, Goto Y. 2016. Nucleus factory on cavitation bubble for amyloid β fibril. Sci Rep 6: 22015.

Nakayama KH, Lee CCI, Batchelder CA, Tarantal AF. 2013. Tissue specificity of decellularized rhesus monkey kidney and lung scaffolds. PLOS One 8(5): e64134.

Namimatsu S, Ghazizadeh M, Sugisaki Y. 2005. Reversing the effects of formalin fixation with citraconic anhydride and heat: a universal antigen retrieval method. J Histochem Cytochem 53(1):3–11.

Nel AJM, Garnett S, Blackburn JM, Soares NC. 2015. Comparative reevaluation of FASP and enhanced FASP methods by LC-MS/MS. J Proteome Res 14(3):1637–1642.

Ngoka LC. 2008. Sample prep for proteomics of breast cancer: Proteomics and gene ontology reveal dramatic differences in protein solubilization preferences of radioimmunoprecipitation assay and urea lysis buffers. Proteome Sci 6: 30.

Nirmalan NJ, Harnden P, Selby PJ, Banks RE. 2008. Mining the archival formalin-fixed paraffin-embedded tissue proteome: Opportunities and challenges. Mol BioSyst 4(7):712.

Nirmalan NJ, Hughes C, Peng J, McKenna T, Langridge J, Cairns DA, Harnden P, Selby PJ, Banks RE. 2011. Initial development and validation of a novel extraction method for quantitative mining of the formalin-fixed, paraffin-embedded tissue proteome for biomarker investigations. J Proteome Res 10(2): 896–906.

Nomura E, Katsuta K, Ueda T, Toriyama M, Mori T, Inagaki N. 2004. Acid-labile surfactant improves in-sodium dodecyl sulfate polyacrylamide gel protein digestion for matrix-assisted laser desorption/ionization mass spectrometric peptide mapping. J Mass Spectrom 39(2):202–207.

Norris JL, Porter NA, Caprioli RM. 2003. Mass spectrometry of intracellular and membrane proteins using cleavable detergents. Anal Chem 75(23):6642–6647.

Ok E, Basnakian AG, Apostolov EO, Barri YM, Shah SV. 2005. Carbamylated low-density lipoprotein induces death ofendothelial cells: A link to atherosclerosis in patients with kidney disease. Kidney Int 68(1):173–178.

Olszowy PP, Burns A, Ciborowski PS. 2013. Pressure-assisted sample preparation for proteomic analysis. Anal Biochem 438(1):67–72.

Önnerfjord P, Khabut A, Reinholt FP, Svensson O, Heinegård D. 2012. Quantitative proteomic analysis of eight cartilaginous tissues reveals characteristic differences as well as similarities between subgroups. J Biol Chem 287(23):18913–18924.

Ostasiewicz P, Zielinska DF, Mann M, Wiśniewski JR. 2010. Proteome, phosphoproteome, and N-glycoproteome are quantitatively preserved in formalin-fixed paraffin-embedded tissue and analyzable by high-resolution mass spectrometry. J Proteome Res 9(7):3688–3700.

Palmer-Toy DE, Krastins B, Sarracino DA, Nadol JB, Merchant SN. 2005. Efficient method for the proteomic analysis of fixed and embedded tissues. J Proteome Res 4(6):2404–2411.

Patel E, Clench MR, West A, Marshall PS, Marshall N, Francese S. 2015. Alternative surfactants for improved efficiency of in situ tryptic proteolysis of fingermarks. J Am Soc Mass Spectrom 26(6):862–872.

Peer D. 2014. Precision medicine—Delivering the goods? Cancer Lett 352(1):2–3.

Peterson VM, Zhang KX, Kumar N, Wong J, Li L, Wilson DC, Moore R, McClanahan TK, Sadekova S, Klappenbach JA. 2017. Multiplexed quantification of proteins and transcripts in single cells. Nat Biotechnol 35(10): 936–939.

Pinho SS, Reis CA. 2015. Glycosylation in cancer: Mechanisms and clinical implications. Nat Rev Cancer 15(9):540–555.

Polgár L. 2005. The catalytic triad of serine peptidases. Cell Mol Life Sci 6205: 2161–2172.

Powers TW, Holst S, Wuhrer M, Mehta AS, Drake RR. 2015. Two-dimensional N-glycan distribution mapping of hepatocellular carcinoma tissues by MALDI-imaging mass spectrometry. Biomolecules 5(4): 2554–2572.

Powers TW, Jones EE, Betesh LR, Romano PR, Gao P, Copland JA, Mehta AS, Drake RR. 2013. Matrix assisted laser desorption ionization imaging mass spectrometry workflow for spatial profiling analysis of N-linked glycan expression in tissues. Anal Chem 85(20): 9799–9806.

Prakadan SM, Shalek AK, Weitz DA. 2017. Scaling by shrinking: Empowering single-cell' omics' with microfluidic devices. Nat Rev Genet 18: 345–361.

Proc JL, Kuzyk MA, Hardie DB, Yang J, Smith DS, Jackson AM, Parker CE, Borchers CH. 2010. A quantitative study of the effects of chaotropic agents, surfactants, and solvents on the digestion efficiency of human plasma proteins by trypsin. Proteome 9(10): 5422–5437.

Quach TTT, Li N, Richards DP, Zheng J, Keller BO, Li L. 2003. Development and applications of in-gel CNBr/tryptic digestion combined with mass spectrometry for the analysis of membrane proteins. J Proteome Res 2(5):543–552.

Quanico J, Franck J, Dauly C, Strupat K, Dupuy J, Day R, Salzet M, Fournier I, Wisztorski M. 2013. Development of liquid microjunction extraction strategy for improving protein identification from tissue sections. J Proteomics 79: 200–218.

Rabilloud T. 1996. Solubilization of proteins for electrophoretic analyses. Electrophoresis 17(5):813–829.

Rapp C, Warta R, Stamova S, Nowrouzi A, Geisenberger C, Gal Z, Roesch S, Dettling S, Juenger S, Bucur M, Jungk C, DaoTrong P, Ahmadi R, Sahm F, Reuss D, Fermi V, Herpel E, Eckstein V, Grabe N, Schramm C, Weigand MA, Debus J, von Deimling A, Unterberg A, Abdollahi A, Beckhove P, Herold-Mende C. 2017. Identification of T cell target antigens in glioblastoma stem-like cells using an integrated proteomics-based approach in patient specimens. Acta Neuropathol 134(2): 297–316.

Rial-Otero R, Carreira RJ, Cordeiro FM, Moro AJ, Santos HM, Vale G, Moura I, Capelo JL. 2007. Ultrasonic assisted protein enzymatic digestioÿn for fast protein identification by matrix-assisted laser desorption/ionization time-of-flight mass spectrometry. Sonoreactor versus ultrasonic probe. J Chromatogr A 1166(1-2): 101–107.

Riondino S, Ferroni P, Spila A, Alessandroni J, D'Alessandro R, Formica V, Della-Morte D, Palmirotta R, Nanni U, Roselli M, Guadagni F. 2015. Ensuring sample quality for biomarker discovery studies - Use of ict tools to trace biosample life-cycle. Cancer Genomics Proteomics 12(6): 291–299.

Rodríguez-Rigueiro T, Valladares-Ayerbes M, Haz-Conde M, Blanco M, Aparicio G, Fernández-Puente P, Blanco FJ, Lorenzo MJ, Aparicio LA, Figueroa A. 2011. A novel procedure for protein extraction from formalin-fixed paraffin-embedded tissues. Proteomics 11(12): 2555–2559.

Ronci M, Bonanno E, Colantoni A, Pieroni L, Ilio CDi, Spagnoli LG, Federici G, Urbani A. 2008. Protein unlocking procedures of formalin-fixed paraffin-embedded tissues: Application to MALDI-TOF. Proteomics 8: 3702–3714.

Rosenberger G, Koh CC, Guo T, Röst HL, Kouvonen P, Collins BC, Heusel M, Liu Y, Caron E, Vichalkovski A, Faini M, Schubert OT, Faridi P, Ebhardt HA, Matondo M, Lam H, Bader SL, Campbell DS, Deutsch EW, Moritz RL, Tate S, Aebersold R. 2014. A repository of assays to quantify 10,000 human proteins by SWATH-MS. Sci Data 1: 140031.

Russell WK, Park Z-Y, Russell DH. 2001. Proteolysis in mixed organic −aqueous solvent systems: applications for peptide mass mapping using mass spectrometry. Anal Chem 73(11):2682–2685.

Santos HM, Capelo JL. 2007. Trends in ultrasonic-based equipment for analytical sample treatment. Talanta 73(5):795–802.

Santos HM, Kouvonen P, Capelo J-L, Corthals GL. 2013. On-target ultrasonic digestion of proteins. Proteomics 13(9):1423–1427.

Sarsby J, Griffiths RL, Race AM, Bunch J, Randall EC, Creese AJ, Cooper HJ. 2015. Liquid extraction surface analysis mass spectrometry coupled with field asymmetric waveform ion mobility spectrometry for analysis of intact proteins from biological substrates. Anal Chem 87(13): 6794–6800.

Satija R, Shalek AK. 2014. Heterogeneity in immune responses: From populations to single cells. Trends Immunol 35(5):219–229.

Sato N, Taniguchi T, Goda Y, Kosaka H, Higashino K, Sakai T, Katoh S, Yasui N, Sairyo K, Taniguchi H. 2016. Proteomic analysis of human tendon and ligament: Solubilization and analysis of insoluble extracellular matrix in connective tissues. J Proteome Res 15(12): 4709–4721.

Saveliev SV, Woodroofe CC, Sabat G, Adams CM, Klaubert D, Wood K, Urh M. 2013. Mass spectrometry compatible surfactant for optimized in-gel protein digestion. Anal Chem 85(2): 907–914.

Schey KL, Anderson DM, Rose KL. 2013. Spatially-directed protein identification from tissue sections by top-down LC-MS/MS with electron transfer dissociation. Anal Chem 85(14):6767–6774.

Scicchitano MS, Dalmas DA, Boyce RW, Thomas HC, Frazier KS. 2009. Protein extraction of formalin-fixed, paraffin-embedded tissue enables robust proteomic profiles by mass spectrometry. J Histochem Cytochem 57(9):849–860.

Scott DA, Casadonte R, Cardinali B, Spruill L, Mehta AS, Carli F, Simone N, Kriegsmann M, Del Mastro L, Kriegsmann J, Drake RR. 2019. Increases in tumor N-glycan polylactosamines associated with advanced HER2-positive and triple-negative breast cancer tissues. Proteomics 13(1): 1800014.

Seddon AM, Curnow P, Booth PJ. 2004. Membrane proteins, lipids and detergents: not just a soap opera. Biochim. Biophys. Acta - Biomembr. 1666(1):105–117.

Shah P, Zhang B, Choi C, Yang S, Zhou J, Harlan R, Tian Y, Zhang Z, Chan DW, Zhang H. 2015. Tissue proteomics using chemical immobilization and mass spectrometry. Anal Biochem 469: 27–33.

Shalek AK, Satija R, Shuga J, Trombetta JJ, Gennert D, Lu D, Chen P, Gertner RS, Gaublomme JT, Yosef N. 2014. Single cell RNA Seq reveals dynamic paracrine control of cellular variation. Nature 510(7505): 363–369.

Shao S, Guo T, Aebersold R. 2015. Mass spectrometry-based proteomic quest for diabetes biomarkers. Biochim Biophys Acta-Proteins Proteomics 1854(6):519–527.

Shao S, Guo T, Gross V, Lazarev A, Koh CC, Gillessen S, Joerger M, Jochum W, Aebersold R. 2016. Reproducible tissue homogenization and protein extraction for quantitative proteomics using micropestle-assisted pressure cycling technology. J Proteome Res 15: 1821–1829.

Shen K, Sun J, Cao X, Zhou D, Li J. 2015. Comparison of different buffers for protein extraction from formalin-fixed and paraffin-embedded tissue specimens. PLOS One 10(11):e0142650.

Shi S-R, Liu C, Balgley BM, Lee C, Taylor CR. 2006. Protein extraction from formalin-fixed, paraffin-embedded tissue sections: Quality evaluation by mass spectrometry. J Histochem Cytochem 54(6):739–743.

Shi SR, Key ME, Kalra KL. 1991. Antigen retrieval in formalin-fixed, paraffin-embedded tissues: An enhancement method for immunohistochemical staining based on microwave oven heating of tissue sections. J Histochem Cytochem 39(6):741–748.

Shi SR, Taylor CR, Fowler CB, Mason JT. 2013. Complete solubilization of formalin-fixed, paraffin-embedded tissue may improve proteomic studies. Proteomics Clin Appl 7(3-4):264–272.

Silberring J, Ciborowski P. 2010. Biomarker discovery and clinical proteomics. Trends Analyt Chem 29(2):128–140.

Speers AE, Wu CC. 2007. Proteomics of integral membrane proteins theory and application. Chem Rev 107(8):3687–3714.

Sprung RW, Brock JWC, Tanksley JP, Li M, Washington MK, Slebos RJC, Liebler DC. 2009. Equivalence of protein inventories obtained from formalin-fixed paraffin-embedded and frozen tissue in multidimensional liquid chromatography-tandem mass spectrometry shotgun proteomic analysis. Mol Cell Proteomics 8(8): 1988–1998.

Srzentić K, Zhurov KO, Lobas AA, Nikitin G, Fornelli L, Gorshkov MV, Tsybin YO. 2018. Chemical-mediated digestion: An alternative realm for middle-down proteomics? J Proteome Res 17(6): 2005–2016.

Sun S, Zhou JY, Yang W, Zhang H. 2014. Inhibition of protein carbamylation in urea solution using ammonium-containing buffers. Anal Biochem 446(1):76–81.

Svensson V, Vento-Tormo R, Teichmann SA. 2018. Exponential scaling of single-cell RNA-seq in the past decade. Nat Protoc 13(4):599–604.

Swaney DL, Wenger CD, Coon JJ. 2010. Value of using multiple proteases for large-scale mass spectrometry-based proteomics. J Proteome Res 9(3):1323–1329.

Swatkoski S, Gutierrez P, Wynne C, Petrov A, Dinman JD, Edwards N, Fenselau C. 2008. Evaluation of microwave-accelerated residue-specific acid cleavage for proteomic applications. J Proteome Res 7(2): 579–586.

Tanca A, Abbondio M, Pisanu S, Pagnozzi D, Uzzau S, Addis M. 2014. Critical comparison of sample preparation strategies for shotgun proteomic analysis of formalin-fixed, paraffin-embedded samples: Insights from liver tissue. Clin Proteomics 11(1):28.

Tanca A, Pagnozzi D, Addis MF. 2012. Setting proteins free: Progresses and achievements in proteomics of formalin-fixed, paraffin-embedded tissues. Proteomics Clin Appl 6(1–2):7–21.

Tanca A, Pagnozzi D, Burrai GP, Polinas M, Uzzau S, Antuofermo E, Addis MF. 2012. Comparability of differential proteomics data generated from paired archival fresh-frozen and formalin-fixed samples by GeLC-MS/MS and spectral counting. J Proteomics 77: 561–576.

Tao F, Li C, Smejkal G, Lazarev A, Lawrence N, Schumacher RT. 2007. Pressure cycling technology (PCT) applications in extraction of biomolecules from challenging biological samples. Proc 4th Int confrence High Press Biosci Biotechnol 1(1):166–173.

Thomas JJ, Shen Z, Crowell JE, Finn MG, Siuzdak G. 2001. Desorption/ionization on silicon (DIOS): A diverse mass spectrometry platform for protein characterization. Proc Natl Acad Sci USA 98(9):4932–4937.

Thompson SM, Craven RA, Nirmalan NJ, Harnden P, Selby PJ, Banks RE. 2013. Impact of pre-analytical factors on the proteomic analysis of formalin-fixed paraffin-embedded tissue. Proteomics Clin Appl 7(3–4):241–251.

Tian Y, Bova GS, Zhang H. 2011. Quantitative glycoproteomic analysis of optimal cutting temperature-embedded frozen tissues identifying glycoproteins associated with aggressive prostate cancer. Anal Chem 83(18):7013–7019.

Tian Y, Gurley K, Meany DL, Kemp CJ, Zhang H. 2009. N-linked glycoproteomic analysis of formalin-fixed and paraffin-embedded tissues. J Proteome Res 8(4):1657–1662.

Tian Y, Zhou Y, Elliott S, Aebersold R, Zhang H. 2007. Solid-phase extraction of N-linked glycopeptides. Nat Protoc 2(2):334–339.

Tirosh I, Izar B, Prakadan SM, Wadsworth MH, Treacy D, Trombetta JJ, Rotem A, Rodman C, Lian C, Murphy G, Fallahi-Sichani M, Dutton-Regester K, Lin JR, Cohen O, Shah P, Lu D, Genshaft AS, Hughes TK, Ziegler CG, Kazer SW, Gaillard A, Kolb KE, Villani AC, Johannessen CM, Andreev AY, Van Allen EM, Bertagnolli M, Sorger PK, Sullivan RJ, Flaherty KT, Frederick DT, Jané-Valbuena J, Yoon CH, Rozenblatt-Rosen O, Shalek AK, Regev A, Garraway LA. 2016. Dissecting the multicellular ecosystem of metastatic melanoma by single-cell RNA-seq. Science (80-.) 352(6282): 189–196.

Toews J, Rogalski JC, Clark TJ, Kast J. 2008. Mass spectrometric identification of formaldehyde-induced peptide modifications under in vivo protein cross-linking conditions. Anal Chim Acta 618(2): 168–183.

Toews J, Rogalski JC, Kast J. 2010. Accessibility governs the relative reactivity of basic residues in formaldehyde-induced protein modifications. Anal Chim Acta 676(1):60–67.

Tsiatsiani L, Heck AJR. 2015. Proteomics beyond trypsin. FEBS J 282(14):2612–2626.

Turiák L, Misják P, Szabó TG, Aradi B, Pálóczi K, Ozohanics O, Drahos L, Kittel Á, Falus A, Buzás EI, Vékey K. 2011. Proteomic characterization of thymocyte-derived microvesicles and apoptotic bodies in BALB/c mice. J Proteomics 74(10): 2025–2033.

Turiák L, Shao C, Meng L, Khatri K, Leymarie N, Wang Q, Pantazopoulos H, Leon DR, Zaia J. 2014. Workflow for combined proteomics and glycomics profiling from histological tissues. Anal Chem 86(19): 9670–9678.

Vaysse P-M, Heeren R, Porta T, Balluff B. 2017. Mass spectrometry imaging for clinical research–latest developments, applications, and current limitations. Analyst 142: 2690–2712.

Vincenti DC, Murray GI. 2013. The proteomics of formalin-fixed wax-embedded tissue. Clin Biochem 46(6):546–551.

Waas M, Bhattacharya S, Chuppa S, Wu X, Jensen DR, Omasits U, Wollscheid B, Volkman BF, Noon KR, Gundry RL. 2014. Combine and conquer: Surfactants, solvents, and chaotropes for robust mass spectrometry based analyses of membrane proteins. Anal Chem 86(3): 1551–1559.

Wakabayashi M, Yoshihara H, Masuda T, Tsukahara M, Sugiyama N, Ishihama Y. 2014. Phosphoproteome analysis of formalin-fixed and paraffin-embedded tissue sections mounted on microscope slides. J Proteome Res 13(2):915–924.

Wall MJ, Crowell AMJ, Simms GA, Liu F, Doucette AA. 2011. Implications of partial tryptic digestion in organic–aqueous solvent systems for bottom-up proteome analysis. Anal Chim Acta 703(2):194–203.

Wang C, Reed JM, Ma L, Qiao Y, Luo Y, Zou S, Hickman JJ, Su M. 2012. Biomimic light trapping silicon nanowire arrays for laser desorption/ionization of peptides. J Phys Chem C 116(29): 15415–15420.

Wang H, Qian W-J, Mottaz HM, Clauss TRW, Anderson DJ, Moore RJ, Camp DG, Khan AH, Sforza DM, Pallavicini M, Smith DJ, Smith RD. 2005. Development and evaluation of a micro- and nanoscale proteomic sample preparation method. J Proteome Res 4(6): 2397–2403.

Wang Z, Nicholls SJ, Rodriguez ER, Kummu O, Hörkkö S, Barnard J, Reynolds WF, Topol EJ, DiDonato JA, Hazen SL. 2007. Protein carbamylation links inflammation, smoking, uremia and atherogenesis. Nat Med 13(10): 1176–1184.

Wei J, Buriak JM, Siuzdak G. 1999. Desorption–ionization mass spectrometry on porous silicon. Nature 399(6733):243–246.

Weston LA, Hummon AB. 2013. Comparative LC-MS/MS analysis of optimal cutting temperature (OCT) compound removal for the study of mammalian proteomes. Analyst 138(21):6380–6384.

Wisniewski JR, Dus-Szachniewicz K, Ostasiewicz P, Ziolkowski P, Rakus D, Mann M. 2015. Absolute proteome analysis of colorectal mucosa, adenoma, and cancer reveals drastic changes in fatty acid metabolism and plasma membrane transporters. J Proteome Res 14(9):4005–4018.

Wisniewski JR, Duś K, Mann M. 2013. Proteomic workflow for analysis of archival formalin-fixed and paraffin-embedded clinical samples to a depth of 10000 proteins. Proteomics Clin Appl 7(3–4):225–233.

Wisniewski JR, Ostasiewicz P, Mann M. 2011. High recovery FASP applied to the proteomic analysis of microdissected formalin fixed paraffin embedded cancer tissues retrieves known colon cancer markers. J Proteome Res 10(7):3040–3049.

Wisniewski JR, Pruś G. 2015. Homogenous phase enrichment of cysteine-containing peptides for improved proteome coverage. Anal Chem 87(13):6861–6867.

Wisniewski JR, Zougman A, Nagaraj N, Mann M. 2009. Universal sample preparation method for proteome analysis. Nat Methods 6(5):359–362.

Wiśniewski JR. 2016. Quantitative evaluation of filter aided sample preparation (FASP) and multienzyme digestion FASP protocols. Anal Chem 88(10):5438–5443.

Wiśniewski JR, Mann M. 2012. Consecutive proteolytic digestion in an enzyme reactor increases depth of proteomic and phosphoproteomic analysis. Anal Chem 84(6):2631–2637.

Wiśniewski JR, Wegler C, Artursson P. 2018. Multiple-enzyme-digestion strategy improves accuracy and sensitivity of label- and standard-free absolute quantification to a level that is achievable by analysis with stable isotope-labeled standard spiking. J Proteome Res. acs.jproteome.8b00549.

Wiśniewski JR, Zielinska DF, Mann M. 2011. Comparison of ultrafiltration units for proteomic and N-glycoproteomic analysis by the filter-aided sample preparation method. Anal Biochem 410(2):307–309.

Wisztorski M, Fatou B, Franck J, Desmons A, Farré I, Leblanc E, Fournier I, Salzet M. 2013. Microproteomics by liquid extraction surface analysis: application to FFPE tissue to study the fimbria region of tubo-ovarian cancer. Proteomics Clin Appl 7(3–4): 234–240.

Wolff C, Schott C, Porschewski P, Reischauer B, Becker K-F. 2011. Successful protein extraction from over-fixed and long-term stored formalin-fixed tissues. PLOS One 6(1):e16353.

Wu Z, Huang J, Lu J, Zhang X. 2018. Reversible lysine derivatization enabling improved Arg-C digestion, a highly specific Arg-C digestion using trypsin. Anal Chem 90(3):1554–1559.

Xiao Z, Li G, Chen Y, Li M, Peng F, Li C, Li F, Yu Y, Ouyang Y, Xiao Z, Chen Z. 2010. Quantitative proteomic analysis of formalin-fixed and paraffin-embedded nasopharyngeal carcinoma using iTRAQ labeling, two-dimensional liquid chromatography, and tandem mass spectrometry. J Histochem Cytochem 58(6): 517–527.

Xie B, Li YY, Jia L, Nie YQ, Du H, Jiang SM. 2011a. Experimental ablation of the pancreas with high intensity focused ultrasound (HIFU) in a porcine model. Int J Med Sci 8(1):9–15.

Xie R, Chung J-Y, Ylaya K, Williams RL, Guerrero N, Nakatsuka N, Badie C, Hewitt SM. 2011b. Factors influencing the degradation of archival formalin-fixed paraffin-embedded tissue sections. J Histochem Cytochem 59(4): 356–365.

Xu H, Yang L, Wang W, Shi S, Liu C, Liu Y, Fang X, Taylor C, Lee C, Balgley B. 2008. Antigen retrieval for proteomic characterization of formalin-fixed and paraffin-embedded tissues. J Proteome Res 7(3): 1098–1108.

Yamamoto T, Kudo M, Peng W-X, Takata H, Takakura H, Teduka K, Fujii T, Mitamura K, Taga A, Uchida E, Naito Z. 2016. Identification of aldolase A as a potential diagnostic biomarker for colorectal cancer based on proteomic analysis using formalin-fixed paraffin-embedded tissue. Tumor Biol 37(10): 13595–13606.

Yang H-J, Hong J, Lee S, Shin S, Kim J, Kim J. 2010. Pressure-assisted tryptic digestion using a syringe. Rapid Commun Mass Spectrom 24(7):901–908.

Yeung YG, Nieves E, Angeletti RH, Stanley ER. 2008. Removal of detergents from protein digests for mass spectrometry analysis. Anal Biochem 382(2):135–137.

Yoshida A, Okamoto N, Tozawa-Ono A, Koizumi H, Kiguchi K, Ishizuka B, Kumai T, Suzuki N. 2013. Proteomic analysis of differential protein expression by brain metastases of gynecological malignancies. Hum Cell 26(2): 56–66.

Young D, Bermes E, Haverstick D. 2008. Specimen collection and other preanalytical variables. In: Burtis DE, Ashwood CA, Bruns ER, editors, Fundementals of clinical chemistry. 6th Edition, pp. 42–62. St. Louis: Saunders Elsevier.

Yousem SA. 2012. Role of molecular studies in the diagnosis of lung adenocarcinoma. Mod Pathol 25(S1):S11–S17.

Zhang B, Wang J, Wang X, Zhu J, Liu Q, Shi Z, Chambers MC, Zimmerman LJ, Shaddox KF, Kim S, Davies SR, Wang S, Wang P, Kinsinger CR, Rivers RC, Rodriguez H, Townsend RR, Ellis MJ, Carr SA, Tabb DL, Coffey RJ, Slebos RJ, Liebler DC, NCI CPTAC. 2014. Proteogenomic characterization of human colon and rectal cancer. Nature 513(7518): 382–387.

Zhang H, Liu T, Zhang Z, Payne SH, Zhang B, McDermott JE, Zhou J-Y, Petyuk VA, Chen L, Ray D, Sun S, Yang F, Chen L, Wang J, Shah P, Cha SW, Aiyetan P, Woo S, Tian Y, Gritsenko MA, Clauss TR, Choi C, Monroe ME, Thomas S, Nie S, Wu C, Moore RJ, Yu K-H, Tabb DL, Fenyö D, Bafna V, Wang Y, Rodriguez H, Boja ES, Hiltke T, Rivers RC, Sokoll L, Zhu H, Shih I-M, Cope L, Pandey A, Zhang B, Snyder MP, Levine DA, Smith RD, Chan DW, Rodland KD CPTAC Investigators. 2016. Integrated proteogenomic characterization of human high-grade serous ovarian cancer. Cell 166(3): 755–765.

Zhang W, Sakashita S, Taylor P, Tsao MS, Moran MF. 2015. Comprehensive proteome analysis of fresh frozen and optimal cutting temperature (OCT) embedded primary non-small cell lung carcinoma by LC–MS/MS. Methods 81: 50–55.

Zhang Y, Muller M, Xu B, Yoshida Y, Horlacher O, Nikitin F, Garessus S, Magdeldin S, Kinoshita N, Fujinaka H, Yaoita E, Hasegawa M, Lisacek F, Yamamoto T. 2015. Unrestricted modification search reveals lysine methylation as major modification induced by tissue formalin fixation and paraffin embedding. Proteomics 15(15): 2568–2579.

Zhou JY, Dann GP, Shi T, Wang L, Gao X, Su D, Nicora CD, Shukla AK, Moore RJ, Liu T, Camp DG, Smith RD, Qian W-J. 2012. Simple sodium dodecyl sulfate-assisted sample preparation method for LC-MS-based proteomics applications. Anal Chem 84(6): 2862–2867.

Zhou Y-F. 2011. High intensity focused ultrasound in clinical tumor ablation. World J Clin Oncol 2(1):8–27.

Zhu J, Nie S, Wu J, Lubman DM. 2013. Target proteomic profiling of frozen pancreatic CD24+ adenocarcinoma tissues by immuno-laser capture microdissection and nano-LC-MS/MS. J Proteome Res 12(6):2791–2804.

Zhu Y, Clair G, Chrisler WB, Shen Y, Zhao R, Shukla AK, Moore RJ, Misra RS, Pryhuber GS, Smith RD, Ansong C, Kelly RT. 2018. Proteomic analysis of single mammalian cells enabled by microfluidic nanodroplet sample preparation and ultrasensitive nanoLC-MS. Angew. Chemie Int. Ed. 57(38): 12370–12374.

Zhu Y, Dou M, Piehowski PD, Liang Y, Wang F, Chu RK, Chrisler W, Smith JN, Schwarz KC, Shen Y, Shukla AK, Moore RJ, Smith RD, Qian WJ, Kelly RT. 2018. Spatially resolved proteome mapping of laser capture microdissected tissue with automated sample transfer to nanodroplets. Mol Cell Proteomics 17: 1864–1874. mcp.TIR118.000686.

Zhu Y, Piehowski PD, Zhao R, Chen J, Shen Y, Moore RJ, Shukla AK, Petyuk VA, Campbell-Thompson M, Matthews CE, Smith RD, Qian W-J, Kelly RT. 2018. Nanodroplet processing platform for deep, quantitative proteome profiling of 10 – 100 mammalian cells. Nat Commun 9(1): 882.

Zielinska DF, Gnad F, Wiśniewski JR, Mann M. 2010. Precision mapping of an in vivo N-glycoproteome reveals rigid topological and sequence constraints. Cell 141(5):897–907.

Zou J, Talbot F, Tata A, Ermini L, Franjic K, Ventura M, Zheng J, Ginsberg H, Post M, Ifa DR, Jaffray D, Miller RJ, Zarrine-Afsar A. 2015. Ambient mass spectrometry imaging with picosecond infrared laser ablation electrospray ionization (PIR-LAESI). Anal Chem 87(24): 12071–12079.